

SEA ICE Research and Engineering Development

Naoki Nakazawa

■ Abstract

Ice exists in multiple forms, such as sea ice, glaciers, permafrost ice, river ice, and ice formed from frozen water vapor. This book focuses on sea ice, in particular, tracing the development of research and engineering techniques over time.

Various regions on Earth such as the Arctic Ocean, Antarctic Ocean, Sea of Okhotsk, Baltic Sea, Caspian Sea, and Bohai Sea experience sea ice in winter (and sometimes in summer). Research on sea ice has been conducted in these areas.

Although human activity in ice-covered seas was occurring thousands of years ago, European exploration began historically with maritime navigation. After many tragic Arctic expeditions, Nils Adolf Erik Nordenskiöld successfully opened the Northeast Passage along the Russian Arctic coast in the late 19th century, and explorers like Fridtjof Nansen and Roald Amundsen traversed the Northwest Passage along the Canadian Arctic coast in the early 20th century. These explorations laid the groundwork for Arctic development.

After World War II (WW2), the Cold War turned the Arctic Ocean into a strategic area, with the United States and Soviet Union conducting military-focused sea-ice research. In the 1960s, the discovery of oil in the Arctic led to further sea-ice engineering research for resource development.

When extracting oil and natural gas in icy seas, drilling facilities face significant ice forces from moving ice floes, requiring accurate assessment to ensure safe design and construction. In the 1960s, with the beginning of oil exploration in the Arctic, sea ice and ice-resistant structure research intensified in the regions of Northern Europe and North America close to the Arctic. While in Japan, Dr. Ukichiro Nakaya's snow research began in the 1930s, and by the 1960s, observations of drifting sea ice in the Sea of Okhotsk were underway; engineering research into sea ice increased in the 1970s, leading to the construction of Arctic-bound mobile oil drilling platforms for North American oil companies in the 1980s.

The construction of SSDC (Single Steel Drilling Caisson, 1982, Hitachi Zosen Corporation), a drill barge built for year-round oil exploration; Kulluk (1983, Mitsui Engineering & Shipbuilding Co.), an ice-strengthened drill barge; Molikpaq (1984, Ishikawajima-Harima Heavy Industries Co.), a bottom-grounded Arctic drilling platform; and Super CIDS (Concrete Island Drilling System, 1984, NKK Corporation) demonstrated Japan's advanced shipbuilding skills and ice engineering expertise.

To further advance Japanese ice engineering, the Study Project on Ice Loads on Offshore Structures (commonly known as the JOIA Ice Load Research Project), running from 1993 to 2001, brought together researchers and engineers from industry, academia, and the government and earned international acclaim. However, the Plaza Accord in 1985 strengthened the Japanese yen, gradually diminishing Japan's manufacturing competitiveness and making the construction of new offshore ice-resistant structures in Japan more challenging after the 1990s, with Japan's highly regarded sea ice research not always resulting in manufacturing contracts.

By the 2000s, global warming was causing a reduction in sea ice, with a sharp decline in Arctic sea ice during summer. Although raising concerns about its environmental impact, this reduction has opened new opportunities, such as opening the Northern Sea Route for oil and natural gas transport and increasing trade between Asia and Europe. Japan, with its expertise in building icebreakers gained from constructing Antarctic research ships since 1956, plans to launch a new Arctic research vessel in 2026.

This book outlines the history of technological advancements in sea ice engineering, emphasizing Japan's potential role in addressing climate change and supporting research in the Arctic region, with a goal of contributing to Japan's future scientific and technological achievements in the Arctic.

* The original Japanese version of this report is available for download from the museum's official website at:

<https://sts.kahaku.go.jp/diversity/document/system/pdf/127.pdf>

■ Profile

Naoki Nakazawa

Senior Researcher, Center of the History of Japanese Industrial Technology, National Museum of Nature and Science

1979: Bachelor of Engineering, Department of Civil Engineering, Hokkaido University, Sapporo.

1979: Pacific Consultants Co., Ltd., Tokyo.

1987-1989: Visiting researcher, U.S. Army Cold Regions Research and Engineering Laboratory, Hanover, New Hampshire.

1989: Master of Science (M.Sc.) in Arctic Engineering, University of Alaska Fairbanks.

1989-1997: Pacific Consultants Co., Ltd.

1991: Doctor of Engineering, Hokkaido University.

1997 to present: President, Systems Engineering Associates, Inc.

2007-2023: Technical Advisor, Foundation of Advanced Construction Technology Center.

2014-2020: Research Fellow, Graduate School of Frontier Sciences, The University of Tokyo.

2021-2022: Senior Researcher, Center of the History of Japanese Industrial Technology, National Museum of Nature and Science, Tokyo.

■ Contents

1	Introduction	3
2	Understanding <i>Ice</i>	5
3	Evolution of Offshore Ice Engineering	9
4	Pioneers in Snow and Ice Research	15
5	Mechanical Properties of Sea Ice	28
6	Ice Model Basin.....	38
7	Japan Ocean Industries Association (JOIA): Ice Load Research Project	44
8	Offshore Ice-Resistant Structures	62
9	Icebreakers of Japan	78
10	Epilogue	84
	Acknowledgements	85

1 | Introduction

We live with seasonal weather. After the cold winter subsides, frozen earth and snow thaw, allowing plants to sprout. The melting snow from mountainous regions flows down streams, gathering in reservoirs to become water resources. Rivers flow, sustaining life and nourishing people's livelihoods. Water that flows across land, forms lakes, and finally flows into seas, evaporates, forming clouds in the atmosphere. These clouds, in turn, bring spring rains, summer monsoons, and autumn showers.

During the chilly winter, ice crystals in the clouds grow, forming snowflakes that return to the earth. Dr. Ukichiro Nakaya (1900-1962), pioneering Japanese physicist in glaciology and low-temperature sciences, famously wrote, "Snowflakes are letters from the sky," while revealing the beauty of snow crystals through his creation of the first artificial snowflake.

Water can exist in a variety of *states*, e.g., experienced in nature as a liquid, a vapor (gas), or ice (solid) depending on its temperature. This phenomenon isn't exclusive to water; many substances change state with temperature fluctuations. The transitions between these states are called *phase changes*. The various kinds of weather on Earth demonstrate the phase changes of water in our daily lives.

Water remains in a liquid state between 0°C to 100°C (specifically, 99.974°C) at normal atmospheric pressure (i.e., at sea level). We can observe phase changes in everyday environments, such as ice (solid) in a container melting into water (liquid) and water vapor (gas) in contact with the container wall condensing into water droplets (liquid) (see Fig. 1.1). The fact that we can observe the three states of matter within the range of everyday temperatures suggests that water, and consequently ice, can be considered a unique substance. In general, as almost all substances transition from gas to liquid to solid, their mass remains constant, but their volume decreases. However, when water freezes into ice, it is one of the few substances that expands.

This book focuses on the engineering aspects of this unique substance, water, specifically in its solid state as *ice*, primarily sea ice.

Beginning with expeditions in the late 19th century, many explorers and scientists navigating the Arctic Ocean had to overcome challenges posed by ice. Their endeavors transformed the Arctic Ocean from a realm of adventure into one of scientific exploration/research and economic activity.

During the Cold War era after WW2, ice engineering experienced significant research and development for military purposes. In the Arctic, submarines surfaced by breaking through sea ice, while airstrips had to be constructed on Greenland's ice sheet. Simultaneously, research into the geophysics of snow and ice began in Antarctica. In addition, there were advancements in icebreaker (ship) technology.

The discovery of fossil fuel resources in the Arctic Ocean

in the 1960s linked ice research with market economics, prompting numerous companies to enter the field of ice engineering since extracting oil and natural gas from the seabed beneath sea ice requires specialized tools and facilities.

When seawater freezes into sea ice, it uniquely expands in volume. The force of this ice expansion, i.e., *ice force*, can be significant enough to damage structures. Additionally, structures are affected by forces induced by the movement of sea ice under the influence of ocean currents and winds. To understand these forces, research has focused on the physical and mechanical properties of ice, including experiments to measure ice force and efforts to develop calculation methods for ice force as well as to develop design techniques for structures and the materials and construction methods required in this environment (see Fig. 1.2).



Fig. 1.1 Ice (solid) with water (liquid) in a glass with (slightly) visible water condensation from atmospheric water vapor, photographed by the author.



Fig. 1.2 Experiment to measure ice force against a structure, photograph.¹⁻¹⁾

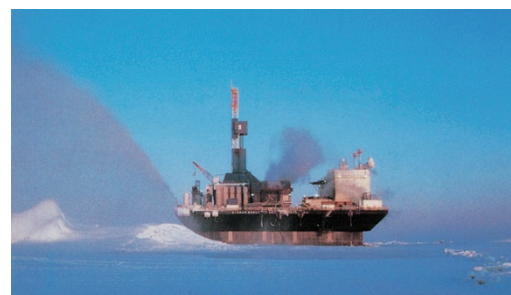


Fig. 1.3 Oil drilling platform in icy waters, photograph: SuperCIDS.¹⁻²⁾

This book traces the development of offshore ice engineering (excluding effects from permafrost), starting from fundamental research on snow and ice, through studies conducted by researchers and engineers on the design and construction of ice-resistant structures like oil drilling platforms (see **Fig. 1.3**) and icebreakers, to commercial development and construction. It's worth noting that the fundamental research and technological developments mentioned in this book also apply to structures such as bridges and revetments for rivers and lakes as well as coastal defenses.

References

- 1-1) JOIA. (2000). *FY1993-2000, Marine Petroleum Development Technology Survey: Fundamental Research on Offshore Structures in Extreme Marine Environments—A Study on Ice Loads Impacting on Offshore Structures*, Final Report. Japan Ocean Industry Association (JOIA). (in Japanese).
- 1-2) Shimizu Corporation. (n.d.). *Mobile Artificial Island For Oil Drilling SuperCIDS* [trans. from Japanese]. https://www.shimz.co.jp/works/jp_har_198403_supersizzu.html.

2 | Understanding Ice

2.1 Snow and Ice: Aggregates of Water Molecules

This book primarily focuses on ice, particularly sea ice. However, it's important to touch on *snow*, another form of water aggregation. In the book *Structure and Physical Properties of Snow and Ice*,²⁻¹ the relationship between snow, ice, water, and water vapor is explained as follows (see Fig. 2.1):

When water freezes, forming a solid, it's called *frozen ice*, or simply ice; when water vapor condenses directly into ice, it's termed *desublimation ice*, or simply snow. Moreover, when examining snow's structure and properties, note that when a conglomeration of snowflakes contains entrapped air, the resulting impermeable mass is referred to as ice. In this context, the boundary between snow and ice lies at a density of 820 - 840 kg/m³, corresponding to a porosity of 8-11%. (trans. by author)

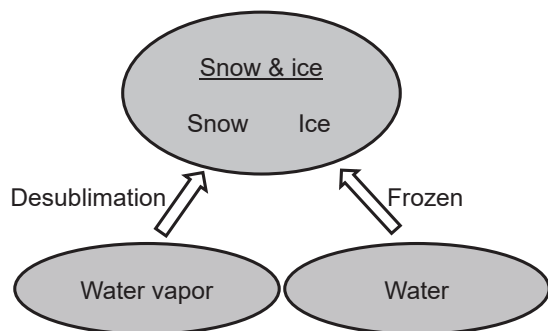


Fig. 2.1 Formation of snow and ice: Water vapor condensing directly into ice - *Desublimation ice*, or simply snow; ice formed by the freezing of water - *Frozen ice*, or ice.²⁻¹

The structure of ice consists of numerous water molecules interconnected through chemical bonds, i.e., hydrogen bonds. In ice and water, hydrogen bonds can be depicted schematically, as shown in Fig. 2.2, with adjacent water molecules attracted to each other via the hydrogen bond between the hydrogen and oxygen atoms.

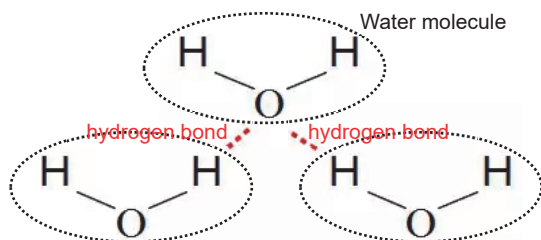


Fig. 2.2 Hydrogen bonding of water molecules: Hydrogen (H) atoms of each water molecule (H₂O) form bonds with the oxygen (O) atoms of neighboring water molecules.²⁻¹

2.2 Unique Properties of Ice

1) Ice Floats on Water

Typically, as substances transition from gas to liquid and then to solid, the spaces between particles narrow, leading to a decrease in volume. However, when water turns into a solid, as ice, the spaces between particles widen (see Fig. 2.3). Consequently, unlike most other substances, ice expands with its density decreasing to below 1000 kg/m³, causing it to float on water (see Fig. 2.4). If ice were denser than water and sank, it would accumulate thickness not at the water's surface, but at the bottom (seafloor). In such a situation, it would likely be impossible for aquatic plants and animals to survive winter in rivers, lakes, and seas that freeze over. The ecosystem we know today in the nearly fully ice covered Arctic Ocean during winter would likely not exist.

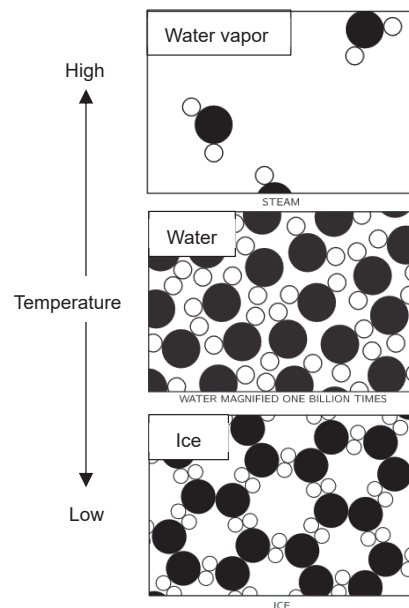


Fig. 2.3 Diagram of molecular structures—ice, water, and water vapor. Note: Ice molecules are less densely packed than in their liquid state—contrary to what is normally seen with other materials.²⁻²



Fig. 2.4 Iceberg, illustration: When water turns into ice, its density becomes less than 1000 kg/m³, causing it to float on water.²⁻³

2) Ice Sinking in Water: Ice Formed Under High Pressure

All ice that forms under normal temperature and pressure conditions on Earth is regular hexagonal ice, known as *Ice Ih* (h denotes a hexagonal crystal). This type of ice has a density below 1000 kg/m³, causing it to float on water. However, applying extremely high pressures on the order of gigapascals (GPa) can lead to the emergence of ice with different crystal structures. Such substances, which have different crystal structures despite having the same chemical composition, are referred to as *polymorphs*. Ice exhibits polymorphism, and the variety of its forms far exceeds that of other substances.

Since the early 1900s, high-pressure experimental techniques capable of generating pressures exceeding 1 GPa have been developed by numerous researchers. With advancements in this field, new polymorphs of ice are being continuously discovered. For instance, Percy Bridgman, the father of high-pressure physics and Nobel laureate in physics in 1946, discovered four phases of ice: Ice IV, V, VI, and VII. More recently, in February 2021, a research group at the University of Tokyo announced the discovery of the 20th phase of ice, known as Ice XIX.²⁻⁴⁾

Figure 2.5 depicts the temperature-pressure phase diagram of ice. When the pressure exceeds 20,000 atmospheres (2 GPa) and the temperature drops below -100°C, various high-pressure forms of ice appear in addition to Ice Ih. These include Ice II, Ice III, Ice IV, Ice V, Ice VI, Ice VII, Ice VIII, Ice IX as well as glassy ice and Ice X to Ice XIX, totaling 20 different types of ice.

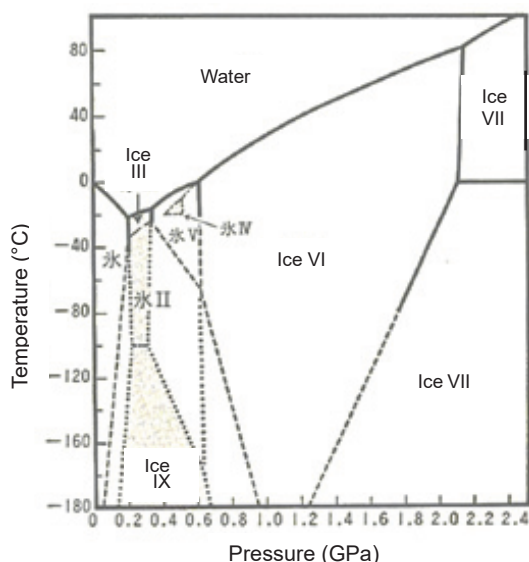


Fig. 2.5 Ice temperature-pressure phase diagram.²⁻¹⁾

Table 2.1 illustrates the crystal systems and densities of ice up to Ice IX. The only forms of ice that can exist in Earth's natural environment have densities below 1000 kg/m³: common Ice Ih and occasionally Ice Ic (a cubic crystalline variant of ice) present in the upper atmosphere. The rest, with densities exceeding 1000 kg/m³, can only be produced un-

der high-pressure and extremely low-temperature conditions, such as in laboratory settings.

The remainder of this book will be concerned solely with natural ice (Ice Ih).

Table 2.1 Types of ice: Crystal systems and densities of 11 types of ice.²⁻⁵⁾

Ice Phase*	Crystal System	Density (kg/m ³)
Ice Ih	Hexagonal crystal	931
Ice Ic	Cubic crystal	930
Amorphous ice	Amorphous (non-crystalline)	1100
Ice II	Rhombohedral crystal	1180
Ice III	Tetragonal crystal	1160
Ice IV	Rhombohedral crystal	1270
Ice V	Monoclinic crystal	1270
Ice VI	Tetragonal crystal	1310
Ice VII	Cubic crystal	1490
Ice VIII	Cubic crystal	1490
Ice IX	Tetragonal crystal	1160

*As of February 2021, 20 phases of ice have been discovered; table includes only the 11 types for which density is known.

3) Albedo of Snow and Ice

Albedo, i.e., surface reflectivity, is the ratio of reflected energy to incident energy. A lower albedo value indicates greater absorption of incoming energy. In regard to Earth's environment, albedo generally ranks from low to high as follows: water (oceans and lakes), forests, grasslands, savannas, dry soil, deserts, ice, and snow. As seen in **Fig. 2.6**, water has an albedo of about 0.1 (10%), while sea ice covered with snow has an albedo of around 0.8 (varies depending on snow condition); the albedo of water may be less than 0.1 and that of fresh snow cover is approximately 0.9.

The average albedo of the Earth's surface is about 0.3, i.e., Earth absorbs about 70% of incoming solar energy and reflects 30% back into space. Despite the ocean, which covers about 70% of the Earth's surface, having an albedo of less than 0.1, the presence of snow and ice raises the overall Earth albedo to 0.3. Although the total area covered by sea ice varies through the year, in February and September (the approximate periods of minimum and maximum sea ice coverage seen in the Arctic and Antarctic Oceans), sea ice represents about 50% and 60%, respectively, of Earth's total ice surface area. Clearly, the high albedo of snow and ice plays a crucial role in shaping the environment around us.

In recent years, there has been a significant decrease in Arctic sea ice. Below is information on the minimum sea ice extent (i.e., coverage) observed in the Arctic Ocean.²⁻⁶⁾

- September 17, 2012: Smallest Arctic sea ice extent in recorded history — 3.39×10^6 km².
- Average minimum sea ice extent from 1981 to 2010: 6.374×10^6 km².
- Note: The 2012 minimum sea ice extent is approximately 50% smaller than the average for 1981 to 2010.

During the summer of 2012, the sea ice coverage in the Arctic Ocean decreased to about 50% of the average minimum extent recorded from 1981 to 2010. As sea ice diminishes, the exposed surface area of seawater increases, resulting in a decrease in overall albedo. Consequently, Earth's overall reflectivity decreases, leading to increased absorption of solar radiation on the Earth's surface, accelerating global warming. This phenomenon is known as the ice albedo feedback. Therefore, careful observation of changes in the distribution and quantity of snow and ice is crucial in understanding global warming and climate change.

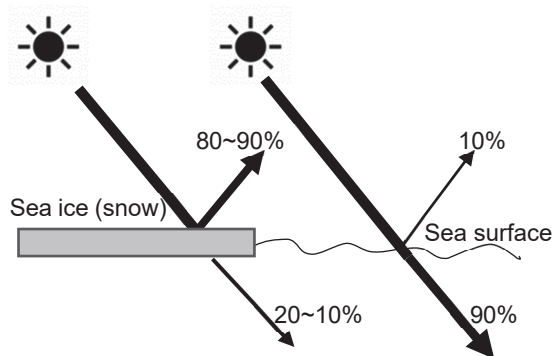


Fig. 2.6 Diagram: Albedo of sea ice (snow) and seawater. Note: Sea ice (snow) plays a significant role as a thermal regulator for the Earth, illustrated by the author.

2.3 Distribution of Snow/Ice and Ice Volume in Antarctic/Arctic Regions

Various forms of *ice* exist on Earth, including ice sheets on Antarctica and Greenland, permafrost, sea ice, snow accumulation, icebergs, and atmospheric ice. Approximately 99% of these forms of ice exist as ice sheets located on Antarctica (about 89%) and Greenland (about 10%), with the next largest portion being permafrost in the Arctic region (about 0.8%). While the quantity of sea ice is small relative to Earth's total ice, sea ice significantly affects the world environment as noted above in the discussion of albedo.

The reduction of sea ice in the Arctic Ocean has become particularly significant since the late 20th century due to its effect on global warming. In 2020, the annual average sea ice volume in the Arctic Ocean was the third lowest on record, 13,500 cubic kilometers (km^3).²⁻⁷⁾ Assuming a density of 0.91 t/m^3 for sea ice, this amounts to 1.228×10^{13} tons (t). In 2013, the ice sheet volume in Antarctica was $26,500,000 \text{ km}^3$,²⁻⁸⁾ which at a density of 0.90 t/m^3 , amounts to $2,385 \times 10^{13}$. (Note: variations in the 21st century Arctic sea ice densities are much larger than previously measured.) The amount of sea ice in the Arctic Ocean is approximately one two-thousandth of the ice sheet volume in Antarctica. However, since almost the entire Arctic Ocean is covered with sea ice during winter, and even in summer, several million square kilometers (around $6,000,000 \text{ km}^2$ in August 2021) are covered with sea ice, fluctuations in sea ice volume have a significant impact

on global weather and marine conditions. Table 2.2 shows the distribution of snow and ice on Earth.

Table 2.2 Distribution of snow and ice: Volume of ice on Antarctica and in the Arctic Ocean.²⁻¹⁾

Locations and Types of Snow and Ice	Mass Ratio (%)
Antarctic ice sheet	89
Greenland ice sheet	10
Permafrost in the Arctic region	0.8
Sea ice, snow cover, icebergs, atmospheric ice, others	0.2
Total	100
Locations: Snow-Ice	Mass (t)
Antarctica ice sheet (2013)	2385×10^{13}
Annualized average sea ice in the Arctic Ocean for 2020	1.228×10^{13}
Note: The volume/mass of sea ice in the Arctic Ocean is approximately 1/2000th of the volume of the Antarctica ice sheet.	

2.4 Conclusion

As of February 2021, 20 phases of ice have been discovered, the great majority being ice with a density of over 1000 kg/m^3 created through high-pressure experiments. All ice formed at normal temperatures and pressures that we encounter on Earth is Ice Ih—with a hexagonal crystal structure and a density of less than 1000 kg/m^3 , this ice floats in water. The (floating) sea ice covering the Arctic and Antarctic Oceans, with its high albedo, plays a crucial role in decreasing the heating of the Earth.

This book focuses on the history of offshore ice engineering, so it does not delve further into the physical properties or phase changes of ice. For those wishing to learn more about water molecules, hydrogen bonding, and high-pressure ice that does not float in water, I recommend the books (in Japanese) *Structure and Physical Properties of Snow and Ice*²⁻¹⁾ and *Science of Ice*.²⁻⁵⁾

References

- 2-1) Maeno, N. and M. Fukuda (eds.). (1986). *Structure and Physical Properties of Snow and Ice*. Kokon Shoin. ISBN 4-7722-1094-6. (in Japanese).
- 2-2) Feynman, R. P., R. B. Leighton, and M. Sands. (n.d.). *The Feynman Lectures on Physics*, Vol. 1, Chapter 1 Atoms in Motion. https://www.feynmanlectures.caltech.edu/I_01.html.
- 2-3) FREEPIK Company S.L. (n.d.). *Iceberg Png Images*. <https://www.freepik.com/free-photos-vectors/iceberg-png>.
- 2-4) The University of Tokyo, School of Science. (2021, Feb. 19). *Discovery of a New Ice Phase (Ice XIX) at Low Temperatures and High Pressure*, Press Releases [trans. from Japanese]. <https://www.s.u-tokyo.ac.jp/ja/press/2021/7238/>.
- 2-5) Maeno, N. (2004). *Science of Ice* (new ed.). Hokkaido University Press. ISBN:978-4-8329-7371-8. (in Japanese).

2-6) National Snow & Ice Data Center. (n.d.). *Charctic Interactive Sea Ice Graph*, A Sea Ice Today Tool.
<https://nsidc.org/arcticseaicenews/charctic-interactive-sea-ice-graph/>.

2-7) Polar Science Center. s(n.d.). *PIOMAS Arctic Sea Ice Volume Reanalysis*, Arctic Sea Ice Volume Anomaly.

<http://psc.apl.uw.edu/research/projects/arctic-sea-ice-volume-anomaly/>.

2-8) Amos, J. (2013, Mar. 08). *Antarctic ice volume measured*. BBC News Services.
<https://www.bbc.com/news/science-environment-21692423>.

– Addendum 1 –

Ice: Antarctica and the Arctic Ocean

Antarctica is like a giant ice warehouse.

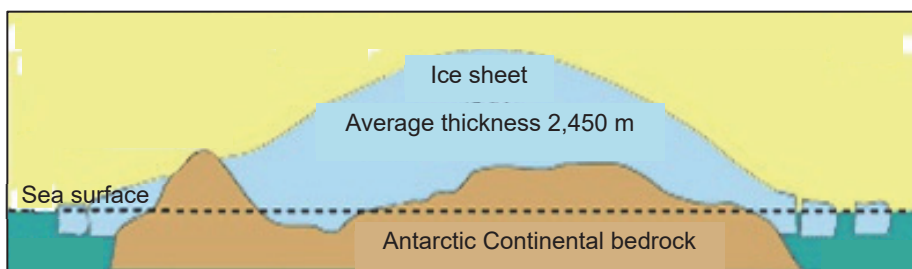
Compare the sizes of Antarctica, the Arctic Ocean, and the United States:

- Antarctica: 14,200,000 km²
- Arctic Ocean: 14,060,000 km²
- United States: 9,834,000 km² (8,116,000 km² excluding Alaska)

When comparing Antarctica to the United States (excluding Alaska), as shown in the figure below, the great size of Antarctica is clear. This huge landmass is covered by an ice sheet that’s about 2,450 m thick on average. Even though the area of the Arctic Ocean is almost the same as that of Antarctica, the ice floating on it is much thinner, only a few meters thick on average, and it’s getting thinner every year. Compared to the thick ice sheets of Antarctica, the ice in the Arctic Ocean is like a thin layer.



Size comparison: Antarctica and the United States (excluding Alaska).



Cross-section of Antarctica: Covered by an ice sheet, average thickness about 2,450 m.

3 | Evolution of Offshore Ice Engineering

3.1 Frozen Seas: Northern Hemisphere

The interaction between human activities and the icy environments of the Arctic has evolved significantly across time, with different eras focusing on different sea regions and objectives. This chapter examines the evolution of research topics related to marine ice across these historical periods.

Figure 3.1 illustrates the seas in the Northern Hemisphere that are subject to freezing during the winter months, marked as B2 to B21. Near Japan, the Sea of Okhotsk and the Bohai Sea are noted as B11 and B13, respectively. The seas referred to as B3, B4, B7, B11, B13, B14, B16, and B17 denote ar-

reas with currently active oil and natural gas development and production.

Table 3.1 provides a summary of the sea ice conditions in the areas of active oil and natural gas development depicted in Fig. 3.1. Chapter 8 describes in more detail specific examples of ice-resistant structures engineered for oil and natural gas extraction, many of which are located in the regions identified in Table 3.1. Given that approximately 70% of the Earth's surface is covered by oceans with an average depth of about 3,800 m, the shallow depths of the seas listed in Table 3.1 stand out. These shallow areas being exploited, primarily occurring on the continental shelf, present unique engineering challenges and opportunities for marine ice engineering.

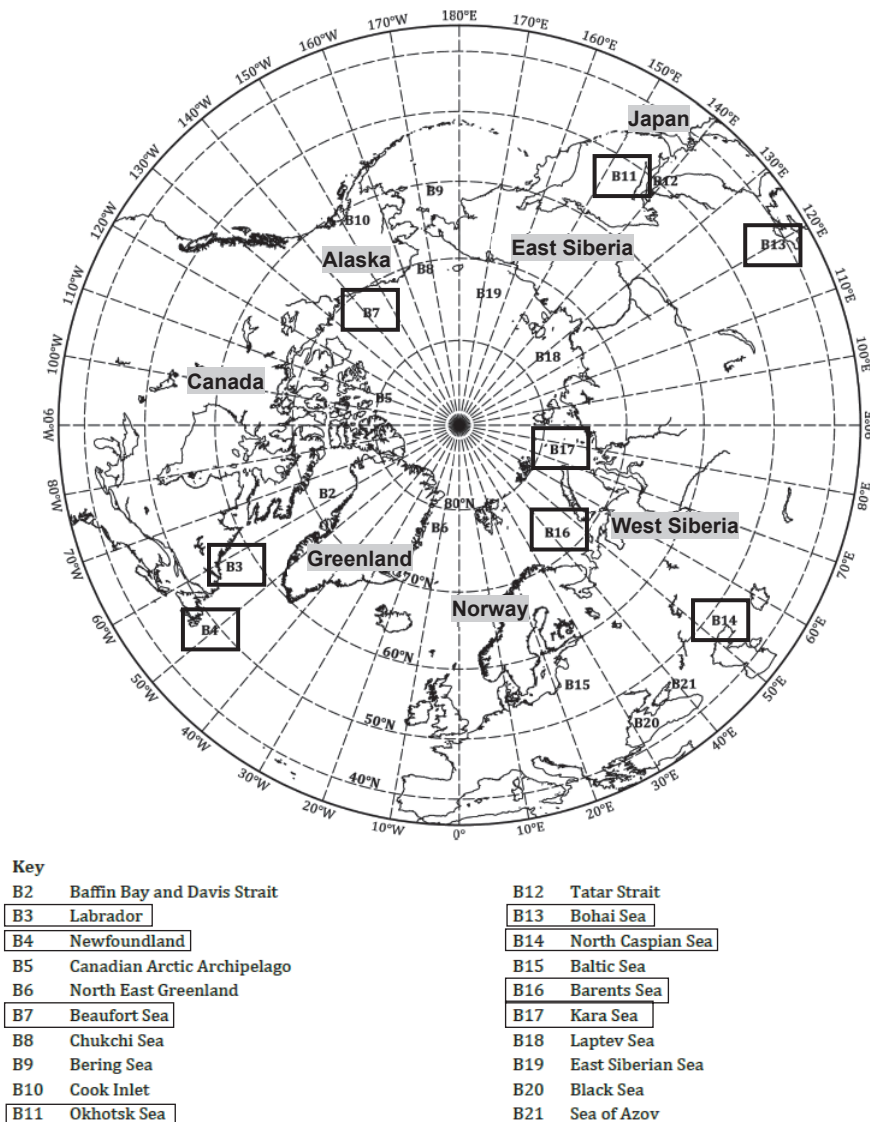


Fig. 3.1 Seas that freeze during winter—Northern Hemisphere: boxed areas—Regions with currently active oil and natural gas development.³⁻¹⁾

Table 3.1 Ice thickness and sea water depth: Northern hemisphere locations with ongoing oil and natural gas development.³⁻¹⁾

No.	Location	Level ice thickness		Water depth
		First-year ice	Multi-year ice	
B3	Labrador (offshore)	1 to 2 m	2 to 8 m	20 to 1000 m or more
B4	Newfoundland (offshore)	0.7 to 1.2 m	1 to 2 m	75 to 1200 m
B7	Beaufort Sea	1.5 to 2.3 m	2 to 20 m	2 to 90 m, to several thousand
B11	Okhotsk Sea	1.1 to 1.7 m	none	0 to 700 m
B13	Bohai Sea	0.1 to 0.6 m	none	0 to 78 m
B14	Caspian Sea	0.5 m	none	0 to 10 m
B16	Barents Sea	0.7 to 1.5 m	none	222 m (ave.), 600 m (max.)
B17	Kara Sea	1.4 to 1.8 m	1.8 to 2.2 m	111 m (ave.), 600 m (max.)

3.2 Arctic Exploration: Development of Arctic Sea Routes

1) Beginnings of the Great Arctic Navigational Era

Clive Holland (1946-2000), affiliated with the Scott Polar Research Institute at Cambridge University, provides a comprehensive examination of Arctic explorations from 500 BC to 1915 in his book *Arctic Exploration and Development*.³⁻²⁾ His analysis highlights the beginning of significant Arctic voyages in 1553, when three British ships under the command of Sir Hugh Willoughby (d. 1554) embarked from London, aiming to discover the Northeast Passage. This era saw Russia, the Netherlands, Denmark, and Canada dispatch fleets to pioneer Arctic sea routes. All failed to reach the North Pole, and many encountered tragic fates due to severe conditions such as thick sea ice and extreme cold.

The quest for new maritime routes intensified during the 16th and 17th centuries, resulting in explorations of the Labrador Peninsula (Canada), Novaya Zemlya (Russia), and the Kara Sea (Russia). Dutch explorer Willem Barentsz (1550-1597) led three voyages of exploration and discovery of regions like the Yamal Peninsula (Russia) and islands such as Spitsbergen (Norway). His final expedition was shipwrecked for most of a year on Novaya Zemlya (Russia), and he died while sailing back home.

The voyages of Barentsz failed to establish a trans-Arctic passage, but subsequent intense whaling activities in the 17th and 18th centuries near Spitsbergen nearly exterminated the local whale population. The 18th century had another significant exploration milestone with Vitus Bering's (1681-1741) journeys that discovered Kamchatka (Russia), the Bering Sea (Russia, the USA), and the East Siberian Sea (Russia), further contributing to the mapping and understanding of Arctic territories.

2) Nordenskiöld: Arctic Ocean Northeast Passage

In the 19th century, the Arctic Ocean shifted from being primarily a region of exploration to one of scientific surveys. This transition was marked by the geological survey of the Svalbard archipelago (formerly Spitsbergen) by the Norwegian geologist Baltazar Keilhau (1797-1858) in 1827, followed by the discovery of the North Magnetic Pole at Cape Adelaide (Canada) by British naval officer James C. Ross

(1800-1862) in 1831.

The first person to successfully navigate the entire Northeast Passage from Northern Europe along the Siberian coast to the Pacific Ocean was Adolf Erik Nordenskiöld (1832-1901), a Swedish geologist and explorer. In June 1878, he left Sweden on the *Vega* (357 t, 30 crew members), **Fig. 3.2**, and sailed eastward through the Arctic Ocean; after spending the winter trapped in ice in the Chukchi Sea (Russia, the USA), Nordenskiöld passed through the Bering Strait into the Pacific Ocean, arriving to a warm welcome in Yokohama on September 2, 1879—even having an audience with Emperor Meiji. On his return to Sweden, he brought back a large number of Japanese books, which are still in the collection of the Royal Swedish Library in Stockholm. Details of Nordenskiöld's voyage and the Japanese books are described in *The Story Of How The Explorer Adolf Nordenskiöld Built a Collection of Japanese-Related Books in Sweden*, by Masayoshi Oku.³⁻³⁾

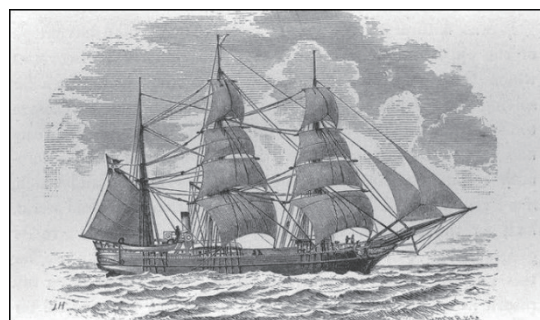


Fig. 3.2 Nordenskiöld's *Vega* (357 t), illustration: ship that pioneered the Northeast Passage.³⁻⁴⁾

3) Achievements of Nansen and Amundsen: Arctic Ocean Exploration and Northwest Passage

As the exploration of the Northeast Passage progressed, Norwegian explorer Roald Amundsen (1872-1928) became the first to successfully navigate the Northwest Passage, a sea route linking Europe with the Pacific Ocean via the Canadian Arctic Archipelago and Alaska. From 1903 to 1906, Amundsen navigated this passage aboard the *Gjøa*, a 47-ton vessel with a crew of six depicted in **Fig. 3.3**. Prior to Amundsen's expedition, another Norwegian explorer, Fridtjof Nansen (1861-1930), embarked on significant Arctic Ocean explorations from 1893 to 1896 aboard the *Fram*, a 400-ton ship with a crew of thirteen, shown in **Fig. 3.4**.



Fig. 3.3 Amundsen's *Gjøa* (47 t), photograph: ship that pioneered the Northwest Passage.³⁻⁵⁾



Fig. 3.4 Nansen's team and the *Fram* (400 t), photograph: conducting scientific and engineering research in the Arctic Ocean.³⁻⁶⁾



Fig. 3.5 Historic Arctic Ocean routes: Nordenskiöld's Northeast Passage (1878-79) and Amundsen's Northwest Passage (1903-06).³⁻⁸⁾

The pivotal voyages of Nansen and Amundsen are critical in the context of modern Arctic navigation, as described below:

Nansen's journey aboard the *Fram* is frequently highlighted in discussions of Arctic maritime history, often paralleling Nordenskiöld's exploits aboard the *Vega*. While the significance of opening Arctic Sea routes may sometimes be understated, Nansen's contributions were fundamentally transformative and indirectly pivotal. His pioneering work in drift observations and in the design and construction of vessels suited for Arctic conditions has had a lasting impact, establishing foundational principles for contemporary Arctic research.

Regarding the Northwest Passage, Amundsen's early expeditions, including a preparatory journey along the northwest coast of Greenland in 1901, culminated in his successful navigation of the passage from 1903 to 1905 aboard the *Gjøa*. Inspired by the earlier achievements of the *Vega* and stimulated by Nansen's polar explorations, Amundsen dedicated his efforts passionately to the exploration of the Northwest Passage. He later became the first person to reach the South Pole, further establishing his legacy in polar exploration.³⁻⁷⁾ (trans. by author)

Figure 3.5 illustrates the historic Arctic Ocean routes taken by Nordenskiöld during the Northeast Passage expedition (1878-1879) and by Amundsen through the Northwest Passage (1903-1906).

3.3 The Cold War and Arctic Ice: Military Research

The Cold War era, commencing shortly after the conclusion of WW2, was characterized by the global division between capitalist nations, predominantly led by the United States, and socialist states, centered around the USSR, the Soviet Union. This geopolitical tension extended into the Arctic Ocean, which served as a physical barrier between the USSR and North America, i.e., Canada and the USA. Throughout the Cold War, the Arctic region was transformed into a strategic theatre for undersea military operations. The USS *Nautilus*, an American nuclear-powered submarine, embarked on a historic expedition in August 1958, successfully navigating beneath the Arctic Ocean ice to reach the North Pole. This voyage was followed by the USS *Skate*, which became the first vessel to surface at the North Pole in March 1959, see Fig 3.6. Unlike the *Nautilus*, which merely passed beneath the North Pole,



Fig. 3.6 USS *Skate*, photograph: Surfacing through ice-covered seas, North Pole, winter 1959.³⁻⁹⁾

the USS *Skate* performed extensive operational maneuvers in the Arctic Ocean, initially surfacing through the ice in August 1958. It subsequently conducted winter operational maneuvers in March 1959 and, along with the USS *Seadragon*, participated in pioneering under-ice naval exercises in July 1962. These activities demonstrated the operational capabilities of nuclear submarines in the Arctic's ice-laden waters during the Cold War.

Additionally, the strategic importance of Thule Air Base, constructed in northern Greenland in the early 1950s, was significant during the Cold War. The base was equipped with radar systems designed to detect missiles passing over the polar route. In support of these developments, the US Army Corps of Engineers established the Snow, Ice, and Permafrost Research Establishment (SIPRE, 1949) and the Arctic Construction and Frost Effects Laboratory (ACFEL, 1953). These two laboratories were consolidated later into the Cold Regions Research and Engineering Laboratory (CRREL, 1961-present). It should be noted that the results of previously conducted original cold region research by Dr. Ukichiro Nakaya and other Japanese scientists contributed significantly to the foundation of CRREL.

As the Arctic Ocean was considered the front line of the U.S.-Soviet confrontation during the Cold War, military research played a substantial role in studies focused on ice and permafrost—the end of the Cold War diminished the Arctic Ocean's strategic importance. However, the significant reduction in sea ice observed in the 2000s has reinvigorated interest in the region beyond the obvious environmental significance, extending to the potential for resource exploitation and new security implications.

3.4 Oil, Natural Gas, and Arctic Ice: Engineering Research

The Arctic region has been a focal point for oil and natural gas development since the 1920s, with substantial operations beginning in northwest Canada and northern Russia and intensifying during WW2. In the 1960s, large oil and natural gas reserves were discovered along the Russian Arctic Ocean coast as well as in the Beaufort Sea, a region bordered by

the United States and Canada. These discoveries led to engineering research aimed at resource development under challenging icy conditions. Further significant oil and natural gas discoveries were made on the northeastern continental shelf of Sakhalin (Russia) in the 1970s and in the Barents Sea (Norway, Russia) in the 1980s, highlighting the potential for resource development in icy seas.

In 2009, a report based on research by the U.S. Geological Survey (USGS) identified areas with a potential for major oil and natural gas fields in the Barents Sea, the eastern and western waters off Greenland, the Beaufort Sea, and the Kara Sea, see Fig. 3.7.³⁻¹⁰⁾ Specifically, the report estimated that 13% and 30% of the world's undiscovered oil and natural gas resources, respectively, are located within the Arctic Circle, predominantly in waters less than 500 m deep—regions characterized by thick sea ice in the winter and the presence of large icebergs.

Developing oil and natural gas resources in difficult icy waters requires structures capable of withstanding ice forces from moving ice sheets (shown in Fig. 3.8) as well as specialized ships for transportation and ice-resistant port facilities

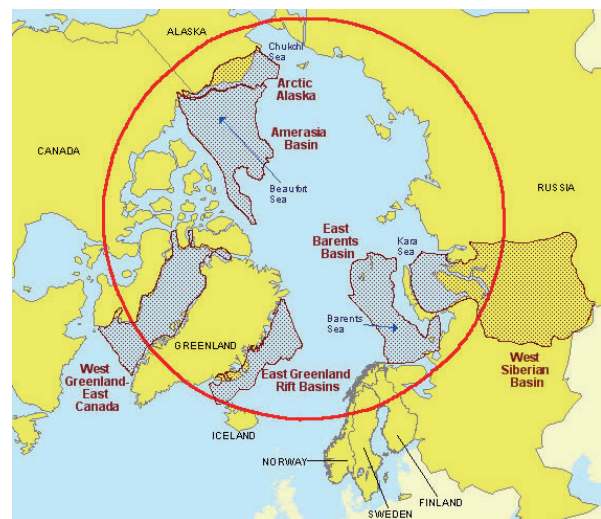


Fig. 3.7 Potential areas (shaded) of oil and natural gas deposits. Note: Arctic region represented within the Arctic Circle (red line at 66°33'N latitude).³⁻¹⁰⁾



Fig. 3.8 Ice-resistant oil production platform operating on the Russian arctic continental shelf, photograph.³⁻¹¹⁾

(Fig. 3.9). The design and construction of these structures and ships have stimulated engineering research, fostering collaboration among universities, public research institutions, oil companies, design firms, shipbuilding companies, construction firms, and materials manufacturers. This collective effort in engineering research is not limited to the countries bordering the Arctic region such as those in northern Europe, Russia, the United States, and Canada but also involves Japan, Germany, South Korea, and China.



Fig. 3.9 Icebreaking LNG carrier and ice-resistant port facilities (Port of Prigorodnoye, Sakhalin), photograph.³⁻¹²⁾

3.5 Global Warming and Arctic Sea Ice: Scientific Research

The exploration for resources in the Arctic Ocean, greatly increasing in the 1960s, has been significantly affected in recent decades by the dramatic decline in sea ice, attributable to global warming. This shift has redirected the focus of research toward geophysical and scientific studies.

Figure 3.10 illustrates the extent of Arctic sea ice in the month of September, which almost invariably represents the annual minimum. The data for September 11, 2024 (ice shown as white) indicates a significant reduction relative to



Fig. 3.10 Arctic sea ice extent minimum (white): September 11, 2024. Note the significant reduction relative to the 1981-2010 Sept. average (orange line).³⁻¹³⁾

the 1981 to 2010 average ice extent for that day (indicated by orange line).³⁻¹³⁾ Figure 3.11 tracks the changes in the area of the September average Arctic sea ice extent from 1979 to 2024: The blue trend line points to a 12.1% drop per decade, or approximately 78,000 km² per year. From 2000 to 2024, September lost 1.61 million km² of sea ice, which is roughly equivalent to the area occupied by the (U.S.) state of Alaska or the country of Iran.³⁻¹⁴⁾

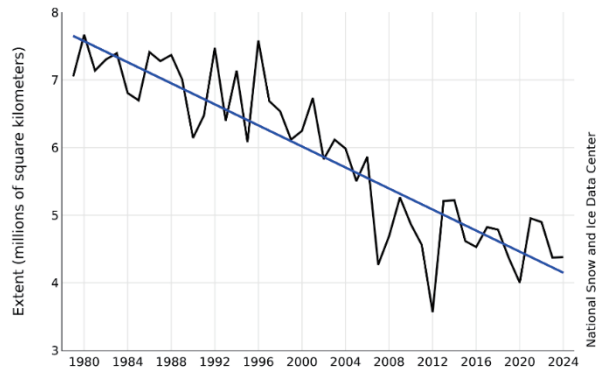


Fig. 3.11 Arctic sea ice extent: September average 1979-2024.³⁻¹⁴⁾

This substantial decline has heightened global concern over climate change, prompting extensive research into the implications of diminishing sea ice for global warming and climate change in general.

In Japan, while polar research has historically focused on Antarctic studies primarily conducted by the National Institute of Polar Research (NIPR), recent initiatives have broadened the scope: the Arctic Environment Research Consortium (JCAR) established in 2011 and the Japan Arctic Research Center (J-ARC Net) Hokkaido University in 2015. These institutions have broadened the scope of research beyond sea ice to also include the effects of atmospheric and oceanic circulation in the Arctic region that result from global climate change.

3.6 Conclusion

The field of offshore ice engineering, encompassing scientific and engineering research aimed at Arctic exploration and the development of navigational routes, has evolved significantly over time. In the post-WW2 era, this field was dominated by military research. And in the 1970s to 1990s, there was a surge in fossil fuel resource development research. The current focus has shifted towards geophysical studies that monitor environmental changes in the Arctic resulting from changes in the global climate. However, the implications of three Russian nuclear ballistic missile submarines surfacing simultaneously through Arctic ice, combining a launch of a missile and a torpedo with a combined arms military exercise in March 2021, merit further consideration.

References

- 3-1) International Organization for Standardization. (2019, July). *ISO19906:2019: Petroleum and natural gas industries—Arctic offshore structures* (2nd ed.). ISO, International Organization for Standardization.
- 3-2) Holland, C. (1993). *Arctic Exploration and Development, c. 500 B.C. to 1915: An Encyclopedia*. Garland Publishing. ISBN-10:0824076486.
- 3-3) Oku, M. (n.d.). *The Story of How the Explorer Adolf Nordenskiöld Built a Collection of Japanese-Related Books in Sweden*. Library special collection, Kyoto University of Foreign Studies. (in Japanese).
- 3-4) Overseas Images of Japan Database. (2002). *The Vega under sail*, (Photo CD No. 88001). International Research Center for Japanese Studies.
<https://sekiei.nichibun.ac.jp/GAI/ja/detail/?gid=GJ001010&hid=2729&thumbp=>.
- 3-5) FRAM - The Polar Exploration Museum. (2019). *Vessels, The Polar Ship Gjøa*. The Fram Museum.
<https://framuseum.no/polar-history/vessels/the-polar-ship-gjoa/>.
- 3-6) Bazilchuk, N. (2013, June 12). *Frozen in the ice—polar research then and now*. Sciencenorway.no.
<https://www.sciencenorway.no/arctic-forskningno-fridtof-nansen/frozen-in-the-ice---polar-research-then-and-now/1387372>.
- 3-7) Ship and Ocean Foundation. (2000, Mar.). *The Achievements of Nansen and Amundsen, Northern Sea Routes—The Shortest Maritime Route Connecting East Asia and Europe*. Digital book [in Japanese].
<https://nippon.zaidan.info/seikabutsu/1999/00862/contents/015.htm>
- 3-8) Takahashi, S. (2018, Jan.). Spirits of Exploration and Inquiry. *Journal of Japan Society of Hydrology and Water Resources, Vol. 31, No.1*, 1-3. (in Japanese).
- 3-9) NavSource Naval History. (2006, Sept. 19). Skate (SSN-578) (USN photo # NPC 1149126, US Navy Arctic Submarine Laboratory).
<http://navsource.org/archives/08/575/0857815.jpg>.
- 3-10) Gautier, D. L., et al. (2009, May 29). Assessment of Undiscovered Oil and Gas in the Arctic, U.S. Geological Survey. *SCIENCE, Vol. 324*.
- 3-11) Humpert, M. (2011, Aug. 31). *ExxonMobil Gains Access to Arctic Oil and Gas Reserves in Deal with Rosneft*. The Arctic Institute.
<https://thearticinstitute.org/exxonmobil-gains-access-arctic-oil/>.
- 3-12) Sakhalin Energy. (viewed 2021, Dec.).
<http://sakhalinenergy.ru/en/company/20th-anniversary/>.
- 3-13) National Snow and Ice Data Center. (2024, Sept. 24). *Arctic sea ice extent levels off; 2024 minimum set*.
<https://nsidc.org/sea-ice-today/analyses/arctic-sea-ice-extent-levels-2024-minimum-set>.
- 3-14) National Snow and Ice Data Center. (2024, Oct. 3). *The new abnormal*.
<https://nsidc.org/sea-ice-today/analyses/new-abnormal>.

4 | Pioneers in Snow and Ice Research

4.1 Ukichiro Nakaya: World's First Artificial Snow

1) Early Career: Beginning Snow Research, Professor at Hokkaido Imperial University

Dr. Ukichiro Nakaya (1900-1962), the physicist who created the world's first artificial snow crystals, is also remembered for his words, "Snowflakes are letters sent from the sky." His research on snow crystals began around 1932 when he became a professor at Hokkaido Imperial University (now Hokkaido University). On March 12, 1936, he achieved the world's first successful creation of artificial snow in the university's low-temperature laboratory, clarifying the relationship between weather conditions and the crystal formation process. His other significant contributions to the field of low-temperature science include research on frost heave and icing prevention. Dr. Nakaya's life and career highlights are listed below.⁴⁻¹⁾

- 1900: Born in Kaga, Ishikawa Prefecture.
- 1925: Graduate, Department of Physics, Faculty of Science, Tokyo Imperial University (now the University of Tokyo), mentored by Professor Torahiko Terada (1878-1935).
- 1932: Appointed professor at Hokkaido Imperial University; began researching natural snow crystals at Mount Tokachi (one of the highest mountains in Hokkaido).
- 1936, March 12: Successfully produced the world's first artificial snow crystals; **Fig. 4.1** shows Dr. Nakaya in the Low Temperature Science Laboratory that he created in 1935.
- 1938: Published his first collection of essays: *Winter Flowers and Snow*. Founded Nakaya Laboratory, the predecessor of Iwanami Film Production (1950-1980), focusing on groundbreaking educational and scientific documentaries.



Fig. 4.1 Dr. Nakaya in the Low Temperature Science Laboratory (Hokkaido University), photograph.⁴⁻²⁾

- 1945: Established and directed the Agricultural Physics Research Institute based on the Niseko Ice Observation Station, conducting research on floods, frozen ground, and snowmelt.
- 1952: Became a researcher at SIPRE and moved to the United States, conducting research on the physical properties of ice for two years.
- 1954: Published *Snow Crystals: Natural and Artificial* at Harvard University.⁴⁻³⁾
- 1957: Began research on the Greenland ice sheet, continuing his studies on the physical properties of ice.
- 1962: Passed away at the University of Tokyo Hospital due to osteomyelitis at the age of 61.

2) Remarkable Observations of Snow Crystals in the Field

Dr. Nakaya, renowned for his success in creating the world's first artificial snow crystals, also developed the Nakaya Diagram, which classifies snow crystal shapes. However, before these achievements, he conducted significant field research using Hokkaido's very long winter with an unlimited supply of naturally falling snow.

Before continuing with details of Dr. Nakaya's achievements, it's important to emphasize the importance of meticulous record keeping as a cornerstone of scientific research. And, of course, one difficulty associated with observing and recording snowflakes is their ephemeral nature. This obstacle was first overcome by Wilson Alwyn Bentley (1865-1931), a self-taught meteorologist-photographer American farmer who pioneered microphotography in the 19th century and was the first to photograph single snowflakes using techniques that remarkably continue to the present. His final book of snowflake microphotographs, *Snow Crystals* (containing 2,500 photos), was published in 1931.

After his appointment at Hokkaido Imperial University in 1932, Dr. Nakaya, while living in snow-covered Sapporo and reflecting on the appearance of Japanese snow while studying Bentley's book, stated, "First, observe the snow itself carefully, and avoid being reluctant to start."

During the winter of 1934-35, Dr. Nakaya took about 3,000 photographs of snow crystals in the field at temperatures below -10°C and classified the crystal shapes. **Table 4.1** specifies ice crystals by their shape: Category, Subcategory, and Frequency (frequent, moderate, infrequent and rare). **Figure 4.2** illustrates the various crystal shapes. Dr. Nakaya: "Observations were conducted in Sapporo and at Mount Tokachi over 54 days of snowfall, totaling 974 observation sessions. The clear conclusion from this extensive data is that almost all snowfall consists of a mix of different crystal types. The beautiful hexagonal snowflakes that we often imagine make up only a small part of natural snowfall. In reality, snow comes

in many diverse shapes.”⁴⁻⁴⁾

The author sees in this field research the essence of Dr. Nakaya’s dedication to his work.

Table 4.1 Snow crystal categories, subcategories, and frequency of appearance.⁴⁻⁴⁾

No.	Category	Subcategory	Frequency
I	Needle	Single needle	low
		Needle aggregates	low
II	Prismatic	Single prism	low
		Prism aggregates	low
III	Plate	Regular hexagon	high
		Three-dimensional hexagon	high
		Three-dimensional radiating form	high
		Binary nucleus crystal	medium
		Deformed crystal	medium
IV	Prism-plate combination	Drum-shaped	medium
		Twelve-sided flower form	rare
		Plate-bullet combination	low
V	Side crystals	—	rare
VI	Crystals with cloud particles	Crystals with cloud particles	high
		Thick plate	medium
		Graupel-like snow	high
		Graupel	high
VII	Amorphous form	—	medium

3) World’s First Artificial Snow Crystals

Dr. Nakaya documented the process of creating the world’s first artificial snow crystals in his book *Yuki* [Snow],⁴⁻⁴⁾ in the chapter “Making Snow.” The artificial snow-making apparatus developed by him is shown in Fig. 4.3. Below is an excerpt detailing the moment of success in artificial snow crystal production:⁴⁻⁴⁾

While the conditions for the formation of frost and snow crystals are nearly identical, frost forms on solid surfaces, such as the ground, that add an additional thermal influence. In the case of artificial snow, it was necessary to approximate the conditions under which natural snow forms, specifically, floating in the atmosphere. Replicating the multi-hour descent of snow from the sky within a confined laboratory was impractical, so I devised a method to simulate this state.

The initial approach involved using fine fibers to attach the nucleus of the crystal at a single point, allowing it to develop from there—essentially suspending the snow crystals as if on a spider’s web. Implementing this method, I set up the apparatus in a low-temperature chamber, hung the fibers, and introduced warm water vapor. However, the fibers became encrusted with frost crystals, resembling caterpillars, which posed a significant challenge. Therefore, it became necessary to attach ice crystals to a single point on the fiber and grow snow crystals from that point

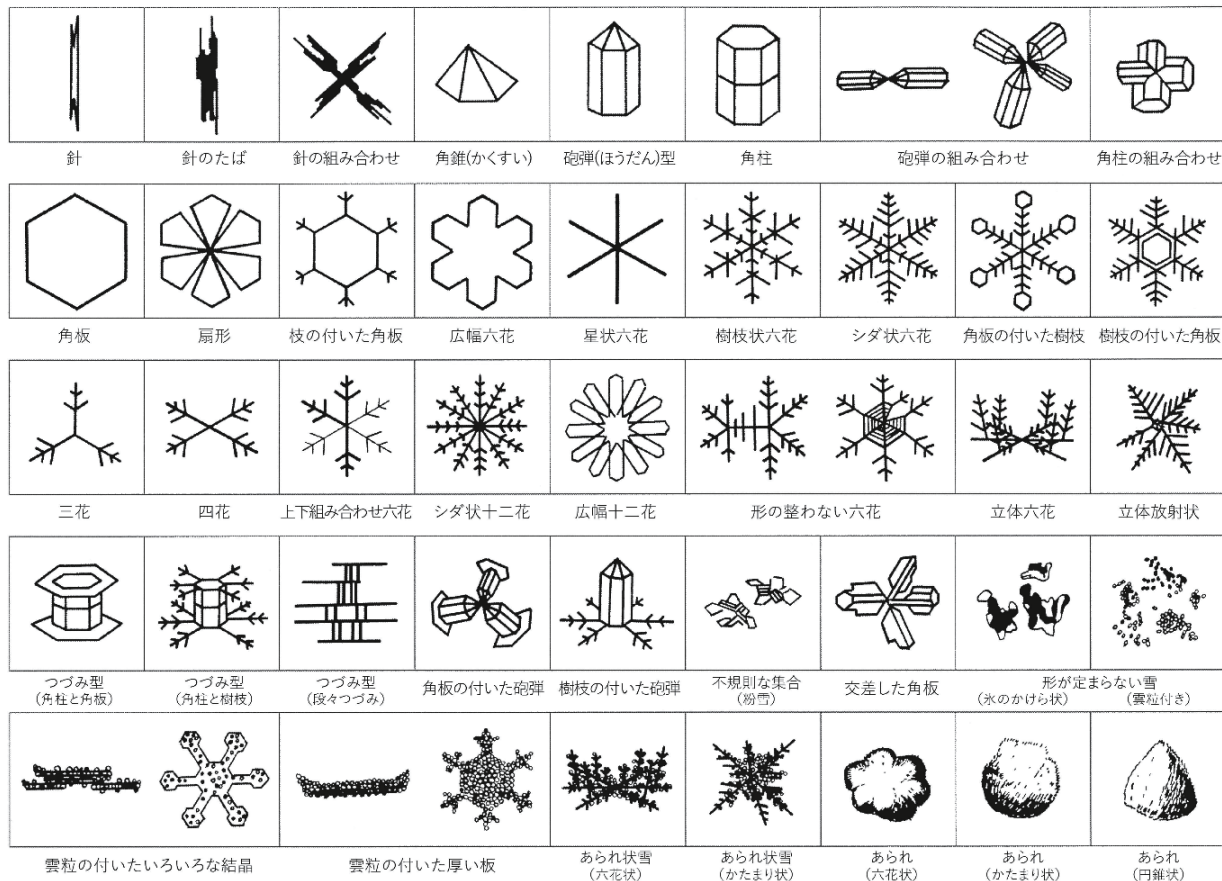


Fig. 4.2 Sketches of the various crystal shapes: Illustrated by Dr. Nakaya.⁴⁻²⁾

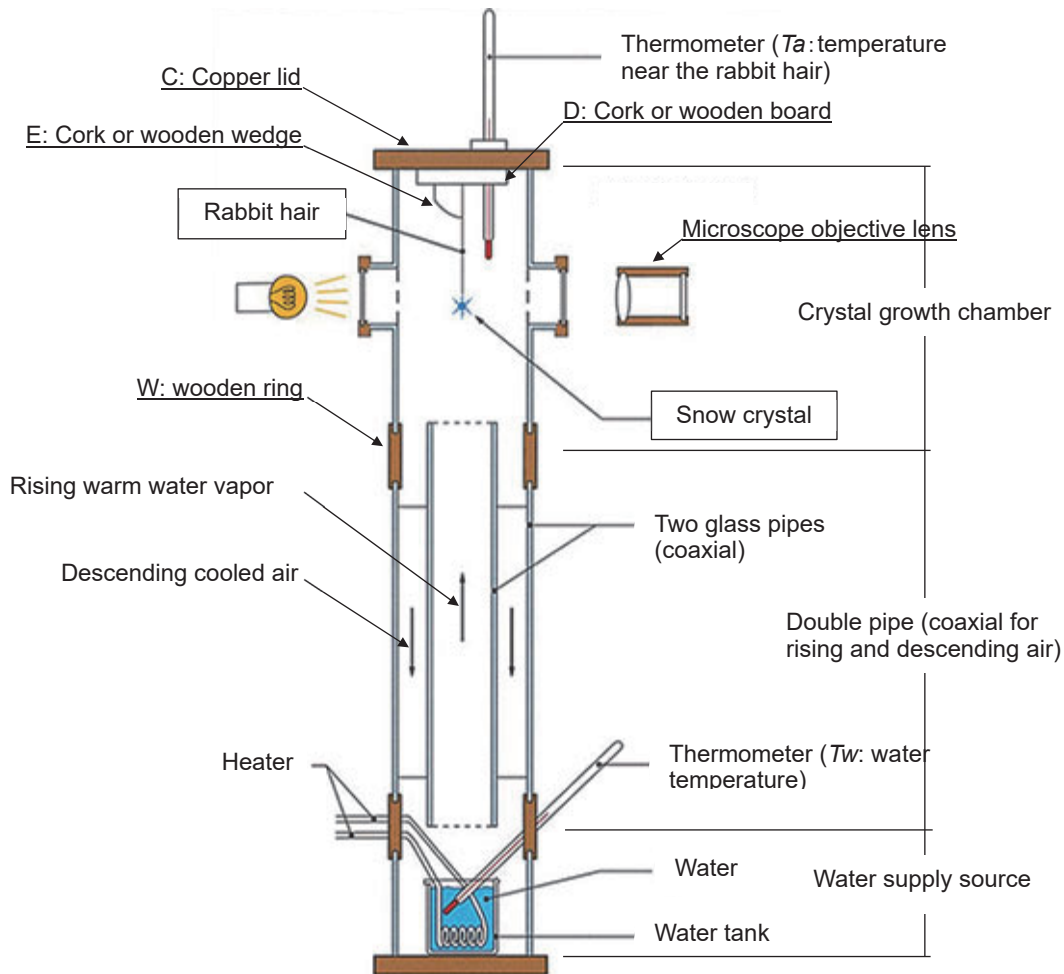


Fig. 4.3 Artificial snow crystal production apparatus (approx. 1 m in height): created by Dr. Nakaya (additional notes by author).⁴⁻²⁾

while preventing frost formation on the rest of the fiber.

At first, achieving this precise control seemed impossible, but through persistent experimentation, I discovered an effective solution: using extremely fine rabbit hair. The rationale behind the efficacy of rabbit hair is discussed in detail later, but essentially, under optimal conditions, rabbit hair facilitated the formation of perfect snow crystals. These conditions involved thoroughly drying the rabbit hair and gradually raising the water temperature from an initially low setting.

By meticulously adjusting the water temperature, I succeeded in producing snow crystals identical to natural hexagonal snowflakes, as well as various other forms, such as hexagonal plates, columns, and bullet shapes. (trans. by author)

4) Artificial Snow Crystal Production Apparatus

The details of Dr. Nakaya's device (see Fig. 4.3) to create artificial snow crystals are described below.

- a) The device consists of three main parts: a moisture supply source at the bottom, a coaxial double (glass) pipe system for ascending and descending airflow, and a crystal growth chamber.
- b) Warm water vapor rises through the inner pipe, while

cooled air descends between the two glass pipes, creating a convective flow.

- c) In the figure, C represents a copper plate lid with either a cork or wood plate (D) attached to the inside surface. The cork (or wood) plate (D) minimizes direct contact between the air circulating inside the crystal growth chamber and the cold copper plate. The presence of plate D significantly affects the temperature T_a at the crystal growth site.
- d) The wedge E is made of copper or wood. This use of different materials for E and D introduces additional adjustment factors for varying the temperature (T_a) near the rabbit hair, allowing the creation of various types of crystals.
- e) The crystal shape is primarily determined by the room temperature (T_r) and water temperature (T_w), but the thermal conditions around the crystal growth site also have a considerable secondary influence.
- f) W is a wooden ring that allows the upper section of the outer glass pipe to be removed. By shortening the upper pipe, the crystal growth site (the tip of the rabbit hair) can be positioned closer to the warm water vapor outlet, increasing the vapor supply under the same room and water temperatures. Conversely, the upper pipe can be

extended, demonstrating that the convective state of the water vapor affects the crystal shape.

As Dr. Nakaya stated: “With this setup, artificial snow could be created at any time. By varying the chamber’s environmental condition, water temperature, and device configuration, approximately 700 types of crystals were produced and photographed under a microscope.”⁴⁻⁴⁾ (trans. by author)

Dr. Nakaya’s work underscores the importance of design, ingenuity, and ideas in test apparatuses for research purposes. The passion of the researchers in creating snow crystals led to the development of a groundbreaking test device. Indeed, enthusiasm is the mother of invention.

5) Nakaya Diagram

The famous Nakaya Diagram (Fig. 4.4) classifies snow crystal shapes based on temperature (horizontal axis) and supersaturation with respect to ice (vertical axis, defined as the ratio of measured moisture content to the saturated vapor density of ice). In a practical sense, snow crystals reaching the ground can be thought of as conveying messages, i.e., information about the temperature and moisture content of the clouds high above.

Regarding the vertical axis of Supersaturation, some have raised a question: How can clouds become supersaturated (i.e., above the saturation level) with water if the clouds are composed of tiny water droplets? Supersaturation above the water saturation level seems impossible. For a detailed discussion on this topic, I recommend “Problems of Nakaya’s Diagram and Diffusion Cloud Chamber for Growing Ice Crystals” by Katsutosi Tsushima (2004).⁴⁻⁵⁾

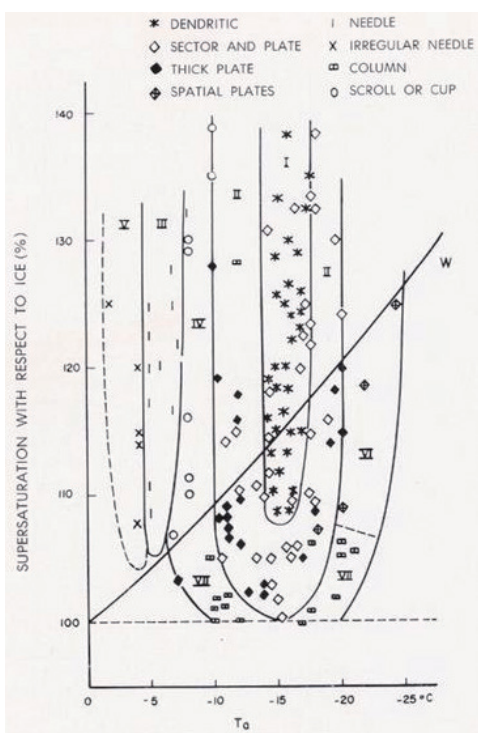


Fig. 4.4 Nakaya Diagram: Identifies type of snow crystal formed as a function of temperature and supersaturation.⁴⁻²⁾

6) Snowflakes as Letters Sent From the Sky

Again, referring to *Yuki* [Snow] from the chapter “Making Snow”:

Snow forms in the upper atmosphere, starting with a central core, and as it descends to the ground, it undergoes various stages of growth in different atmospheric layers, resulting in the complex shapes that reach the surface. By understanding the conditions under which the shapes and patterns of snow crystals are formed, one can deduce the conditions present in the atmosphere from the upper layers to the surface by examining microscopic photographs of the crystals. If we can artificially recreate all types of naturally occurring snow crystals and measure their conditions in the laboratory, we can infer the atmospheric conditions present when such snow falls.

Thus, snow crystals can be seen as letters sent from the sky, with their shapes and patterns written in a cryptic code. Deciphering this code is the essence of artificial snow research.⁴⁻⁶⁾ (trans. by author)

Figure 4.5 is a card handwritten by Dr. Nakaya: “Snowflakes are letters sent from the sky,” accompanied by his own drawing of a snow crystal.

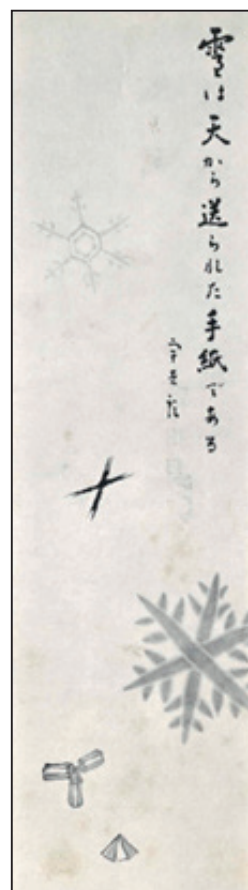


Fig. 4.5 Card handwritten by Dr. Nakaya (author’s photograph; item provided by Sachi Itagaki).

7) Ukichiro Nakaya as a Literary Figure

Dr. Ukichiro Nakaya was not only a highly regarded researcher and educator in the study of snow crystals but also a significant contributor to the study of ice accretion, floods,

permafrost, snowmelt, and the Greenland ice cap. Beyond his scientific achievements, Dr. Nakaya was a prolific writer and artist, leaving behind over 40 works, including essays, critiques, and paintings. Notable works include “Winter Flowers,” “Snow,” “Reminiscences of Torahiko Terada,” and the “Ukichiro Nakaya Art Collection.” He also co-authored several works with prominent figures such as Hideki Yukawa (1907-1981), theoretical physicist Nobel laureate, and Torahiko Terada (1878-1935), physicist and author. His literary contributions were further compiled into collections such as the *Ukichiro Nakaya Essay Collection* (three volumes) published by Asahi Shimbun and the *Ukichiro Nakaya Collection* (eight volumes) published by Iwanami Shoten. Remarkably, he also founded Nakaya Laboratory Production (the precursor to Iwanami Film Production) with participants like Isamu Kobayashi (later president of Iwanami Shoten) and Susumu Hani (later a film director). They produced outstanding educational and scientific documentary films, including *Convex Lenses*, *Frost Flowers*, and *The Snow of Mt. Daisetsuzan*.

Dr. Nakaya was an outstanding scientist and a distinguished literary figure. **Figure 4.6** shows a calligraphy work by Dr. Nakaya intricately drawn with scientific precision.



Fig. 4.6 Dr. Ukichiro Nakaya, *Kochu Tenchi Ari* (World in a Container): Calligraphy on colored paper (author’s photograph; item provided by Fujiko Nakaya).

4.2 Yoshimitsu Kubo: Ice Engineering

1) Introduction to Ice Engineering

In September 1980, a pioneering engineering book—*Introduction to Ice Engineering*⁴⁻⁶⁾ (**Fig. 4.7**)—was published by Tairyusha (Japan). The author, Dr. Yoshimitsu Kubo, was born in Kagawa Prefecture in 1912. After graduating from the Department of Civil Engineering at Tokyo Imperial University, he worked as an engineer for the South Manchuria Railway Company. Post-WW2, he served in various government agencies including the Ministry of Transport, the Economic Stabilization Board, and the Board of Audit before becoming an executive at Japan Bridge & Structurer Institute, Inc. Dr. Kubo is recognized as a pioneer in ice engineering. The pref-

ace to his book contains the following passage:

When discussing the relationship between ice and civil engineering, the primary focus would be on train and vehicle transportation over frozen rivers and lakes during winter. Notable historical examples include the ice train operation on Lake Baikal during the Russo-Japanese War in 1904 and the ice road vehicle transport on Lake Ladoga behind Leningrad during WW2 in 1942. Naturally frozen ice sheets are used as scaffolding for construction of river structures. Permafrost, also useable, presents various challenges. In the Arctic Ocean, ice is used for aircraft landings. Recently, with the discovery of oil in the northern seas of Alaska and Canada, the use of Arctic ice sheets for drilling operations has gained attention, along with the issues of icebreaker ships and ice sea transportation. To effectively utilize natural ice sheets, it is essential to understand the formation, physical and mechanical properties, and load-bearing capacity of river and sea ice.

In 1938, a comprehensive study on the freezing and use of rivers began, primarily for train operations on frozen rivers. At that time, I was part of the Construction Bureau Planning Section of the South Manchuria Railway and was responsible for this research [author note: Dr. Kubo was 26 years old at the time]. Starting from scratch, with no reference literature available, the research began in a state of complete uncertainty. It was by visiting Dr. Sakuhei Fujiwara at the Faculty of Science, Tokyo Imperial University, during a business trip that my ice research started.⁴⁻⁶⁾ (trans. by author)

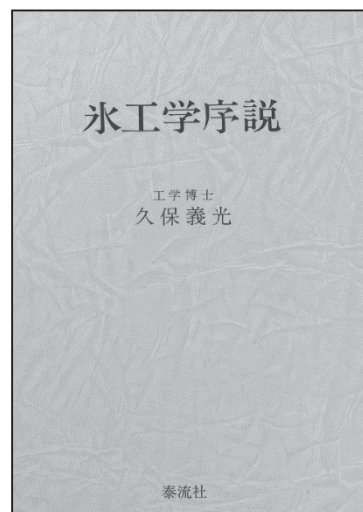


Fig. 4.7 *Introduction to Ice Engineering*, Dr. Yoshimitsu Kubo.⁴⁻⁶⁾

Before *Introduction to Ice Engineering*, books on the crystallographic structure and properties of ice from a scientific perspective had been published, but this book is considered the first in Japan to approach the topic with an engineering viewpoint. With a particularly detailed examination of the load-bearing capacity of ice sheets tested through ice track train operations, the book covers the following topics that are of great importance for engineering evaluations:

- I. Formation of Natural Ice Sheets
- II. Mechanical Properties of Ice
- III. Ice Track Train Operations and Other Tests
- IV. Load-Bearing Capacity of Natural Ice Sheets
- V. Ice-Breaking and Load-Bearing Capacity of Sea Ice
- VI. Ice Terminology
- VII. Overview of International Conferences

2) Ice Track Train Operations: Second Songhua River, Manchuria

From autumn 1939 to spring 1941, Dr. Kubo conducted ice track train operation tests over two winters on the Second Songhua River between Changchun and Harbin in northern Manchuria, China. The goal was to lay tracks on the frozen river and operate trains, but this required thorough preliminary studies that included observations of freezing and thawing, ice thickness measurements, mechanical property tests of the ice, and various load tests on the river ice sheets. The ice track train operation test conducted in February 1941 was later featured on the cover of the 1976 issue of *ICE*, the journal of the International Glaciological Society (IGS) (Fig. 4.8).

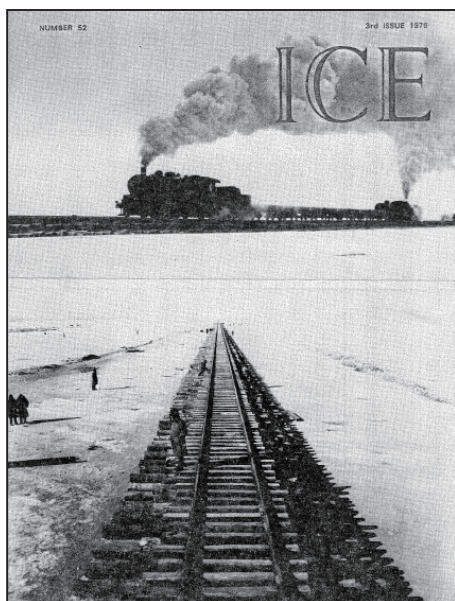


Fig. 4.8 Cover, *ICE* (journal of IGS, 1976 issue): Ice track train operation test, 1941.⁴⁻⁶⁾

The observations and tests listed below were conducted on the Songhua River: Note that Dr. Kubo’s research team meticulously planned and executed these tests within a limited two-winter testing period. The ice sheet bomb drop test, testing the impact on ice sheets, was likely conducted because the Second Sino-Japanese War began in 1937 (continued until 1945).

- i) Investigation of environmental conditions
 - Freezing and thawing conditions
 - Air temperature, water temperature, ice temperature
 - River flow velocity, water depth, ice thickness
- ii) Mechanical tests of ice
 - Tensile strength, compressive strength, bending strength, shear strength, torsional strength

- iii) Ice sheet load tests (static loads)
 - Ice sheet sandbag load test (Fig. 4.9)
 - Ice sheet-rail pile load test (Fig. 4.10)
 - Ice sheet pile load test (refer to the next sub-section, 3)
- iv) Ice sheet moving load test (dynamic loads) (Fig. 4.11)



Fig. 4.9 Ice sheet sandbag load test (in situ), photograph: Examined effect of load weight (max. load 40 t) and loading time (4-8 hours) on naturally frozen ice sheets with thicknesses of 34-98 cm—sandbags (30 kg each).⁴⁻⁶⁾



Fig. 4.10 Ice sheet-rail pile load test, photograph: Test table (four pine log legs, each 30 cm diameter) with 60 t load placed on ice sheet (70 cm thick)—Examined amount of subsidence and the condition of cracks in the ice sheet.⁴⁻⁶⁾

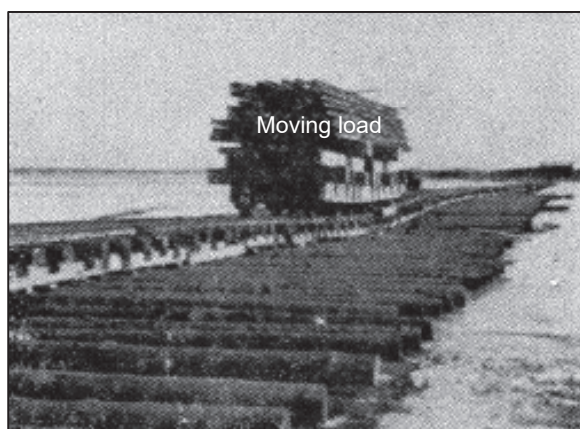


Fig. 4.11 Ice sheet moving load test (i.e., dynamic loading), photograph: Test track laid on the ice sheet—Load simulating the weight of a train moved across to examine the impact on the frozen sheet (conducted as a precursor to operation tests with locomotives and freight cars).⁴⁻⁶⁾

- v) Ice sheet bomb drop test (impact load)
- vi) Ice track train operation test (refer to sub-section 4)

3) Ice Sheet Pile Load Test: Adfreeze Bond Between Log Pile and Ice

This test evaluated the adfreeze bond strength between vertically placed logs (log piles) and in situ river ice. Four rough-hewn white pine logs, each 30 cm in diameter and 2 m long, were joined at the top to form a platform-like structure shown in Fig. 4.12. The four legs of this structure were inserted into pre-drilled holes in the ice sheet and re-frozen. Loads up to 60 t were placed onto the top of this test platform, with the load at failure used to determine the adfreeze bond strength between the logs and the ice sheet—diagram of test setup in Fig. 4.13.

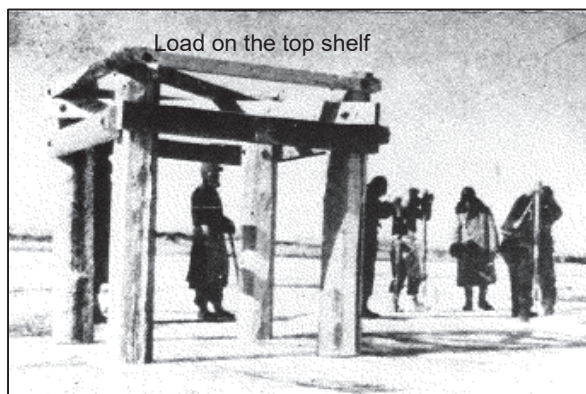


Fig. 4.12 Adfreeze bond strength test between log pile and ice sheet, photograph: Four logs (legs of test platform) inserted into pre-drilled ice sheet and re-frozen into place, loads up to 60 t.⁴⁻⁶⁾

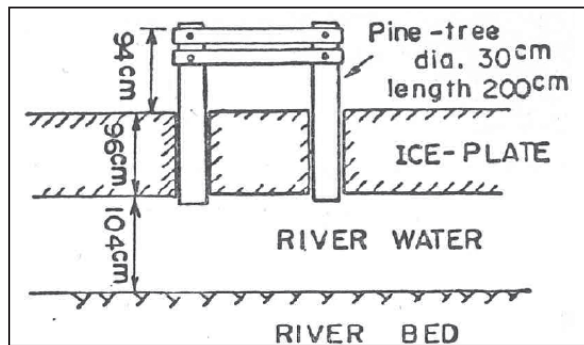


Fig. 4.13 Diagram: Adfreeze bond strength test between log pile and ice sheet.⁴⁻⁶⁾

Based on the results of these experiments and using the air temperature to estimate the ice temperature, Dr. Kubo estimated that the adfreeze bond strength between the ice and the logs was 1.8 kg/cm² (0.18 MPa) under the following conditions: -4°C ice temperature, 86.5 cm ice thickness, and 30 cm log diameter (see formula below). Note, this strength refers to the strength measured when logs are pushed through the ice by applying a (vertical) load from above.

$$f = \frac{\frac{1}{4} \times 60,000}{30\pi \times 86.5} = 1.84 \text{ kg/cm}^2$$

4) Ice Track Train Operation Test

After repeatedly conducting mechanical tests on the local river ice to thoroughly understand the condition of the ice sheet, a rail track was laid on the frozen surface of the Songhua River. Between February 3 and 26, 1941, a total of 162 ice track train operation tests were carried out.

Logs with diameters of 20 to 35 cm were arranged in four layers, as shown in Figs. 4.14 and 4.15, photograph and diagram, respectively. This arrangement of logs helped to distribute the train load on the ice sheet and to absorb the vibrations produced by the passing train. The height of the rail surface above the ice sheet surface was about 140 cm.

Two parallel tracks for the train operation tests were laid 100 m apart (refer to Fig. 4.8): Track 1 and Track 2 extending 437 and 386 m on the ice, respectively. Each end of the ice

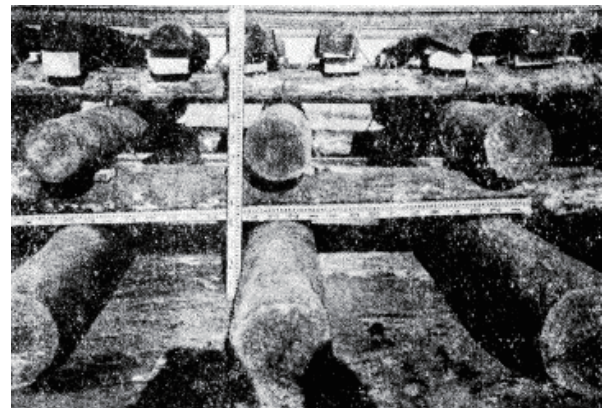


Fig. 4.14 Ice track structure photograph: Logs arranged both parallel and perpendicular to and under the rails and sleepers, photograph.⁴⁻⁶⁾

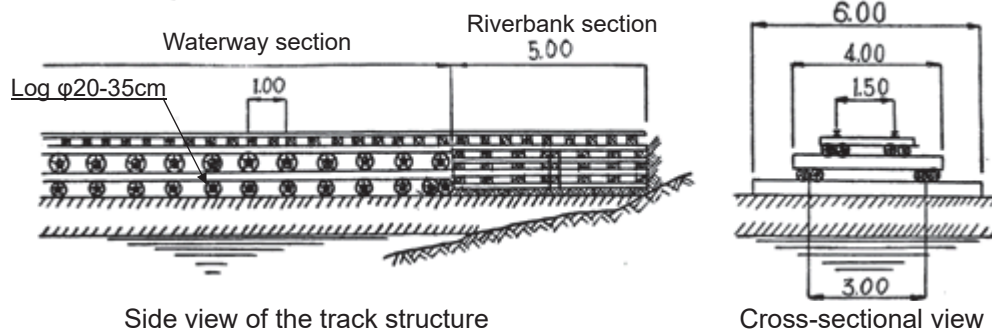


Fig. 4.15 Diagram of the ice track structure.⁴⁻⁷⁾

tracks connected to several hundred meters of land track on either bank of the river. The locomotives used in the tests were a DB1-type (total locomotive weight about 90 t) and a Mikaro-type (total locomotive weight about 140 t). As shown in **Fig. 4.16**, at the end of the tests, the Mikaro-type locomotive hauled 20 freight cars, each weighing 30 t, back and forth on the ice. During the testing period, the ice thickness was 90 to 95 cm, and the average train speed was 10 to 30 km/h.

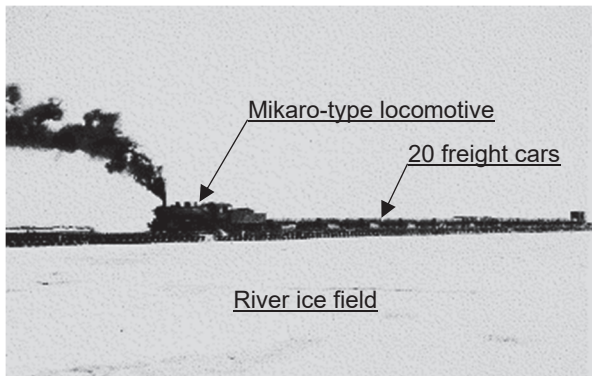


Fig. 4.16 River ice track running test with Mikaro-type locomotive and 20 freight cars, photograph.⁴⁻⁶⁾

From the train operation tests, Dr. Kubo derived the following conclusions regarding the subsidence and cracking of the ice sheet:

i) Ice Sheet Subsidence

- a) For smaller locomotives like the DB1-type (about 90 t), increasing the number of freight cars above 2-3 does not increase the ice sheet subsidence. For larger locomotives like the Mikaro-type (about 140 t), the subsidence does not increase beyond 1-2 cars.
- b) Pushing operations cause greater maximum subsidence than pulling operations.
- c) Higher train speeds result in smaller maximum subsidence but greater maximum uplift, at least for speeds below 20 km/h.
- d) The subsidence and uplift caused by the train load propagate in all directions around the train, taking some time to spread beyond 300 m. However, the main area of subsidence is within 50 m of the train.
- e) After the train passes, the ice sheet under the track oscillates with a period of about one minute, with maximum displacements of about 5 cm, but this movement rapidly diminishes within 3-5 minutes, returning the ice sheet almost to its original level.
- f) When the subsidence of the ice sheet becomes sufficiently large, the range of subsidence remains constant. Therefore, the gradient of the ice sheet surface increases, i.e., the rail surface (in the direction of the track) becomes steeper, possibly affecting locomotive traction. If the maximum allowable gradient of the track is assumed to be 1.5%, then a height difference greater than 30 cm over a 20-meter section of the track would require special attention.

g) During the tests, the maximum subsidence observed was about 30 cm.

ii) Ice Sheet Cracking

- a) Large cracks may develop parallel to the track, either along or near the center line under the track.
- b) Moderately large cracks appear on the surface of the ice sheet adjacent to the track at an angle of about 30 degrees.
- c) Cracks may also form within the ice sheet under or beside the track.

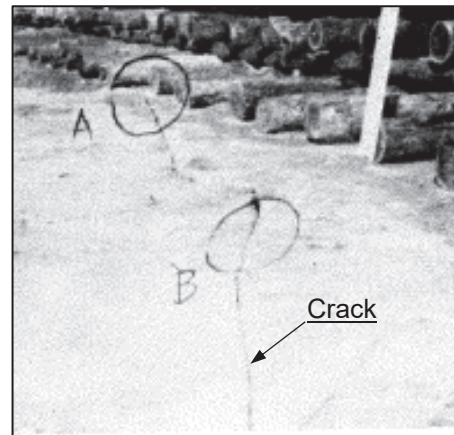


Fig. 4.17 Ice sheet cracking photograph: Cracks, angle of approx. 30 degrees to the track direction in the adjacent area, photograph.⁴⁻⁷⁾

5) Subsequent Research

Dr. Kubo's field tests were conducted over just two winters, but with meticulous planning and adequate personnel and resource support, the results confirmed the practicality of ice track operations. The field tests concluded in March 1941, and by December, the Second Sino-Japanese War escalated into WW2. There is no evidence that the research findings were put into practical use at that time. However, Dr. Kubo's research being featured on the cover of the International Glaciological Society's journal *ICE* in 1976 and the publication of his *Introduction to Ice Engineering* in 1980 led to a reevaluation of his work.

4.3 Tadashi Tabata: Drift Ice Studies

1) Symposium on the Okhotsk Sea & Polar Oceans

On February 12, 1986, the International Symposium on the Okhotsk Sea & Polar Oceans (held in Mombetsu City, Hokkaido) commemorated the 20th anniversary of the establishment of the Drift Ice Research Facility (affiliated with Hokkaido University's Institute of Low Temperature Science) in Mombetsu City in 1965 as well as honored the late Professor Tadashi Tabata. Dr. Tadashi Tabata (1923-1981) played a leading role in drift ice research as the director of this research facility from its inception until his passing. This symposium

has been held annually in Mombetsu since then, with the 38th in 2024 (2021 was canceled due to COVID-19). Despite being held in a small city facing the Sea of Okhotsk, it has become a significant international event where participants from around the world gather to discuss the Sea of Okhotsk and sea ice.

As the first symposium in 1986 was also a memorial tribute for Dr. Tabata, the gathering featured researchers from around the world who had connections with him. The author attended this symposium and still vividly remembers the opening ceremony. Among those in the ceremony paying tribute to Dr. Tabata were Dr. Wilford F. Weeks (then professor, University of Alaska, Fairbanks) on double bass and Dr. Vera Alexander (University of Alaska, Fairbanks) on piano in a performance to his memory with Dr. Tabata's portrait displayed on the stage.

2) Drift Ice Research Facility: Establishment and Regional Contribution

Dr. Tadashi Tabata, in his book *Ryuu-hyo* (Drift Ice)⁴⁻⁸ (1978), **Fig. 4.18**, wrote the following in the preface titled "Encounter":

The first time I saw the drift ice in Abashiri, it was magnificent. The rugged ice fields, covered slightly with snow, stretched as far as the eye could see. The Shiretoko mountain range was clearly visible to the east, with Mount Shari majestically at the end. The gaps between the stacked ice were a deep cobalt blue, captivating anyone who saw it. There were rounded ice hummocks, thick ice sheets standing like sails, and piles of thin ice fragments forming mountains over two meters high. The ice was various shades, some whitish, some relatively transparent with a bluish tint. Snow concealed the cracks in the ice, sometimes making it treacherous to walk. The world was silent, with only the faint sound of the wind. The pleasure of sitting behind a tall ice block and taking a break was immense. The impression left by the drift ice was profound. (trans. by author)

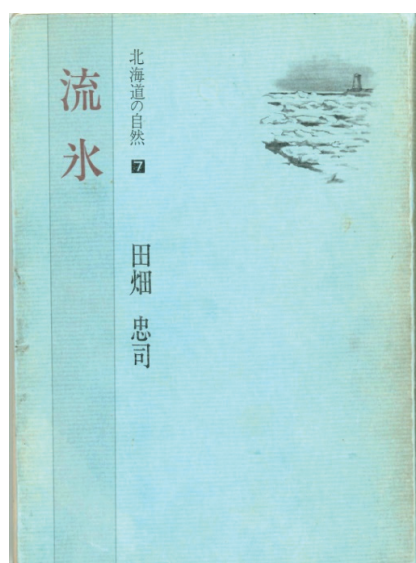


Fig. 4.18 *Ryuu-hyo* (Drift Ice), Dr. Tadashi Tabata, photograph.⁴⁻⁸⁾

The Sea of Okhotsk is a somewhat elongated sea, approximately 2,000 km in length. About 80% (varies yearly) of its surface freezes in winter, with thick drift ice covering even the southernmost parts from mid-January to late March. Within this southernmost area of the Northern Hemisphere to feature nearly solid sea ice cover, there is a transitional zone between the densely packed drift ice and the open sea that is a band of broken ice known as the marginal ice zone (MIZ). Other regions where MIZs exist include the eastern coast of Canada, the Barents Sea, and the Baltic Sea, but the Sea of Okhotsk coast of Hokkaido is the lowest latitude MIZ in the world. As such, it is a relatively warm area for a frozen sea, with thinner ice and more dynamic (unstable) movements compared to other MIZs.

In 1965, the Drift Ice Research Facility was established in Mombetsu City, the southernmost point for drift ice in the Northern Hemisphere (**Fig. 4.19**). Dr. Tadashi Tabata, who played a crucial role in its establishment, served as its first director until his death in 1981.



Fig. 4.19 Drift Ice Research Facility, Mombetsu, est. 1965, photograph.⁴⁻⁹⁾

Dr. Tabata, as a scientist and engineer, conducted a wide range of research from basic science to applied engineering, extending beyond drift ice to include studies on ice accretion on ship hulls and the mechanical properties of sea ice. Ice accretion occurs when seawater spray freezes onto a ship's hull, raising its center of gravity to increase the risk of capsizing. As a counter measure, Dr. Tabata investigated coatings that were both durable and resistant to ice accretion. His mechanical studies on sea ice included research on its elasticity, compressive strength, bending strength, and the coefficient of friction between sea ice and various materials, earning him international recognition.

3) From C-Band to X-Band Doppler Radar

Together with the opening of the Drift Ice Research Facility, the world's first radar system (C-band) dedicated to observing drift ice was being installed. Over three years, radar antennas were set up in Mombetsu, Abashiri, and Esashi, creating a C-band wide-area drift ice observation radar network that monitored the movement of drift ice along approximately 60 km of the Hokkaido coast of the Sea of Okhotsk, day and

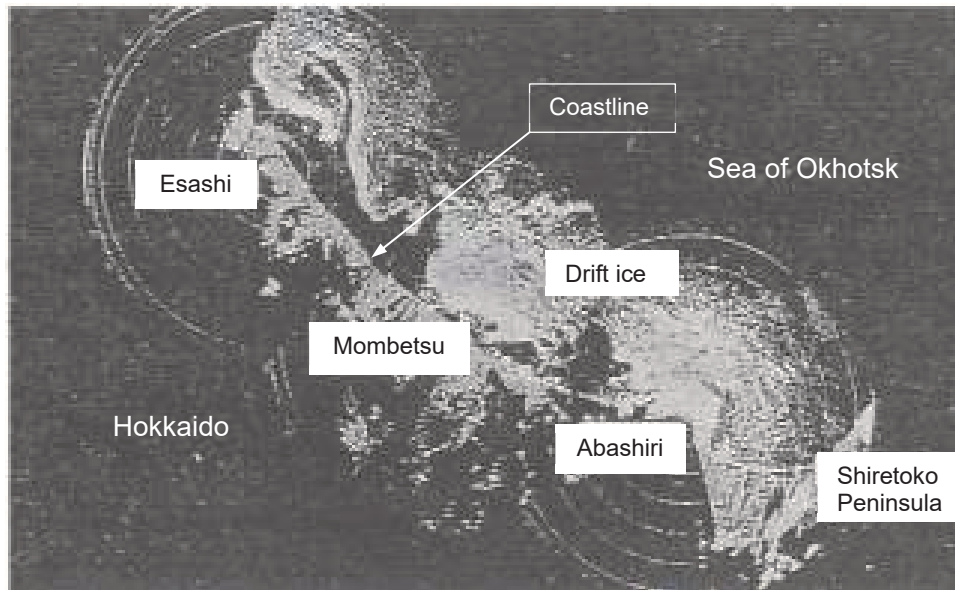


Fig. 4.20 C-band wide-area drift ice observation radar network, Hokkaido coast of the Sea of Okhotsk, photograph.⁴⁻¹⁰⁾

night, regardless of the weather (Fig. 4.20). This permitted detailed studies corresponding radar data to actual ice conditions, such as the behavior of coastal drift ice, including detailed observations of ice distribution. Research on the physical properties of sea ice was enhanced by incorporating radar data. Additionally, studies on the formation and movement of drift ice, as well as meteorological and oceanographic research, particularly on the variations and physical mechanisms of the Soya Warm Current region, were initiated.⁴⁻¹⁰⁾

The radar data was invaluable not only for research on the movement and deformation of drift ice but also for preventing maritime accidents. The fishing vessels operating in coastal waters were primarily the ones affected by drift ice. These vessels often operate just before the drift ice arrives or as soon as the ice begins to recede, sometimes navigating within ice floes and getting trapped. Consequently, the number of maritime accidents used to roughly correlate with the amount of coastal drift ice. After the establishment of the radar network, drift ice distribution maps, created every morning from radar data and distributed to relevant organizations like the Japan Coast Guard, ensure the safety of navigation and fishing, significantly contributing to regional economic activity and maritime safety. These numerous observation and research achievements garnered international attention, leading to the installation of similar drift ice radars in Alaska, Canada, and the Baltic Sea, establishing a globally influential role for the facility.⁴⁻¹⁰⁾

With Hokkaido University's transition from a public to an independent institution, the Drift Ice Research Facility was closed in 2004. However, in November 2005, an X-band Doppler radar facility was installed at the summit of Mt. Ōyama in Mombetsu City (Fig. 4.21). This marked the world's first use of this type of radar for observing sea ice and snow clouds. Compared to C-band radar, X-band radar has a smaller observation range but offers a higher operating frequency and thus, resolution. This radar is used to analyze the movement of drift

ice and clouds (both rain and snow producing), as well as upper wind direction, by measuring the difference in frequency between the transmitted radio waves and those reflected back by objects (Doppler effect). Research groups from the Institute of Low Temperature Science (Hokkaido University) and the Meteorological Research Institute (Japan Meteorological Agency) use this radar to detect ice fields regardless of weather conditions, providing high precision information about the movement of drift ice.



Fig. 4.21 X-Band Doppler Radar, installed at the summit of Mt. Ōyama in 2005, Mombetsu City, photograph.⁴⁻¹¹⁾

In the Sea of Okhotsk, the timing of drift ice arrival and departure, as well as ice volume, fluctuates significantly. Also, the relatively recent rapid decline of Arctic sea ice and its potential impacts on global climate change are alarming. With the possibility of a regular Northern Sea Route between Europe and East Asia becoming a reality and the oil and gas production off Sakhalin expanding, the importance of the drift ice research initiated by Dr. Tabata along the Hokkaido coast of the MIZ is increasingly evident.

4) Mombetsu: Drift Ice Research City

Dr. Masaaki Aota (1938-2012), who succeeded Dr. Tabata as director of the Drift Ice Research Facility in 1981, worked tirelessly to involve Mombetsu citizens in the research. As a result, Mombetsu (population about 24,000) declared itself an “International City of Drift Ice Research” as an important long-term program in the city’s evolving development plans starting in 1989. In 2024, the International Symposium on the Okhotsk Sea & Polar Oceans marked its 38th session. Each year, renowned researchers from both domestic and international institutions gather with the support of citizen volunteers, creating a unique, familial atmosphere not often felt at other international symposiums—a good example of how the establishment of a research facility and its achievements can bring about urban revitalization and internationalization.

4.4 Conclusion

This chapter has highlighted the pioneering figures in Japanese snow and ice research: Dr. Ukichiro Nakaya, Dr. Yoshimitsu Kubo, and Dr. Tadashi Tabata. A common thread in their work is the emphasis on field observations and experiments: A principle that could be characterized as “field-work-based research.” Their contributions were not only scientifically significant but also shared widely with society, with continuing international relevance. Moreover, they were educators who nurtured many successors in their fields.

In 1936, Dr. Ukichiro Nakaya successfully created the world’s first artificial snow crystal at Hokkaido Imperial University. Later, he evaluated and introduced Dr. Yoshimitsu Kubo’s research on ice-covered tracks to the public. In 1952, Dr. Nakaya joined SIPRE (later CRREL) as a researcher and laid the foundation of the institute, as noted below in Addendum 2. Dr. Kubo’s report, even after 40 years, has been preserved and utilized by snow and ice researchers at Hokkaido University and CRREL in the United States. In the 1980s, Japanese researchers and corporate engineers conducted research at CRREL, contributing to the development of ice engineering in Japan and the design and construction of ice-related structures.

Many other pioneers have also contributed significantly

to the advancement of snow and ice research. Their accumulated efforts have led to Japan’s current global leadership in this field. While we have focused only on a few key figures, it is important to acknowledge the contributions of other notable researchers like Dr. Daisuke Kuroiwa (snow and ice physics)(1916-1983) and Dr. Seiichi Kinoshita (permafrost physics)(1924-2003). The author regrets not covering all their achievements in this chapter.

References

- 4-1) Nakaya Ukichiro Museum of Snow and Ice. (n.d.). *Ukichiro Nakaya (1900-1962)* [trans. from Japanese].
<https://yukinokagakukan.kagashi-ss.com/ukichiro/>.
- 4-2) Provided by Nakaya Ukichiro Museum of Snow and Ice.
- 4-3) Nakaya, U. (1954). *Snow Crystals: Natural and Artificial*. Harvard University Press, Cambridge. ISBN-10:0674182758.
- 4-4) Nakaya, U. (1938). *Yuki* [Snow]. Iwanami Shinsho. ISBN 9784004000044. (in Japanese).
- 4-5) Tsushima, K. (2004). Problems of Nakaya’s Diagram and Diffusion Cloud Chamber for Growing Ice Crystals. *TENKI, Journal of the Meteorological Society of Japan, Vol. 51, No. 10, 753-758*. (in Japanese).
- 4-6) Kubo, Y. (1980). *Introduction to Ice Engineering*. Tairyuusha. (in Japanese).
- 4-7) Kubo, Y. (1959). Engineering Applicability of Ice Sheets. *SEPPYO, Journal of the Japanese Society of Snow and Ice, Vol. 21, No. 4, 99-105*. (in Japanese).
- 4-8) Tabata, T. (1978). *Ryuu-hyo* [Drift Ice]. Hokkaido Shimbun Press. (in Japanese).
- 4-9) Hokkaido University: Mosir Project. (2002, July 9). *A Collection of Links* [trans. from Japanese].
<https://www.ep.sci.hokudai.ac.jp/~mosir/work/2002/clione/links/>.
- 4-10) Shirasawa, K. (1992). Sea Ice Research Laboratory, Institute of Low Temperature Science, Hokkaido University. *TENKI, Journal of the Meteorological Society of Japan, Vol. 39, No. 6, 50-52*. (in Japanese).
- 4-11) Hokkaido University: CoSTEP. (2013, June 18). *#18 Find the Drift Ice Accurately and Catch the Movement* [trans. from Japanese].
https://costep.open-ed.hokudai.ac.jp/like_hokudai/article/1140.

– Addendum 2 –

Dr. Ukichiro Nakaya: Continuing Snow and Ice Research

1) Japan-U.S. Collaboration in Snow and Ice Research

In 1952, Dr. Ukichiro Nakaya was invited to become a researcher at the Snow, Ice and Permafrost Research Establishment (SIPRE) of the U.S. Army Corps of Engineers in Illinois. Established in 1949, the main purpose of SIPRE was to conduct fundamental and applied research on snow, ice, and permafrost. SIPRE was particularly involved in snow and ice research at the U.S. Army's Camp Century in Greenland. During the early stages of the Cold War after WW2, Greenland was a geopolitically significant location for the United States.

Dr. Nakaya, already world renowned as a snow and ice researcher, had previously solved the problem of aircraft icing, considered “the greatest enemy of aviation” during WW2, with research conducted at the summit of Mt. Niseko-Annapuri, Hokkaido. Together with Dr. Nakaya, Drs. Kazuhiko Itagaki and Motoi Kumai (snow and ice studies, Hokkaido University) and Dr. Shunsuke Takagi (mathematics, Tokyo University of Agriculture and Technology) laid the foundation for SIPRE. In 1961, SIPRE evolved into the Cold Regions Research and Engineering Laboratory (CRREL) in Hanover, New Hampshire (see photo below). Today, CRREL conducts research related to U.S. homeland security as well as scientific and engineering studies in the Arctic and Antarctic, welcoming numerous researchers and engineers from around the world as a center for snow, ice, permafrost, and cold regions engineering research.

The collaboration between CRREL and Japan developed further in the 1980s. Researchers such as Dr. Ken-ichi Hirayama (hydraulics, later president and professor emeritus of Iwate University),^[1] Dr. Kazuyuki Kato (ice engineering, then at IHI Corporation, later professor at Kinki University),^[2] Dr. Satoshi Akagawa (permafrost engineering, then at Shimizu Corporation, later professor at Hokkaido University),^[3] and the author (ice engineering, then at Pacific Consultants Co., Ltd.)^[4] conducted research at CRREL. Dr. Devinder S. Sodhi of CRREL later participated in the Joint Ocean Industries Association (JOIA) Ice Load Project^[5] (details later in Chapter 7) and conducted research at the laboratory of Dr. Hiroshi Saeki (then professor and later president of Hokkaido University) in the Department of Civil Engineering at Hokkaido University. The research papers produced during the stays of these researchers at CRREL are listed below.

The connections that Dr. Ukichiro Nakaya initially established with a U.S. research institute in 1952 continued for the following 50 years.



Cold Regions Research and Engineering Laboratory (CRREL), Hanover, New Hampshire, photograph.^[6]

- [1] Hirayama, K. (1983, Mar.). Properties of Urea-doped Ice in the CRREL Test Basin. *CRREL Report*, 83-8.
- [2] Sodhi, D. S., K. Kato, and F. D. Haynes. (1983, Dec.). Ice Force Measurements on a Bridge Pier in the Ottauquechee River, Vermont. *CRREL Report*, 83-32.
- [3] Akagawa, S. (1990, Feb.). X-Ray Photography Method for Experimental Studies of the Frozen Fringe Characteristics of Freezing Soil, *CRREL Special Report*, 90-5.
- [4] Nakazawa, N. and D. S. Sodhi. (1990, May). Ice Forces on Flat, Vertical Indentors Pushed through Floating Ice Sheets. *CRREL Special Report*, 90-14.
- [5] Sodhi, D. S., T. Takeuchi, N. Nakazawa, S. Akagawa, and H. Saeki. (1998, Dec.). Medium-scale Indentation Tests on Sea Ice at Various Speeds. *Cold Regions Science and Technology*, Vol. 28, Issue 3, 161-182. Elsevier.
- [6] US Army Corps of Engineers Engineer Research and Development Center. (n.d.). *CRREL Cold Regions Research and Engineering Laboratory* [photo].

<https://www.erd.c.usace.army.mil/Locations/CRREL/>.

2) Dr. Ukichiro Nakaya and Dr. Yoshimitsu Kubo

In his preface of *Introduction to Ice Engineering*, Dr. Yoshimitsu Kubo shares his memories of Dr. Ukichiro Nakaya in “About Dr. Ukichiro Nakaya.”

At that time, Mr. Shin-ichi Ogawa, one year ahead of me at the Manchurian Railway and with whom I was closely acquainted, moved from the Construction Bureau to the Maintenance Section under Chief Kosaku Takano. They were working on measures to counter frost heaving of railway tracks. Chief Takano and Dr. Nakaya were classmates at the Fourth Higher School [author’s note: one of the preparatory institutions for the Imperial Universities pre-WW2]. Dr. Nakaya visited Manchuria twice in a short period to provide technical guidance on frost heaving countermeasures. Although my own research on river ice was unrelated, Dr. Nakaya took the time to offer his opinion and visit my research site. After returning to Japan, Dr. Nakaya quickly published essays in newspapers about his impressions of Manchuria, in which he generously praised the research attitudes of Mr. Ogawa, myself, and others. I was extremely humbled by this.

As described later, I summarized my initial two years of research in a 608-page report titled *Research on River Ice, Particularly Ice-Covered Tracks*, published in August 1941 under the authority of the Construction Bureau of the Manchurian Railway. Like most printed materials in the railway construction sector at the time, it was classified as “top secret” and limited to 300 copies. In December 1976, I visited Hokkaido University and, at the laboratory of Dr. Akira Higashi in the Department of Applied Physics, encountered report copy No. 252 with Dr. Nakaya’s handwritten notes for the first time in 35 years. Although I have copy No. 247 in my possession, I was delighted to discover that out of the approximately 260 copies distributed in 1941, this No. 252 had been preserved and effectively utilized by the researchers at the Institute of Low Temperature Science at Hokkaido University.

The Cold Region Research and Engineering Laboratory (CRREL) of the U.S. Army Corps of Engineers also holds a copy of this report. In November 1979, I had the profound experience of seeing it again, thanks to Dr. Andrew Assur.⁴⁻⁶⁾ (trans. by author)

5 | Mechanical Properties of Sea Ice

5.1 Process of Ice Sheet Formation

The process of sea ice formation is described below and shown in the photos of Fig. 5.1.⁵⁻¹⁾

- i) Freshwater begins to freeze at 0°C, but seawater starts to freeze at around -1.8°C due to its salt content (the freezing temperature varies depending on the salinity of the seawater and other factors such as snowfall). However, only the freshwater component in seawater freezes, with the salty water either expelled back into the seawater or trapped as liquid within the ice. When additional heat (latent heat) is lost from seawater at -1.8°C, some of the freshwater component crystalliz-

es into what is called “frazil ice,” forming either strip-shaped or needle-shaped crystals (Fig. 5.1a).

- ii) With no wind, waves, or swells on the sea surface, the frazil ice grows slowly. As the frazil ice freezes together, it forms “nilas” (a thin, elastic layer of ice that forms on the surface of the sea by the accumulation of frazil ice) or “ice rind” (a brittle surface layer of ice that spreads and thickens on the sea surface), Figs. 5.1b and 5.1c, respectively.
- iii) With waves and swells present, agitation of the newly formed frazil ice disrupts the bonding process, resulting in the growth of larger, slushy ice masses known as “grease ice” (Fig. 5.1d).
- iv) As patches of grease ice, nilas, and ice rind grow, wave



a) Frazil ice: strip-shaped or needle-shaped crystals.



d) Grease ice: slushy ice masses.



b) Nilas: thin, elastic surface layer of ice.



e) Pancake ice: round formations.



c) Ice rind: spreads and thickens on the sea surface.



f) Young ice: plate-like formations.

Fig. 5.1 Formation process of sea ice, photographs.⁵⁻¹⁾

motion causes collisions with each other that result in rounded patches called “pancake ice.” As the pancake ice coverage across the sea surface grows, the waves gradually calm, and the remaining sea surface between the pancake ice formations freezes (Fig. 5.1e).

- v) If the low temperatures continue, nilas and pancake ice increase in hardness and thickness, becoming plate-like ice known as “young ice.” These ice sheets collide and combine by overlapping due to wind, growing even further (Fig. 5.1f).

5.2 Crystal Forms of Sea Ice

1) Granular Ice and Columnar Ice

The crystal forms of sea ice can be broadly categorized into “Granular Ice” and “Columnar Ice.” Under turbulent water conditions, granular ice is formed from frazil ice and snowfall that accumulate on the sea surface. Columnar ice grows as vertically elongated crystals beneath the layer of granular ice. Therefore, a predominance of a granular structure indicates that the growth of sea ice was significantly influenced more by the growth of frazil ice and snowfall than by freezing from the underside. Conversely, a predominance of a columnar structure indicates that the growth was primarily due to freezing from the underside. The crystal form thus provides crucial information about the growth process of sea ice in a particular area.

Figure 5.2 illustrates the crystal forms of sea ice. From

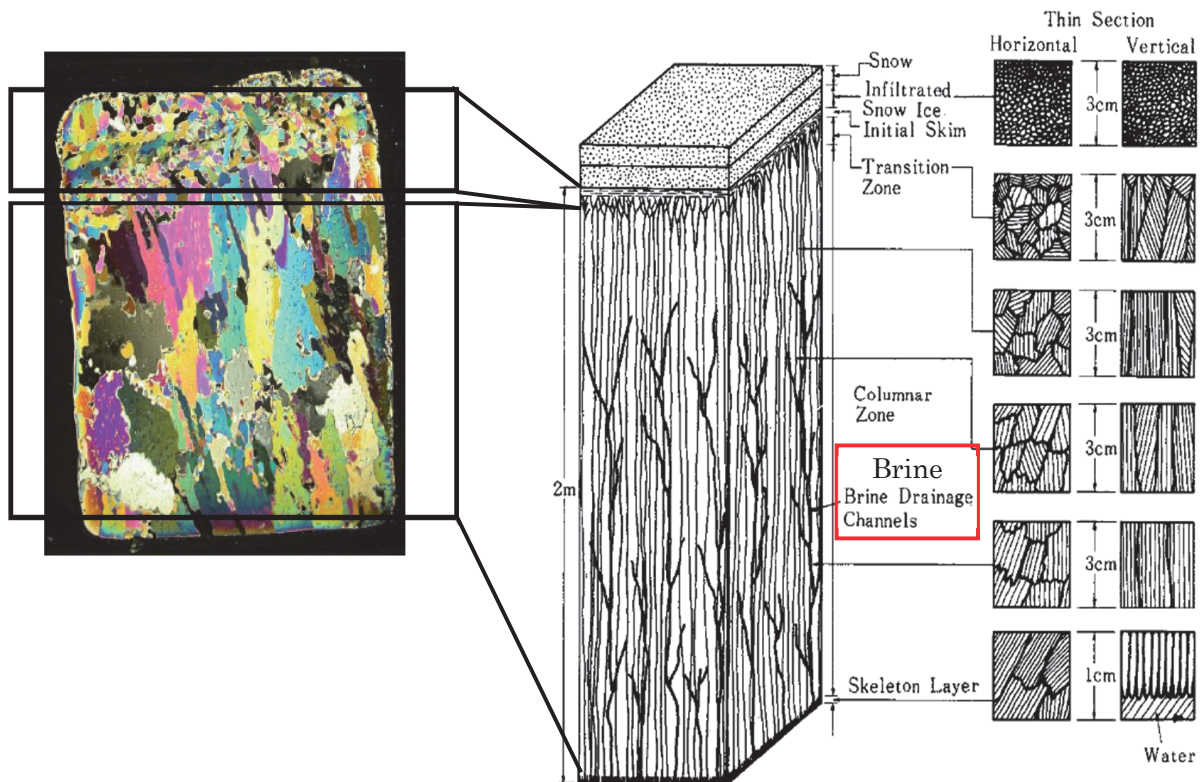


Fig. 5.2 Photograph and diagrams of sea ice crystals: (central figure, top to bottom) Snow and Snow ice surface, Transition zone, Columnar zone growing deeper into the water; (Thin Sections, figure right) Diagrams of sea ice column sampled horizontally (Horizontal) and vertically (Vertical) as thin wafers.⁵⁻²⁾

the top layer down, it includes snow, snow ice, a transition zone, and a columnar zone that grows deeper. When seawater freezes, only the freshwater component of the seawater freezes, leaving behind concentrated saltwater. This concentrated saltwater, called “brine,” can be trapped in the sea ice in the form of vertical tubular or cellular structures. The amount of brine significantly affects the physical and mechanical properties of the sea ice.

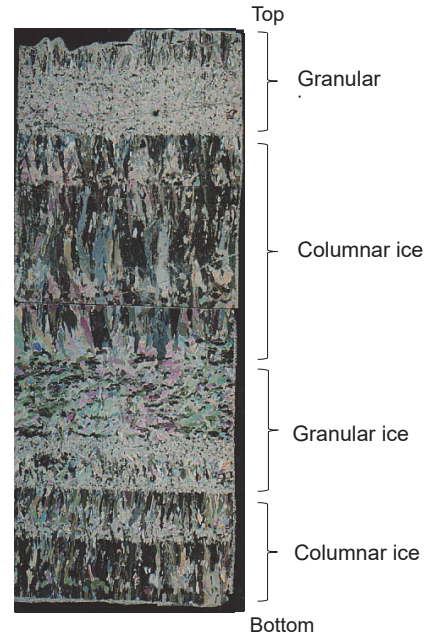


Fig. 5.3 Crystal structure of drift ice sample, Sea of Okhotsk, photograph: alternating layers of granular ice and columnar ice.⁵⁻³⁾

2) Drift ice: Sea of Okhotsk

Every February, drift ice arrives along the Hokkaido coast of the Sea of Okhotsk. This ice forms in the northwestern part of the Sea of Okhotsk and grows as it drifts southward, propelled by the East Sakhalin Current and wind. As the moving ice floes collide and overlap, they thicken before reaching Hokkaido.

Figure 5.3 is a photograph of a thin section of drift ice obtained off the coast of Hokkaido in the Sea of Okhotsk. It shows alternating layers of granular ice and columnar ice from the top down. This suggests that the sea ice was formed by overlapping ice floes.

5.3 Physical and Mechanical Properties of Sea Ice and Ice Forces

1) Required Information: Ice-Resistant Structure Design

When designing offshore structures, coastal structures, and harbor structures—collectively known as ice-resistant structures—that are placed in regions where the sea freezes during winter, it is necessary to consider the effects resulting from a combination of the following external forces:

- Ice force
- Wind force
- Current force
- Wave force
- Seismic force (in affected areas)

In offshore ice-covered regions, ice force is often the dominant external force in the design of structures. The maximum ice force occurs when the sea ice breaks against the structure. To evaluate this ice force and design structures accordingly, the following information is required:

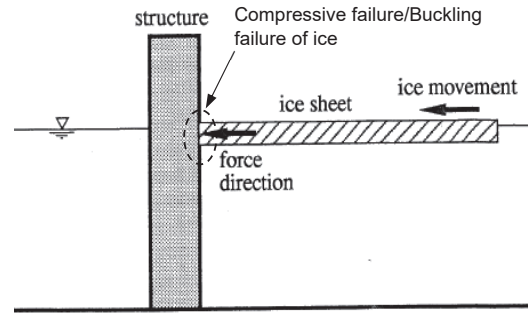
- Physical properties of ice (elastic modulus, Poisson's ratio)
- Ice strength (compressive strength, shear strength, bending strength, tensile strength)
- Mechanical interaction between ice and structural materials (adfreeze bond strength, coefficient of friction)
- Forms of ice failure due to interaction with the structure
- Properties and performance of structural materials at low temperatures
- Methods of construction and installation appropriate in cold regions

2) Ice Forces Acting on Structures

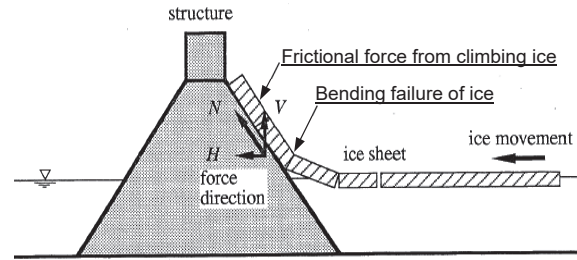
The ice force acting on a structure varies depending on the structure's shape, the form of the ice floe, and the direction of ice movement. Figure 5.4 illustrates the various types of ice forces acting upon structures.⁵⁻⁴⁾

Below are the basic ways that ice forces act on structures:
a) Horizontally: Fig. 5.4a

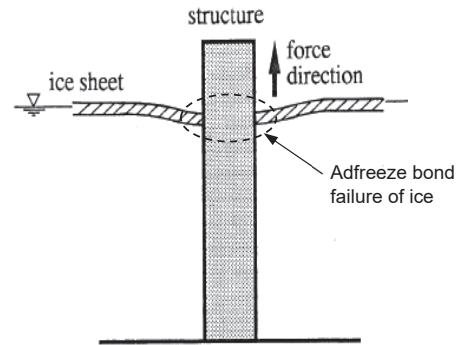
The ice force acting horizontally on vertical-wall structures is the largest among the ice forces. In this case, the ice failure modes are compression failure (crushing) and buckling



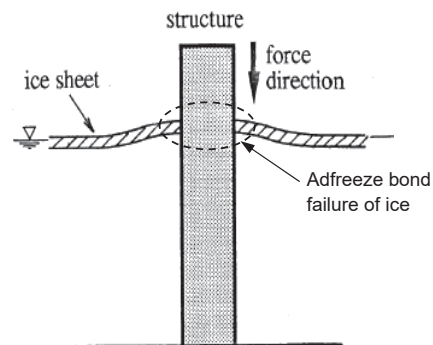
a) Ice force, horizontal action: Ice floe collision with a vertical structure.



b) Ice force acting on inclined structures: Bending failure and frictional force of ice floes.



c-1) Ice force, vertical action: Upward force due to rising water levels.



c-2) Ice force, vertical action: Downward force due to falling water levels.

Fig. 5.4 Diagrams: Types of ice force acting on structures.⁵⁻⁴⁾

failure. Evaluating these failure modes requires information on the compressive and bending strengths of the ice.

b) Ice force acting on inclined structures: Fig. 5.4b

The bending strength of ice is smaller than its compressive

and shear strengths. Therefore, designing structures with inclined surfaces that break colliding ice floes through bending can substantially reduce the effects of the ice force. However, in this case, the friction force between the ice climbing up the inclined surface and the structure must be considered. Thus, evaluating the total ice force requires information on the bending strength of the ice as well as the coefficient of friction between the ice and the structure's surface.

c) Vertically: Figs. 5.4 c-1 and c-2

When the water level rises while an ice floe is frozen to a columnar structure, an upward vertical ice force acts on the structure. Conversely, when the water level drops, a downward ice force acts on the structure. This vertically acting ice force is at its maximum when the bond between the ice and the structure's surface breaks, necessitating information on the adfreeze bond strength between ice and various materials.

Therefore, evaluating ice forces for the design and construction of ice-resistant structures requires understanding the physical parameters, i.e., constants and various strengths, that characterize sea ice. The following Section 5.4 covers the basic strength of sea ice, i.e., its compressive strength, while Section 5.5 introduces the research of Dr. Hiroshi Saeki—recognized domestically and internationally for research on the coefficient of friction between sea ice and structural materials: Ichimura Prize for Distinguished Achievement (1981, Ichimura Foundation for New Technology); Arthur Lubinski Award of Excellence (1984, American Society of Mechanical Engineers (ASME)); the Ice Research and Engineering Award (2004, International Association for Hydro-Environment Engineering and Research (IAHR)), etc.⁵⁻⁵⁾

For those who wish to learn more about the strength characteristics of sea ice and the mechanical properties between sea ice and structures, please refer to H. Saeki.^{5-6,7)}

5.4 Compressive Strength of Sea Ice

When sea ice acts on structures, the maximum ice force exerted on the structure occurs at the moment the sea ice breaks. Therefore, the strength of the ice is the most crucial information for calculating ice forces. As shown in Fig. 5.4, the shape of the structure and the way the ice acts on it can result in different forms of ice failure. The fundamental strengths of ice include compressive strength, shear strength, and bending strength. This section describes the most fundamental—compressive strength.

1) Concrete Strength and Ice Strength

In the case of concrete, strength usually refers to compressive strength. Concrete is made by binding aggregates together with cement paste. Thus, its strength is governed by the adhesive power of the cement paste, which is determined by the water-cement ratio (W/C, by mass): The lower the W/C, the higher the concentration of the cement paste and, thus, the greater the adhesive strength. Therefore, in general, the lower

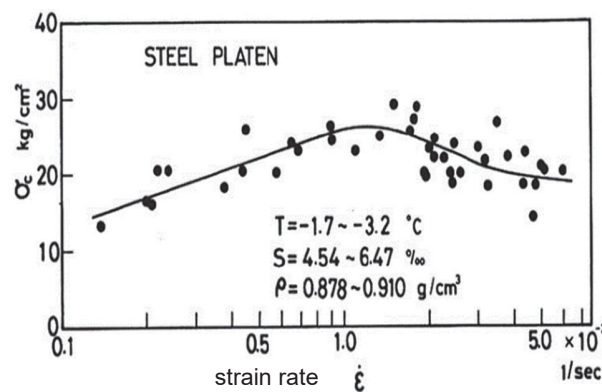
the W/C, the higher the concrete strength and the greater its resistance to freeze-thaw cycles. Of course, other factors such as temperature, humidity, air content, and type of cement also affect strength, but the W/C is the most significant factor. In the construction of the world's first composite structure (steel and concrete) mobile (drilling platform) artificial island, Super CIDS, discussed later in Section 8, strict control of the water content in the aggregate was necessary to ensure the required concrete strength and freeze-thaw durability.

There are a number of factors affecting sea ice strength. As shown in Fig. 5.2, sea ice consists of snow, pure ice, concentrated seawater (brine), and air. Additionally, the pure ice component can be either granular ice or columnar ice, depending on the formation process. Since sea ice grows from the surface downward, it is a highly anisotropic material, i.e., its strength varies depending on the direction of the load relative to the growth direction, significantly different from that of concrete or mortar.

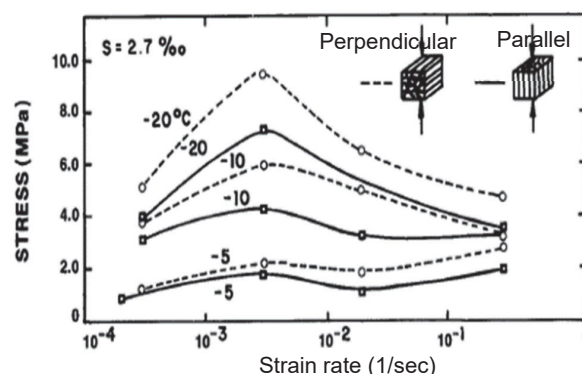
2) Compressive Strength of Sea Ice

Ice is a viscoelastic material, exhibiting both viscous and elastic properties. For example, glaciers flow several hundred meters a year under their own weight, which demonstrates the viscous properties of ice. And the elastic properties of ice result in the maximum force exerted on structures occurring at the moment the ice sheet breaks.

The compressive strength of sea ice is influenced by strain



a) Sea ice: Sea of Okhotsk.⁵⁻⁷⁾



b) Sea ice: Baltic Sea.⁵⁻²⁾

Fig. 5.5 Compressive strength of sea ice: Effects of strain rate (and temperature).

rate and loading rate. **Figure 5.5** shows the effect of strain rate on the compressive strength of sea ice: ice from the Sea of Okhotsk Fig. 5.5a and ice from the Baltic Sea in Northern Europe Fig. 5.5b. In both cases, the compressive strength peaks at a strain rate of about 10^{-3} sec^{-1} . Additionally, Fig. 5.5b shows that the strength increases as the ice temperature decreases from -5°C to -20°C , and that the strength is greater when the load is applied perpendicular to the growth direction (dashed line) than when applied parallel to it (solid line).

3) Compressive Strength of Sea Ice and Frozen Soil

Figure 5.6 shows the effect of temperature on compressive strength for sea ice and different types of frozen soil. Similar to the results for sea ice in Fig. 5.5b, the compressive strength of frozen soil increases as the temperature decreases, but with sea ice showing lower values than all of the frozen soil types. For example, at -10°C , the compressive strength is 13 MN/m^2 for frozen sand, 8 MN/m^2 for frozen silt, and 4 MN/m^2 for frozen clay, while it is 2.5 MN/m^2 for sea ice.

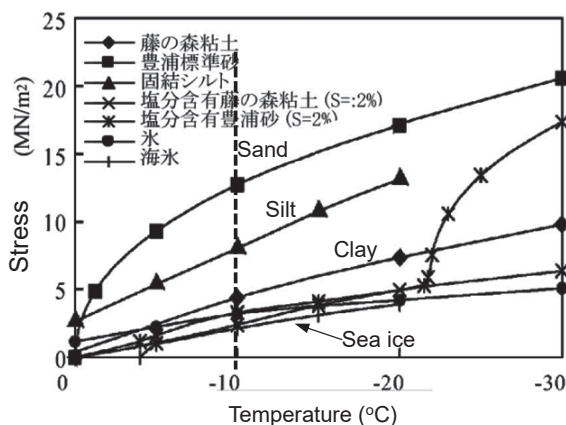


Fig. 5.6 Compressive strength of permafrost by soil type: Effects of temperature.⁵⁻⁸⁾

5.5 Coefficient of Friction Between Sea Ice and Structural Materials

This section introduces Dr. Hiroshi Saeki's research on the coefficient of friction between sea ice and various materials used in offshore structures.

The coefficient of friction between sea ice and structural materials is a crucial factor in evaluating the ice forces acting on inclined ice-resistant structures and on icebreakers. The engineering study of the coefficient of friction of sea ice began with Arnold-Alabieff⁵⁻⁹⁾ (1937), followed by notable research in the 1980s by Tabata and Tsushima^{5-10,11)} (Hokkaido University Institute of Low Temperature Science), Okasanen⁵⁻¹²⁾ (1980, Finland), Forland and Tatintclaux⁵⁻¹³⁾ (1984, USA), and Saeki⁵⁻¹⁴⁾ (1986, Hokkaido University Dept. of Civil Engineering).

1) Development of Experimental Equipment

To understand the characteristics of the coefficient of friction between sea ice and the surface of structural materials, it

is necessary to clarify the influence of the following factors:

- Contact area between ice and material
- Vertical stress at the contact surface
- Direction of movement relative to the ice growth direction
- Relative velocity between ice and material
- Presence of a water film at the contact surface
- Ice temperature
- Surface roughness of the structural material

In experimental research, the test equipment is crucial to meet the research objectives. To investigate the influence of the above factors, the apparatus shown in **Figs. 5.7** and **5.8** was developed by Dr. H. Saeki. In this setup, test material specimens (such as steel plates or concrete slabs) are fixed onto a platform that can be propelled horizontally using a hydraulic jack. The sea ice sample is placed on top of the test material specimen, and a steel cap is placed over the ice sample. A vertical load is applied onto the top of this cap, and the desired velocity of the sled can be achieved using the hydraulic jack.

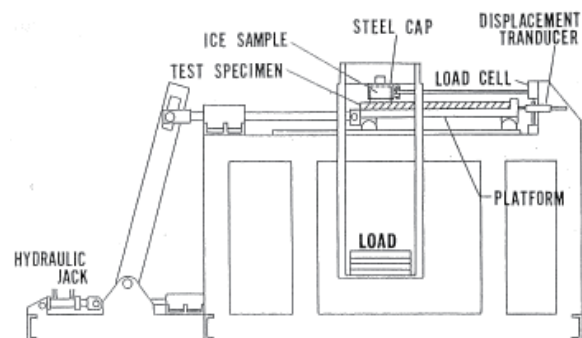


Fig. 5.7 Experimental setup diagram: Coefficient of friction testing apparatus.⁵⁻¹⁴⁾

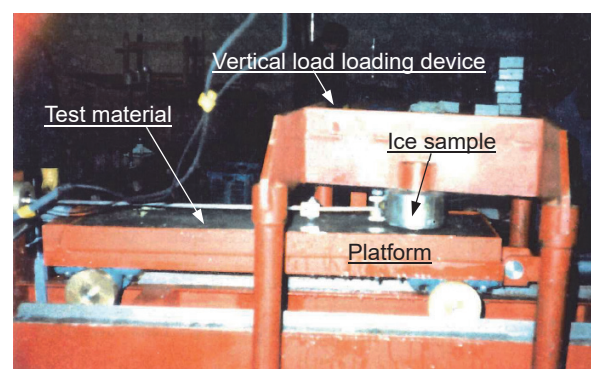


Fig. 5.8 Upper structure, photograph: Coefficient of friction testing apparatus.⁵⁻⁴⁾

2) Ice Used in the Experiment

The experiments were conducted at Lake Saroma in Hokkaido, Japan, in the late 1970s. Lake Saroma is a brackish lake normally connected to the Sea of Okhotsk by a pair of narrow inlets: salinity level close to that of normal Sea of Okhotsk seawater. Ice blocks with a thickness of 30-50 cm were cut

from the lake, and cylindrical ice specimens were prepared using a core drill, as shown in Fig. 5.9.

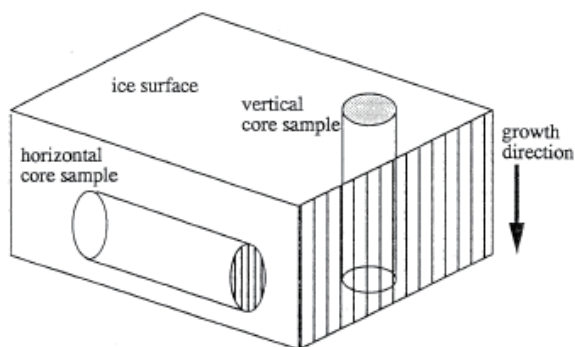


Fig. 5.9 Diagram: Coring directions for sea ice samples.⁵⁻¹⁴⁾

3) Structural Materials Tested

The following five examples of structural materials were used to investigate the coefficient of friction with sea ice. As steel plates are commonly used in coastal and offshore structures and ships, the coefficient of friction was studied for various surface conditions. Four types of steel surfaces and one concrete surface were studied:

- steel plate – uncoated, surface uncorroded
- steel plate – uncoated, surface corroded by seawater
- steel plate – coated with marine paint: ZEBRON
- steel plate – coated with marine paint: INERTA 160
- concrete – smoothed by trowel

4) Findings: Sea Ice-Coefficient of Friction

i) Normal (Vertical) Stress Effects

The normal (vertical) load acting on the ice sample can be varied in the experimental apparatus, see Fig. 5.7. The results for uncoated steel (uncorroded) in Fig. 5.10 show that the coefficient of kinetic friction (μ_k) remains almost constant (0.1) within a vertical stress (σ_v) range of 0.1 MPa to 1.0 MPa, while the coefficient of static friction (μ_s) shows a constant value when σ_v is above 0.5 MPa. These results confirm that sea ice conforms to Amontons' 1st law (see Addendum 3): Friction force is proportional to the normal load between

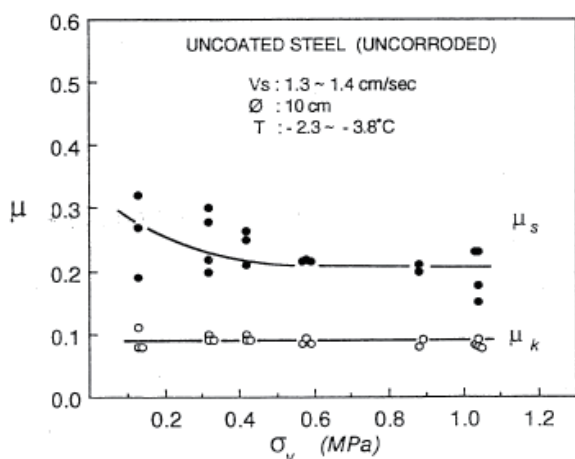


Fig. 5.10 Effects of normal (vertical) stress (σ_v) on the coefficient of friction for uncoated steel (uncorroded).⁵⁻¹⁴⁾

materials, i.e., the coefficient of friction is not influenced by vertical stress.

ii) Contact Area Effects

To investigate the effect of the contact area between ice and the test material surface on the coefficient of friction, ice samples of three different diameters (4.5 cm, 10.0 cm, 15.0 cm) were prepared, all with a thickness of 10.0 cm. The experimental results for uncoated steel (uncorroded) are shown in Fig. 5.11. Both μ_s and μ_k remain nearly constant, indicating that the coefficient of friction is not influenced by the contact area within the examined range, i.e., up to about 11 times the area. The grain size (D_{gr}) of the sea ice used in these experiments was 8-12 mm. This result confirms that sea ice follows Amontons' 2nd law: Friction force is not affected by the contact area between materials.

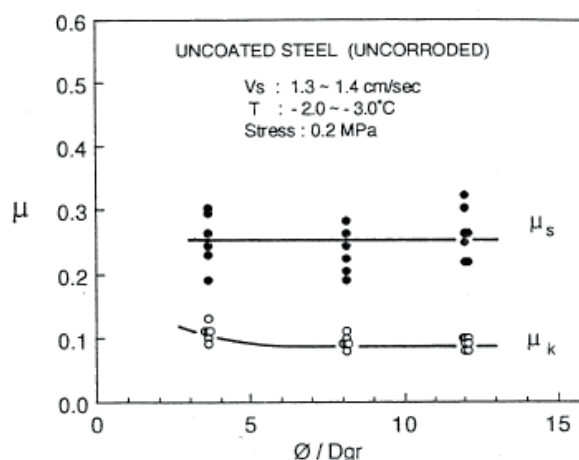


Fig. 5.11 Effects of contact area on the coefficient of friction for uncoated steel (uncorroded).⁵⁻¹⁴⁾

iii) Effects of Relative Velocity

Understanding the impact of relative velocity on the coefficient of friction is crucial for evaluating ice-induced frictional resistance on icebreakers. The test results for uncoated steel (uncorroded) at relative velocities ranging from 0.04 to 110 cm/sec show that both μ_s and μ_k initially decrease with increasing relative velocity, but approach becoming almost

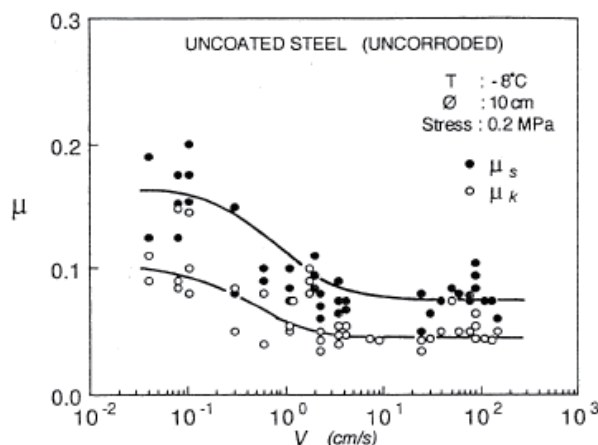


Fig. 5.12 Effects of relative velocity (v) on the coefficient of friction for uncoated steel (uncorroded).⁵⁻¹⁴⁾

constant at velocities above approximately 3 cm/sec, see Fig. 5.12. At lower relative velocities, the coefficients of friction, and as a result, friction force, are higher due to significant interaction between the ice and the roughness of the material surface. As the relative velocity increases, this interaction decreases, resulting in the coefficient of friction becoming almost constant, affirming that sea ice also follows Amontons-Coulomb's 3rd law: The friction force of dynamic friction is independent of the sliding speed.

iv) Effects of Ice Temperature

The strength (hardness) of ice is lower than materials like steel or concrete. As shown in Fig. 5.13, during sliding, the softer contact surface of ice can be sheared (scraped) by a

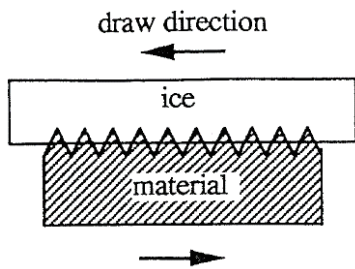
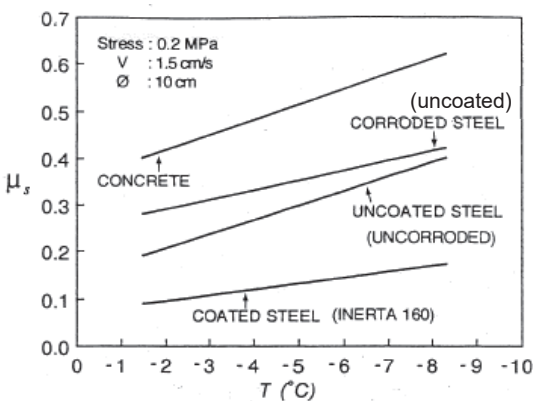
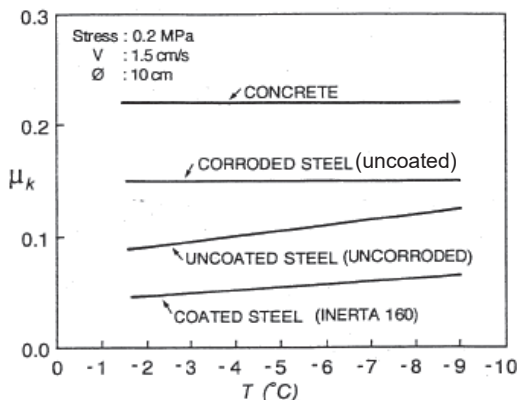


Fig. 5.13 Diagram: Cause of friction between ice and material surfaces.⁵⁻⁴⁾



a) Effects of temperature on the coefficient of static friction (μ_s).



b) Effects of temperature on the coefficient of kinetic friction (μ_k).

Fig. 5.14 Coefficients of friction as functions of ice temperature for various materials.⁵⁻¹⁴⁾

rough, harder material. Therefore, the coefficient of friction between the two depends on the strength of ice and the surface roughness of the other material, with ice strength increasing as the ice temperature decreases. Figure 5.14 shows that μ_s increases with decreasing ice temperature for all materials in the testing range from -1.5°C to -9°C (Fig. 5.14a). However, the test results for μ_k vary according to the material: increasing with decreasing ice temperature for uncoated steel (uncoated) and coated steel (INERTA160) but remaining constant for the concrete and corroded steel (uncoated) test specimens (Fig. 5.14b).

v) Friction and Surface Roughness of Materials

Friction occurs when solid surfaces come into contact, generating a force that opposes relative motion. For ice, this opposing force greatly depends on the strength of ice and the roughness of the other material's surface. Figure 5.15 illustrates the surface roughness profiles of seven types of concrete and steel. Even for the same material, surface treatment can alter roughness, highlighting its importance for reducing surface roughness to minimize friction.

vi) Evaluation of Coefficient of Friction between Sea Ice and Materials

As described above, friction between sea ice and the surface of structural materials is influenced by many factors, including normal (vertical) load, relative velocity, ice temperature, and surface roughness. Therefore, it is not feasible to define coefficients of friction solely on material type like steel or concrete. Figure 5.16 summarizes several years of experimental results on μ_k testing conducted by Dr. H. Saeki. Although there is a range of values for each material, these data provide a useful reference for designers of actual structures.

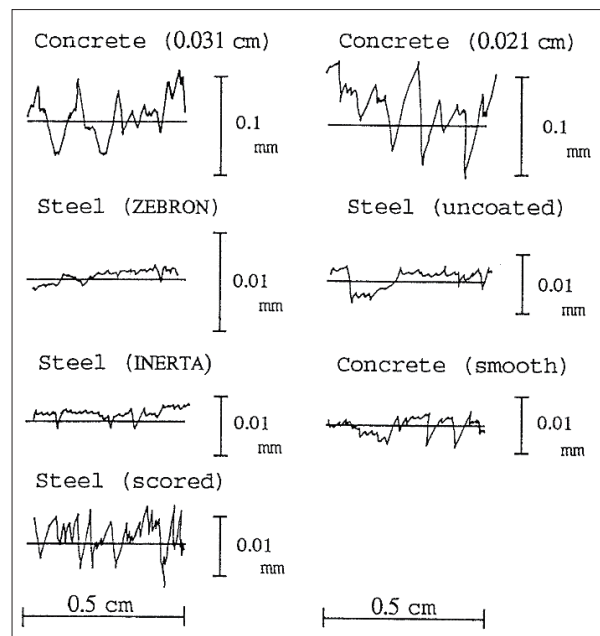


Fig. 5.15 Typical surface roughness profiles of test materials.⁵⁻¹⁴⁾

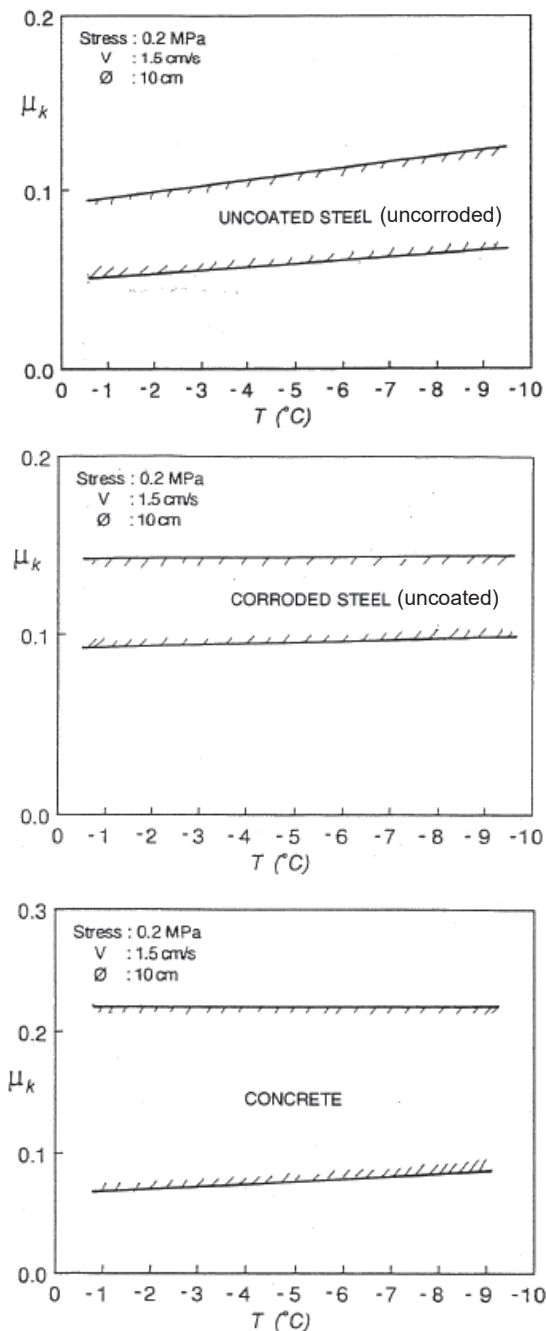


Fig. 5.16 Experimental values: Coefficient of kinetic friction (μ_k) between sea ice and uncoated steel (uncorroded), corroded steel (uncoated), and concrete obtained by Dr. H. Saeki.⁵⁻⁴⁾

5.6 Summary and Commentary

Sea ice is composed of snow, pure ice, concentrated seawater (brine), and air. The pure ice part can exist as granular ice or columnar ice, depending on the formation process. Sea ice growing from the surface downwards (columnar ice) is a highly anisotropic material. When determining its physical and mechanical properties, such as Young's modulus, Poisson's ratio, compressive strength, shear strength, and bending strength, it is essential to understand influencing factors like ice temperature, strain rate, load rate, and applied load

with experiments conducted using specially designed testing equipment.

In Japan, pioneering research on the mechanical properties of snow and ice began with Dr. Ukichiro Nakaya at the Institute of Low Temperature Science, Hokkaido University. This foundational work, continued by notable researchers such as Dr. Hiroshi Saeki (Hokkaido University) and Dr. Ken-ichi Hirayama (Iwate University), led to significant advancements in the construction of ice-exposed structures by Japanese ship-building companies in the 1980s (see Chapter 8).

Recently (as of 2024), snow and ice research in Japan's educational and research institutions has been on the decline. Given the current focus on issues like global warming, the reduction of Arctic sea ice, and the commercial use of Arctic sea routes, it is hoped that Japan's snow and ice research will experience greater development in the future.

References

- 5-1) Japan 1st Regional Coast Guard Headquarters: Ice Information Center, Japan. (n.d.). *Formation and Development Process of Sea Ice* [trans. from Japanese]. https://www1.kaiho.mlit.go.jp/KAN1/drift_ice/knowledge/growth/growth_n.html.
- 5-2) Schwarz, J. and W. F. Weeks. (1977). Engineering Properties of Sea Ice. *Journal of Glaciology*, Vol. 19, No. 81, 499-530.
- 5-3) Hokkaido University: Department of Cosmology, Center for Planetary Science, MOSIR Project. (n.d.). *Crystal Structure of Sea Ice* [trans. from Japanese]. <https://www.ep.sci.hokudai.ac.jp/~mosir/work/2002/clione/research/souya/pub-web/structure.html>.
- 5-4) Nakazawa, N. (1991). *Studies on Factors Influencing the Ice Forces on Structures* [unpublished PhD thesis]. Hokkaido University.
- 5-5) Editorial Committee for the Collection of Research Achievements by Prof. H. Saeki. (2014). *Cold Region Coastal and Ocean Engineering*. Hokkaido University. (in Japanese).
- 5-6) Saeki, H. (1979). *Sea Ice, and Coastal and Offshore Structures* [Course textbook B, 15th Summer Workshop on Hydraulic Engineering]. Coastal Engineering Committee, JSCE (Japan Society of Civil Engineers). (in Japanese).
- 5-7) Saeki, H. (1985). Growth Mechanisms and Mechanical Properties of Sea Ice. *Journal of the Japan Society of Civil Engineers*, Vol. 357, II-3, 13-23. (in Japanese).
- 5-8) Watanabe, K. (2014). Knowledge of Frozen Soil—Technology of Artificial Frozen Soil Wall. *Seppyu* [Snow and Ice], *Journal of the Japanese Society of Snow and Ice*, Vol.76-2, 178-192. (in Japanese).
- 5-9) Arnold-Alabieff, V. I. (1937). The External Friction of Ice. *Journal of Technical Physics*, Vol. 7, No. 8.
- 5-10) Tabata, T. and K. Tsushima. (1979, Aug.). Friction Measurements of Sea Ice on Flat Plates Metals, Plastics and Coatings. *Proceedings of the 5th POAC 79: Vol. 1*, Trondheim.
- 5-11) Tabata, T. and K. Tsushima. (1981, July). Friction Measurements of Sea Ice on Some Plastics and Coatings. *Proceedings of the 6th POAC 81: Vol. 1*, Quebec.
- 5-12) Oksanen, P. (1980, Apr.). *Coefficient of Friction Between Ice*

and Some Construction Materials, Plastics and Coatings. Laboratory of Structural Engineering, Report 7. VTT Technical Research Centre of Finland, Espoo.

5-13) Forland, K. A. and J. C. Tatinclaux. (1984, Aug.). Laboratory Investigation of the Kinetic Friction Coefficient of Ice. *Proceedings of the 7th IAHR Ice Symposium*, [then West] Ger-

many, Hamburg.

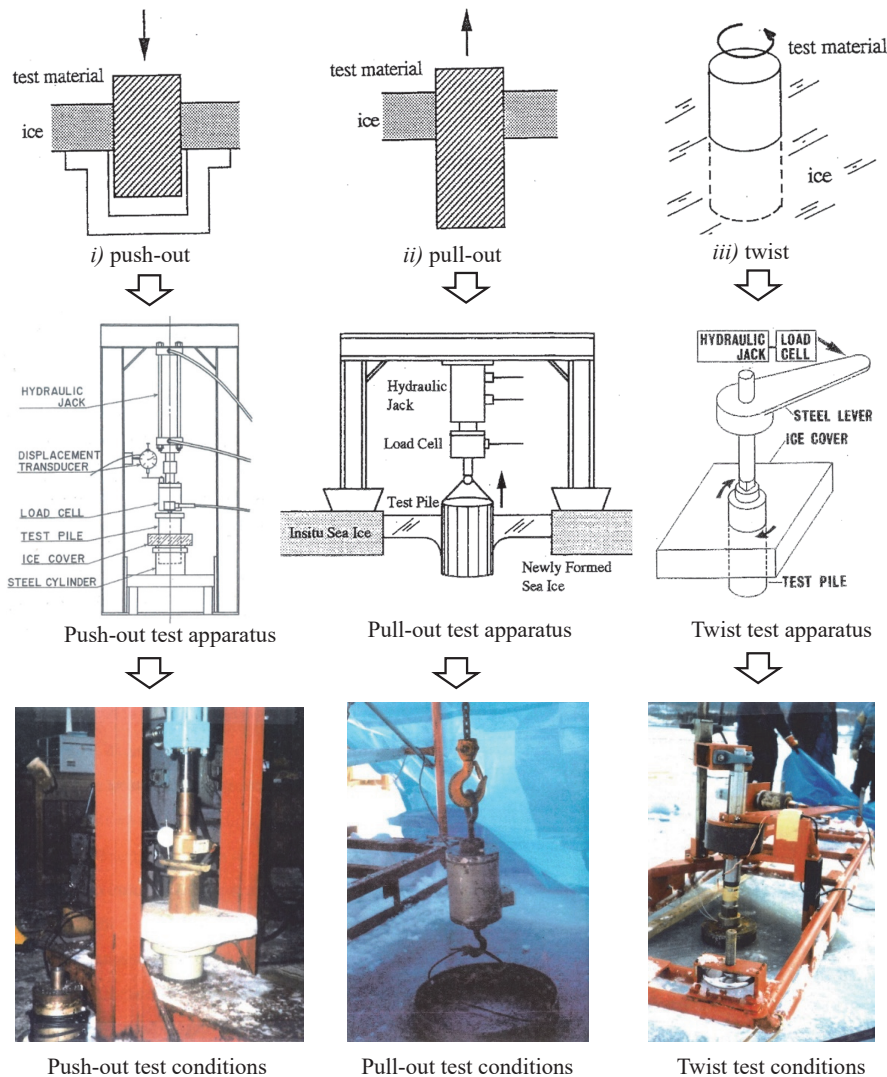
5-14) Saeki, H., T. Ono, N. Nakazawa, M. Sakai, and S. Tanaka. (1986, March). The Coefficient of Friction Between Sea Ice and Various Materials Used in Offshore Structures. *Journal of Energy Resource and Technology*, Vol. 108, Issue 1, 65-72. ASME.

- Addendum 3 -

1) Testing Methods: Adfreeze Bond Strength of Sea Ice

When sea ice adfreezes to a structure (i.e., bonding together via ice), the maximum ice force acting on the structure occurs at the moment the adfreeze bonding breaks (typical examples shown in Figs. 5.4 c-1 and c-2). Therefore, like the coefficient of friction, determining the adfreeze bond strength between sea ice and structures is also crucial for the design of structures in an icy environment.

To determine the crucial parameters of adfreeze bond strength as a function of the failure modes identified in Fig. 5.4, Dr. H. Saeki (Hokkaido University) devised equipment and associated testing procedures for in situ as well as laboratory experiments. The diagrams and photos of the different test methods and equipment for testing three types of adfreeze bond are shown below: *i) Push-out*, *ii) Pull-out*, and *iii) Twist*. This approach compares and verifies the differences in adfreeze bond strength based on the mode of failure, essential for identifying the forces acting in these ice-structure interactions. For detailed information on the research, refer to **Refs. 5-4 and 5-5**.



Adfreeze bond strength of sea ice tests: Three testing methods developed by Dr. H Saeki.^{5-4,5)}

2) Amontons' Laws of Friction

Guillaume Amontons (1663–1705) was a French physicist who published two laws related to friction in 1699. These laws are said to have been discovered originally by Leonardo da Vinci and rediscovered by Amontons about 200 years later. Additionally, about 100 years after that, the third law was discovered by the French physicist Charles-Augustin de Coulomb (1736–1806).

- i) The frictional force is proportional to the (normal) force applied perpendicular to the contact surface: Amontons' 1st law.
- ii) The frictional force is independent of the apparent contact area: Amontons' 2nd law.
- iii) The kinetic frictional force is independent of the sliding velocity: Amontons-Coulomb's law.



Leonardo da Vinci^[1]



Guillaume Amontons^[2]



Charles-Augustin de Coulomb^[3]

[1] Wikipedia. (2019, May 8). *Francesco Melzi - Portrait of Leonardo*.

https://en.wikipedia.org/wiki/Leonardo_da_Vinci#/media/File:Francesco_Melzi_-_Portrait_of_Leonardo.png.

[2] Wikipedia. (2024, Nov.17). *Guillaume Amontons*.

https://en.wikipedia.org/wiki/Guillaume_Amontons.

[3] Wikipedia. (2024, Oct. 6). *Charles-Augustin de Coulomb*.

https://en.wikipedia.org/wiki/Charles-Augustin_de_Coulomb.

6 | Ice Model Basin

6.1 Ice Model Basins Around the World

The development of oil and natural gas resources in icy seas, unlike environments such as the Gulf of Mexico or off the coast of Brazil, requires facilities designed to withstand the effects of ice and low temperatures. Additionally, ships capable of breaking ice are required for the transportation of the oil and natural gas produced. To support research and development in this field, large ice model basins (also known as ice model tanks) equipped with ice-making and advanced experimental functions are essential. These ice model basins replicate and apply the appropriate ice conditions found in icy regions at the scale of the model being tested, allowing tests of the ice loads on offshore structures and the performance of ice-breaking vessels. The discovery of oil and natural gas resources in the Beaufort Sea and the Sea of Okhotsk, which are relatively close to Japan, presented a new marine development market for Japanese shipbuilding and heavy industry. This opportunity drove research and development to enhance international competitiveness in the design and construction of oil drilling facilities and ice-breaking vessels appropriate for icy seas.

Table 6.1 lists some of the world's major ice model basins. With the economic activities surrounding the search for and exploitation of fossil fuel resources in icy seas increasing since the late 1960s, research and development activities intensified in countries bordering the Arctic Ocean and the Baltic Sea like Russia, Finland, the United States, and Canada, leading to the construction of large ice model basins equipped

with state-of-the-art facilities. **Figure 6.1** shows the US Army CRREL ice model basin, established in 1978, where many Japanese researchers have conducted experiments.

In Japan, large ice model basins were built in 1981 by the Ship Research Institute, a national research institution (now National Maritime Research Institute); in 1982 by Nippon Steel Corporation (now Japan Marine United Corporation, JMU); and in 1986 by Mitsubishi Heavy Industries, Ltd. Additionally, low temperature experiment rooms were established by Hokkaido University's Faculty of Engineering in 1977 as well as by Ishikawajima-Harima Heavy Industries Co., Ltd. (now IHI Corporation). Since the 2000s, South Korea and China, having overtaken Japan in the shipbuilding industry, are showing interest in Arctic resource development and Arctic sea routes as national strategies, leading to the construction of ice model basins for their research and development.

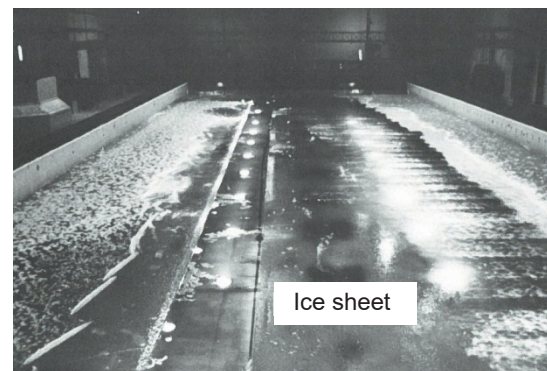


Fig. 6.1 Ice model basin, photograph: US Army CRREL.⁶⁻¹⁾

Table 6.1 Ice model basins around the world.

Year	Country	Institution/Company	Length (m)	Width (m)	Depth (m)
1955	USSR	Arctic and Antarctic Research Institute	13.4	1.85	1.10
1969	Finland	Wartsila Helsinki Shipyard	50.0	4.80	1.15
1970	USA	Arctec Inc.	18.1	2.40	1.20
1971	Germany	Hamburg Ship Model Basin (HSVA)	30.0	6.00	1.20
1974	USA	Arctec Inc.	30.5	3.66	1.52
1978	USA	US Army CRREL	36.6	9.14	1.52
1980	USA	University of Iowa	19.8	4.88	1.22
1981	Japan	National Maritime Research Institute	35.0	6.00	1.80
1982	Japan	Japan Marine United Corporation	20.0	6.00	1.80
1983	Finland	Wartsila Helsinki Shipyard	60.0	6.00	2.30
1984	Germany	Hamburg Ship Model Basin (HSVA)	60.0	10.00	2.50
1985	Canada	National Research Council (NRC)	90.0	12.00	3.00
1986	Japan	Mitsubishi Heavy Industries, Ltd.	28.0	9.00	2.30
2006	Finland	Aker Arctic Technology Inc.	75.0	8.00	2.10
2009	Korea	Korea Research Institute of Ships and Ocean Engineering	42.0	32.00	2.50
2014	Russia	Krylov State Research Centre	100.0	10.00	2.00
2016	China	China Ship Research Center	8.0	2.00	1.00

6.2 Ice Model Basin: National Maritime Research Institute, Japan

In 1981, the National Ship Research Institute (NSRI) (now National Maritime Research Institute, NMRI) constructed Japan's first, the world's eighth, large ice model basin facility to conduct model experiments for ships and marine structures. This facility features a test basin that is 35.0 m long, 6.0 m wide, and 1.8 m deep, enclosed within a refrigerated chamber. Immediately after its completion, model tests were conducted on the ice navigation performance, steering capabilities, and safety of the icebreaker *Shirase* (first generation) for use in the Antarctic.

Figure 6.2 shows a photograph of the NMRI ice model basin, and Fig. 6.3 provides a cross-sectional view of the basin enclosed within a refrigerated chamber capable of -20°C —cold enough for ice to form on the basin's surface. Coolers are installed on the ceiling; an underground pit with observation windows constructed around and beneath the basin enables underwater observations, from the sides and bottom, of ice breaking and the movement of ice fragments around the ship's hull.

One of the primary uses of the ice model basin is to determine the performance of ice-breaking ships by measuring the resistance to forward movement of a ship model break-

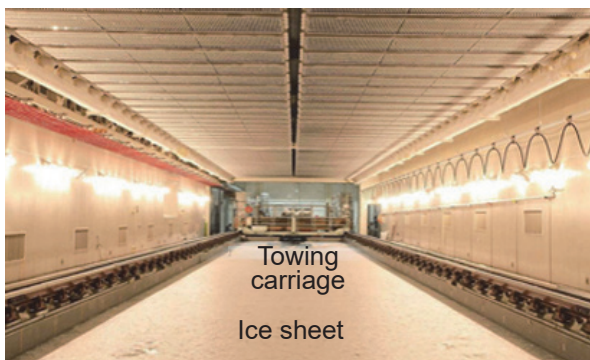


Fig. 6.2 Ice test basin, photograph: MNRI (35.0 m long, 6.0 m wide, and 1.8 m deep).⁶⁻²⁾

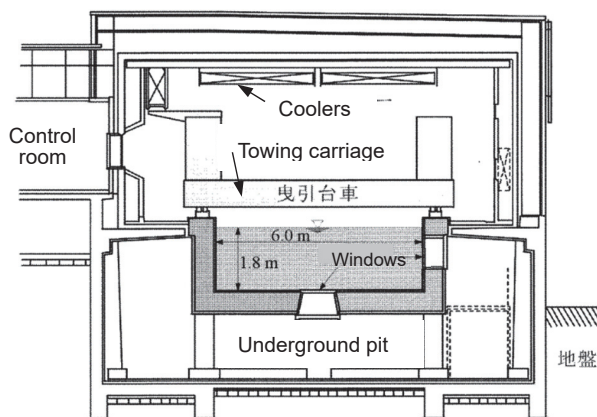


Fig. 6.3 Cross-sectional view, MNRI: test basin, underground observation pit, and refrigerated chamber.⁶⁻³⁾

ing through flat ice sheets and by observing the ice-breaking modes. Figure 6.4 captures the ice-breaking process through one of the test basin's side observation windows: The ice sheet is being pushed down and broken by the inclined bow of the ship as the hull moves forward (from right to left) through the ice fragments. The ice-breaking pattern varies with the ship's design (in particular, the bow shape), but ships typically progress forward while forming crescent-shaped ice fragments.

The NMRI ice model basin is the only facility in Japan conducting research on oil recovery devices deployed in the event of an oil spill in icy seas, see Fig. 6.5. The ice-oil separation device generates bubbles from the left side to move the oil to the right side of the test tank, separating the oil from the ice, with the recovered oil retained in the oil recovery unit and the ice released into the sea.⁶⁻⁴⁾

Although conducting experiments with oil in large basins is generally avoided due to the potential impact on equipment and the difficulty of oil removal post-experiment, this facility has made significant contributions on countermeasures for oil spills in icy waters in addition to its research and development on icebreakers and ice-resistant structures.

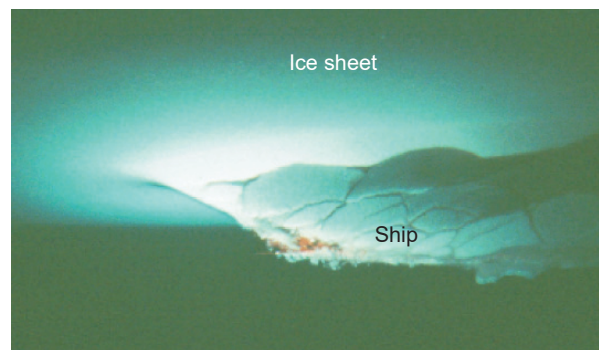


Fig. 6.4 Ship ice breaking experiment—Level ice sheet, photograph: Ice fragment behavior via observation window—Ship's bow breaking ice, traversing right to left.⁶⁻⁴⁾

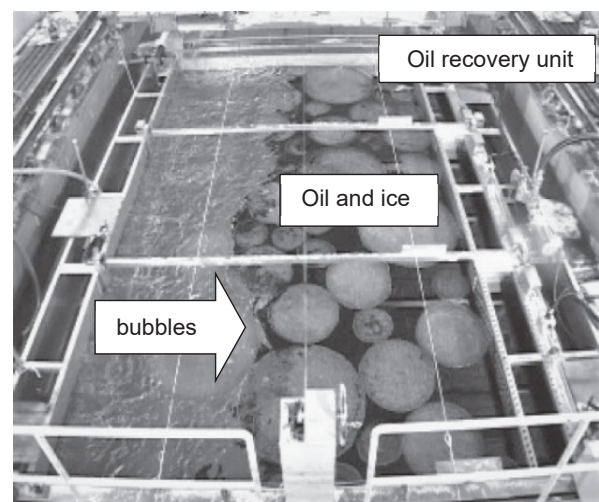


Fig. 6.5 Spilled oil recovery experiment, photograph: Test basin icy waters—bubbles generated at the left side move the oil to the right into the recovery unit.⁶⁻⁴⁾

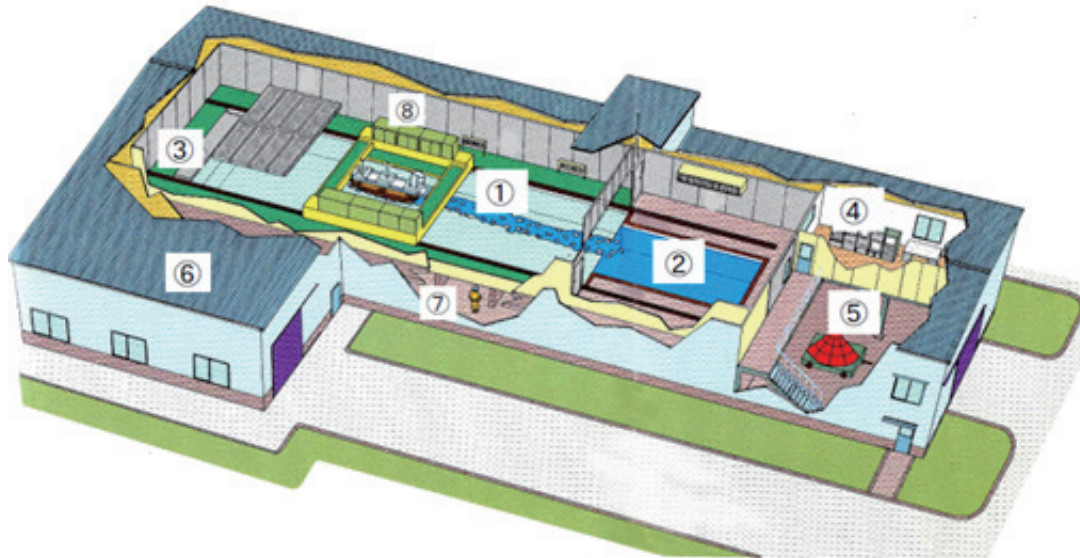


Fig. 6.6 JMU ice model basin—Facility layout: ① ice tank (test basin), ② trim tank, ③ tank for melting ice, ④ data recording room, ⑤ preparation room, ⑥ machine room, ⑦ underground space, and ⑧ towing carriage.⁶⁻⁵⁾

6.3 Ice Model Basin: Japan Marine United

Japan Marine United Corporation (JMU), formerly Nippon Kokan (NKK), established Japan's second ice model basin (first private company operator) at its Tsu Research Institute in September 1982. The company had previously converted the icebreaking-capable lighthouse supply vessel *Soya* into an Antarctic observation ship in 1956, built the *Fuji* (Japan's first icebreaker, 1965), and in November 1982, completed the construction of the first *Shirase*. By the 1980s, the extraction of oil and natural gas resources in icy seas was gaining attention, so the construction of the ice model basin was likely aimed at expanding into the market for designing and building suitable resource development structures and ships.

Using their ice model basin, JMU has designed and built many vessels in Japan for icy seas, including the icebreaking sightseeing ship *Aurora* (1990), the Japan Coast Guard's icebreaking patrol vessel *Teshio* (1995), the icebreaking multi-purpose cargo ship *Umiak I* (2006), ice-resistant "Suezmax" type tankers (maximum dimensions for passages through the Suez Canal), and the Antarctic observation ship (the second) *Shirase* (2009).⁶⁻⁵⁾ Using its ice model basin for the research and development of these vessels established JMU as the leading company in Japan with expertise in ice sea technology. Their ice model basin was also used for experiments in the JOIA Ice Load Research Project (discussed in Chapter 7).

Figure 6.6 shows the facility layout of the JMU ice model basin. The basin consists of the following components: ice tank (test basin), trim tank, and ice melting tank. The test basin is 20.0 m long, 6.0 m wide, and 1.8 m deep. The towing carriage uses a rack and pinion drive system operating at speeds ranging from 0.006 to 1.40 m/sec. The refrigeration unit (installed about 2.5 m above the main ice tank), together with fan heaters positioned along the sides, allows the room

temperature to be controlled between +2°C and -25°C.

Basic ice performance tests, such as measuring the ice resistance of icebreaking vessels, use model level ice sheets. As

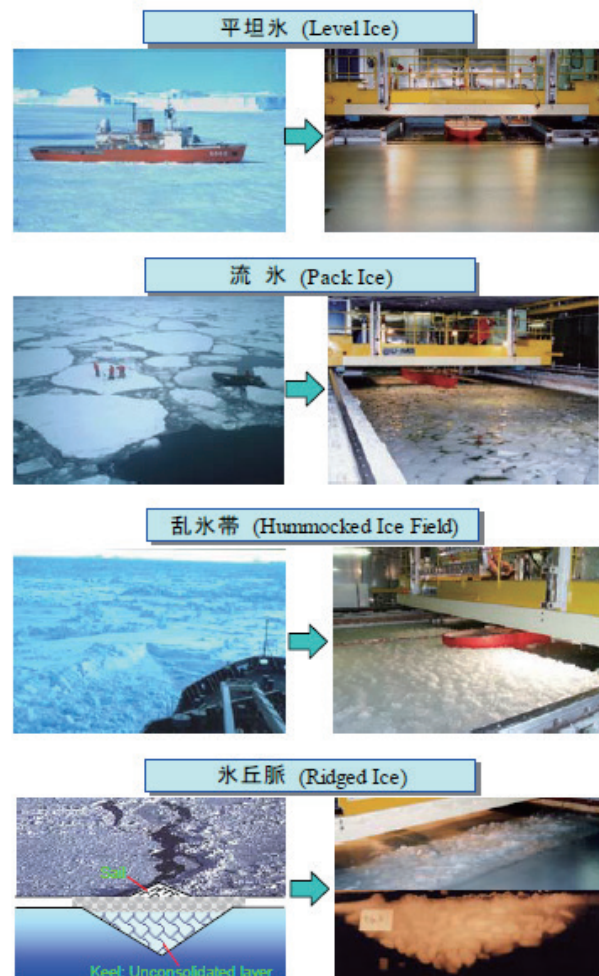


Fig. 6.7 Experiments with various types of model ice, photographs.⁶⁻⁵⁾

shown in Fig. 6.7, when recreating non-level sea ice conditions (e.g., drift ice or ice ridges), model ice sheets are created by breaking and refreezing level ice sheets to reproduce the desired properties of natural ice.⁶⁻⁵⁾

6.4 Ice Model Basin: Mitsubishi Heavy Industries

Mitsubishi Heavy Industries, Ltd. (MHI) installed Japan's third ice model basin at its Nagasaki Research Institute in 1986: Test basin—28.0 m long, 9.0 m wide, and 2.3 m deep. This facility's test basin (Fig. 6.8) was built for large model experiments: research focused on large structures used for resource exploration and production, featuring controlled temperatures down to -40°C. The dimensions of the test basin were comparable to those at internationally renowned institutions such as the Hamburg Ship Model Basin (HSVA) and CRREL, facilitating the comparison and validation of test data.

Table 6.2 lists the main features of the MHI ice model basin facility. The test basin had a freezing capability of 3 mm/hr, comparable to the capability at NMRI, while that of JMU's test basin is 7 mm/hr.

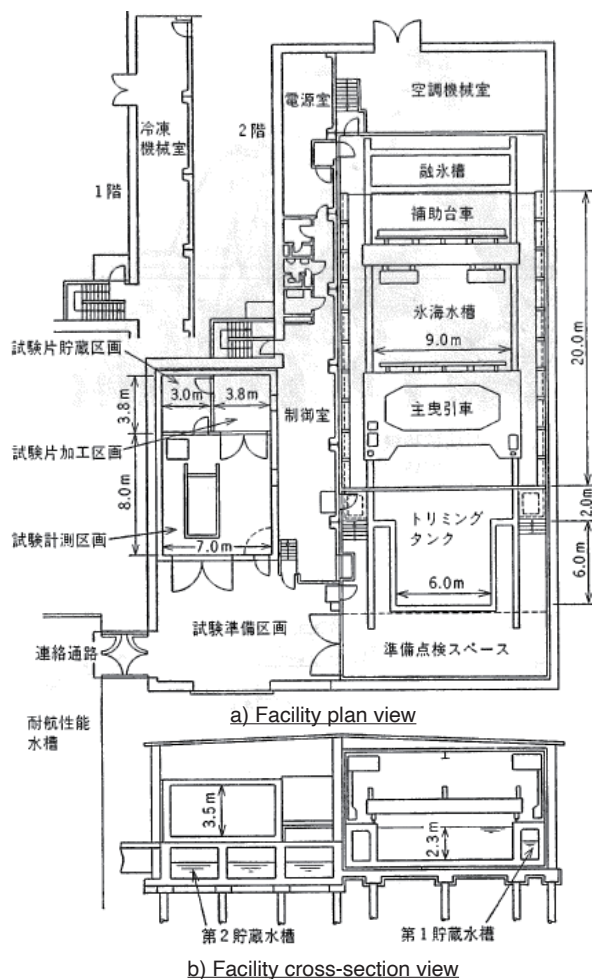


Fig. 6.8 MHI ice model basin, Facility layout: (left dashed box) large cold chamber; (right dashed box) ice test basin.⁶⁻⁶⁾

Table 6.2 Specifications: MHI ice model basin facility.⁶⁻⁶⁾

Facility	Specification	Dimension
Test basin	Length	28.0 m
	Width	9.0 m
	Depth	2.3 m
Towing carriage	Length	6.0 m
	Width	10.0 m
	Towing speeds	0.001-1.0 m/s
	Maximum towing force	49 N (5 t)
Cooling equipment	Screw Compressor	70 kW, 2 sets
	Air Conditioner	2 sets
	Reciprocating Compressor	7.5 kW, 1 set
	Refrigerator	2.2 kW, 1 set

The MHI ice model basin facility was used for strength tests on model ice and materials for structures such as concrete and steel as well as evaluating ice-resistant paint. Figure 6.9 shows an ice load test on a conical wall structure; Fig. 6.10 shows a concrete strength test under low temperatures.

The ice model basin enabled significant research on ice-resistant structures, icebreaking vessels, and low-temperature materials, yielding numerous achievements. However, the facility was closed in 2006.



Fig. 6.9 Ice load test on a conical wall structure, photograph.⁶⁻⁷⁾



Fig. 6.10 Concrete strength test under low temperatures, photograph.⁶⁻⁷⁾

6.5 Ice Model Basins and Model Ice

1) Structure of Model Ice

One of the most crucial elements of conducting experiments in ice model basins is the ice used, i.e., model ice, as its strength and crystalline structure significantly influence the experimental results. Generally, in ice model basins, model ice sheets refer to level ice, which serves as the base ice when creating model sea ice in other forms such as pack ice, hummocked ice fields, and ridge ice. As shown in the polarized light photograph of the crystals in **Fig. 6.11**, model ice sheets can have columnar or granular structures, each formed by different methods.⁶⁻⁵⁾

- Columnar structure: This production method involves cooling the test basin room and growing ice downward from the water surface, similar to the formation of natural sea ice. The resulting ice has a columnar structure composed of vertically elongated, ribbon-like ice crystals.
- Granular structure: This production method involves continuously spraying fine water droplets over the water surface in a cold environment, forming ice layers. The resulting ice has a granular structure composed of fine ice particles.

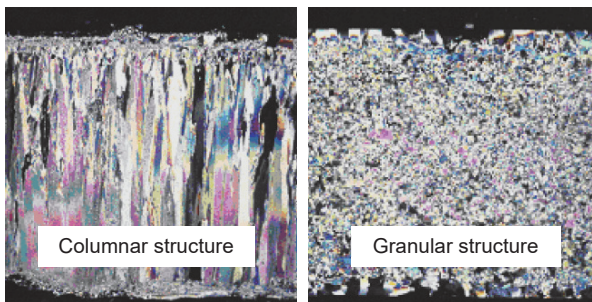


Fig. 6.11 Crystal structure of model ice sheets formed in the JMU ice model basin, photographs.⁶⁻⁵⁾

2) Model Ice Relative to Natural Sea Ice, Types of Model Ice

To estimate the mechanical interactions between sea ice and structures, such as ice loads and ice sheet failure modes, the mechanical properties of model ice must be extrapolated from those of in situ (natural) sea ice. In ice model basin tests, phenomena like ice sheet breaking and the movement of ice fragments must be mechanically similar to natural sea ice conditions. Therefore, model ice sheets must adhere to the following:⁶⁻⁵⁾

- Thickness, bending strength, compressive strength, and elastic modulus: The model ice properties should be scaled down to $1/\lambda$ of the natural sea ice properties, where λ is the scale ratio between the actual structure and its model.
- Coefficient of friction between model ice and model surface, Poisson's ratio, and density: These properties should closely match the values of natural sea ice.

Since sea ice is not as strong as freshwater ice, creating lower-strength ice in ice model basins involves adding solutes to freshwater and freezing the solution. Depending on the research objectives, different types of model ice, such as urea-doped ice, freshwater ice, and saltwater ice, are created for experiments:

- *Urea-doped ice*: Urea ($\text{CH}_2(\text{NH}_2)_2$) is added to water at a concentration of 1-2% to create urea-doped ice. Its strength can be adjusted and is minimally harmful, making it a popular choice in many ice model basins.
- *Freshwater ice*: This is made by freezing freshwater without additives, allowing repeated creation of uniform ice sheets. The formation of cracks (macro and micro) due to interactions between the ice and structures is clearly observable.
- *Saltwater ice*: Initially used to mimic sea ice by adding NaCl (i.e., table salt), saltwater ice is less commonly used now due to issues with concentration control and wastewater treatment.
- *Other types*: Model ice made with ethylene glycol, surfactants, and sugar as solutes have also been developed.

This range of model ice types enables researchers to select the most appropriate ice for their specific experimental needs.

In regard to urea-doped ice, it should be noted that Dr. Ken-ichi Hirayama contributed significantly to establishing the experimental methodology of using this material while conducting research in the CRREL ice model basin, see Fig. 6.1. It should be noted that his tenure at the CRREL laboratory facilitated the research stays of the Japanese researchers that followed. For details concerning research by Dr. Hirayama, the report *Properties of Urea-doped Ice in the CRREL Test Basin*⁶⁻⁸⁾ is recommended.

6.6 Conclusion

Since the 1960s, the discovery of oil and natural gas in icy seas has led to the construction of ice model basins worldwide to support the research and development of facilities for exploration and production as well as of ice-resistant ships for transportation. Initially, these efforts were concentrated in Russia, Northern Europe, Germany, the United States, and Canada. However, by the 1980s, Japan had built three such facilities, followed by the construction of large-scale research facilities in China and South Korea, leading to active research and development in these countries.

References

- 6-1) Nakazawa, N. and D. S. Sodhi. (1990). *Ice Forces on Flat, Vertical Indentors Pushed Through Floating Ice Sheets*. CRREL Special Report 90-14.
- 6-2) National Maritime Research Institute. (2024, Nov. 7). *Main research facilities* (archives) [trans. from Japanese]. https://www.nmri.go.jp/archives/overview/facilities/facilities_j.html.

- 6-3) Sasaki, N. and K. Izumiyama. (2008). Main Towing Tanks of National Maritime Research Institute of Japan. *Journal of the Japan Institute of Marine Engineering (JIME)*, Vol. 43, No. 5, 34-39. (in Japanese).
- 6-4) Izumiyama, K. (2009). Ice Model Basin. *Papers of National Maritime Research Institute (NMRI) of Japan*, Vol. 9, No. 2, 103-109. (in Japanese).
- 6-5) Yamauchi, Y and S. Mizuno. (2008, July). Test Technology of Ice Model Basin. *Japan Marine United Technical Review No.2*. (in Japanese).
- 6-6) Takekuma, K., T. Fujita, and Y. Kayo. (1987, May). Ice Model Basin of the Nagasaki Research and Development Center. *Mitsubishi Heavy Industries Technical Review Vol 24, No. 3*. (in Japanese).
- 6-7) Mitsubishi Heavy Industries, Ltd. (n.d.). *Conquering the Formidable Polar Sea*. Ice model basin brochure H310-08095, (1.0)88-6, B.
- 6-8) Hirayama, K. (1983, Mar.). *Properties of Urea-Doped Ice in the CRREL Test Basin*. CRREL Report, 83-8.

7 | Japan Ocean Industries Association (JOIA): Ice Load Research Project

7.1 Background and Objectives of the Project

In the early 1980s, the proportion of oil produced from offshore oil fields had reached about one-quarter of the total global production, with a rising trend. The production areas were moving towards polar regions and deep-water zones, leading to increased development costs and more challenging drilling conditions.

While technological advancements for deep-water zones were already being pursued globally, making the development of oil and gas fields at depths of 2,000 m a reality, the development in icy regions, such as the Arctic Ocean, had not progressed as much due to technical difficulties. The domi-

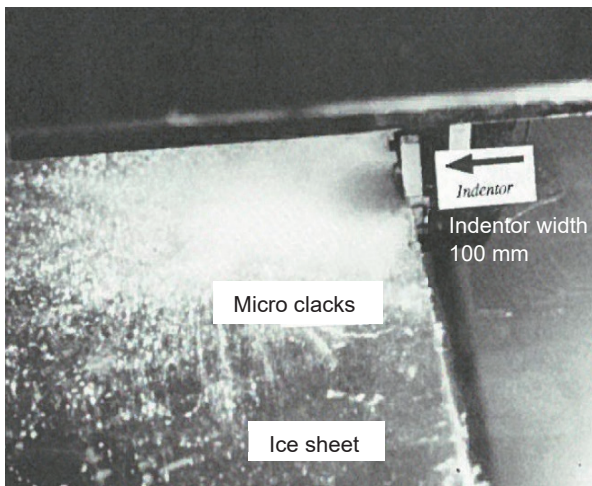
nant environmental factor in icy seas is sea ice. Among the various technical challenges, the capability to evaluate the ice loads on production and drilling structures resulting from interactions with sea ice was crucial for overcoming these difficulties. With this essential ice load evaluation technology, the construction costs and safety assessments of these structures could be determined.

In the 1980s, several ice-resistant structures were operational in the Arctic, including mobile artificial islands such as the SSDC (Single Steel Drilling System) and CRI (Caisson Retained Island), massive steel or concrete structures with widths ranging from 80 to 100 m. The structures were instrumented with sensors to monitor the total ice loads exerted on the entire structure as sea ice advanced as well as monitor the local ice pressures through pressure panels attached at various locations.

Upon analyzing these data, researchers discovered that the structural design was based on overly large estimations of the expected overall ice loads and local ice pressures. This over-estimation was attributed to several factors such as estimating ice loads with empirical formulas that had been developed from ice model basin experiments that focused on narrower structures like bridge piers (see Fig. 7.1). These empirical formulas, being based on coefficients derived from experiments with narrow width models, had neglected the effect of defects in the ice sheet decreasing its strength, i.e., as the contact area between the ice and the structure increased, the incidence of defects (zones of weakness) within the contact zone also increased, leading to a lower ice load. However, the significant drop in oil prices after the mid-1980s reduced operating budgets in the oil industry, resulting in insufficient research and development being conducted to more accurately evaluate ice loads. As a result, traditional empirical formulas continued to be used in the design of structures.

In 1986, the mobile artificial island Molikpaq encountered multi-year ice and experienced intense vibrations similar to those caused by an earthquake. It was reported that the foundation system faced the risk of liquefaction from the vibrations during this event, an issue that had not been anticipated during the design phase. Clearly, the design of offshore structures in icy seas needed to incorporate methods to estimate these vibrations along with the ice load assessments.

The Japan Ocean Industries Association (JOIA), commissioned by the Japanese Ministry of Economy, Trade, and Industry (METI), conducted the Ice Load Research Project on Offshore Structures (or JOIA Ice Load Project) from 1993 to 2000. The project was initiated in response to the discovery, and the need for further exploration, of oil and natural gas resources in ice-covered seas such as the Beaufort Sea, Barents Sea, Kara Sea, the eastern coast of Canada, and the Sea of Okhotsk. Of particular significance, the confirmation of large re-



a) Ice model basin tests: Indenter width 100 mm.⁶⁻¹⁾



b) In situ tests: River pier width 600 mm.⁷⁻¹⁾

Fig. 7.1 Measurement of ice loads on structures with narrow widths, photographs.

serves of oil and natural gas in the Sea of Okhotsk near Japan necessitated the construction of ice-resistant platforms and icebreaking transport ships, providing business opportunities for Japanese companies.

Research study objectives of the project:

- Examine: Interaction between level ice (model ice) and vertical/sloping wall structures and the resulting ice forces—ice model basin experiments.
- Examine: Interaction between rubble ice (unfrozen layers) and vertical/sloping wall structures and the resulting ice forces—ice model basin experiments.
- Examine: Ice pressure distribution and ice sheet failure modes at the contact surface between ice sheets and structures—medium-scale field experiments.
- Establish: Ice load estimation methods based on model experiment results and data obtained from in situ measurements.
- Determine: Seismic effects on and dynamic analysis of structures in icy seas.

7.2 Participating Institutions and Research Implementation

The JOIA Ice Load Research Project, initiated to advance and consolidate ice sea technology, attracted participation from many shipbuilding companies, construction firms, design consultancies, universities, and public research institutions, as detailed in **Table 7.1**. This project was unparalleled in Japan, with no other ice research initiative gaining extensive involvement from such a wide range of organizations and companies.

The project was structured with a standing committee, chaired by Prof. H. Saeki of Hokkaido University, overseeing the overall progress, while various working groups conducted the research. **Table 7.2** outlines the subject areas and schedule of the project from 1993 to 2000. During the initial five years, research was conducted by the Ice Model Basin Experiment Working Group (WG) focusing on indoor experiments, the Medium-Scale Field Indentation Tests WG conducting in

situ experiments at Lake Notoro in Hokkaido, Japan, and the Technical Survey WG investigating ice engineering research both domestically and internationally in addition to collecting empirical data on existing ice-sea structures. Following a mid-term evaluation by a third-party organization in 1997, the project continued from 1998 to its final year with a focus on three objectives: establish ice load estimation methods through the Ice Load WG, develop design manuals for ice-sea structures via the Design Technology WG, and examine the impact of seismic activity on ice sea structures in the Seismic Effects WG.

The project investigated the effects of ice loads from both flat ice (undeformed, level sea ice) and ridge ice onto structural configurations such as vertical and inclined wall structures (see **Fig. 7.2**) (note: ridge ice forms when broken ice is pushed together by wind and waves into mountain- or wall-like configurations).

To produce reliable load evaluation methods essential for structural design in icy environments, the project required detailed experimentation and analyses, leading to the development of ice load estimation programs. The research culminated in the formulation of design guidelines for structures in ice-covered seas.

In 1993, significant time was devoted to planning the experimental procedures. During the first half of the project (1993 to 1997), the research concentrated primarily on exam-

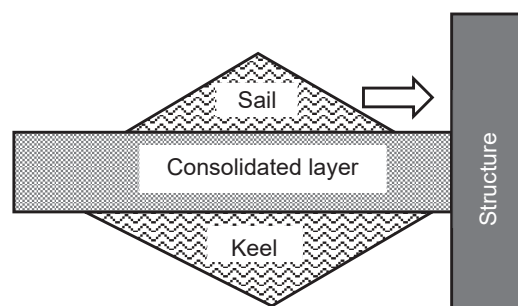


Fig.7.2 Ridge ice: *Sail*, portion that protrudes above the water; *Keel*, portion that is pushed down and forms under the water.⁷⁻²⁾

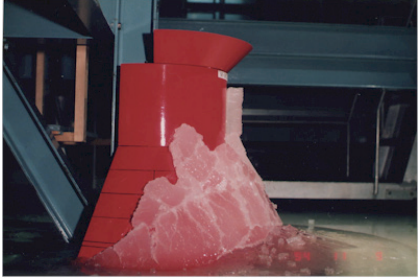
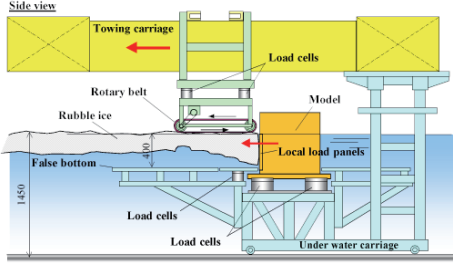
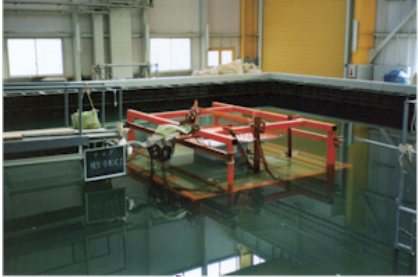
Table 7.1 Participating institutions: JOIA Ice Load Research Project (as of 1996).⁷⁻²⁾

Project Organization	Name, Affiliated Institution
Chair	Prof. Hiroshi Saeki, Hokkaido University
Vice-Chair	Prof. Ken-ichi Hirayama, Iwate University Prof. Masayuki Hyodo, Yamaguchi University
Ice Model Basin Experiment WG	NKK Corp.; Mitsubishi Heavy Industries, Ltd.; Ishikawajima-Harima Heavy Industries Co., Ltd.
Field Indentation Tests WG	Shimizu Corp.; Taisei Corp.; Mitsui Engineering & Shipbuilding Co., Ltd.; Pacific Consultants Co., Ltd.; Shimada Corp.
Seismic Effects WG	HiTech Research Inc.; Penta-Ocean Construction Co., Ltd.; Ohsaki Research Institute, Inc.; Akishima Laboratory Inc.
Technical Survey WG	Saka Consulting Inc.; Obayashi Corp.; Chiyoda Corp.; Kawasaki Heavy Industries, Ltd.; TOA Corp.; Kumagai Gumi Co., Ltd.
Standing Committee Member	National Maritime Research Institute; SODECO*; Kajima Corp.; Nippon Steel Corp.; Fukada Salvage & Marine Works Co., Ltd.; JAPEX Co., Ltd.**; Japan Drilling Co., Ltd.; Hitachi Zosen Corp.; Mitsui Construction Co., Ltd.; Takenaka Corp.

*SODECO (Sakhalin Oil and Gas Development Co.)

**JAPEX Co. Ltd. (Japan Petroleum Exploration Company, Limited)

Table 7.3 (continued) Experiments—level ice/ridge ice acting on vertical/inclined walls, earthquake effects; Responsible organizations; Test details.⁷⁻²⁾

Experiment; Responsible organizations; Test details	Experiment environment
<p>Ice model basin test</p> <ul style="list-style-type: none"> NKK Corp.; Mitsubishi Heavy Industries, Ltd.; Ishikawajima-Harima Heavy Industries Co., Ltd. Test specifications: <ul style="list-style-type: none"> Level ice thickness: 20-100 mm Structure shape: Conical Structure diameter at ice contact: 500, 1000, 1800 mm Conical inclination angle: 45, 60, 75 degrees Coefficient of kinetic friction between ice and structure surface: 0.1, 0.3 Indentation velocity: 4~280 mm/sec 	 <p>MHI Nagasaki Laboratory</p>
<p>Ice model basin test</p> <ul style="list-style-type: none"> NKK Corp. Test specifications: <ul style="list-style-type: none"> Ridge ice thickness: 200 mm Structure shape: Flat, vertical Indentation width: 800 mm Indentation velocity: 10-100 mm/sec 	 <p>NKK Tsu Laboratory</p>
<p>Ice model basin test</p> <ul style="list-style-type: none"> Mitsubishi Heavy Industries, Ltd. Test specifications: <ul style="list-style-type: none"> Ridge ice thickness: 200-300 mm Structure shape: Conical Structure diameter at ice contact: 450 mm Conical inclination angle: 60 degrees Coefficient of kinetic friction between ice and structure surface: 0.1, 0.3 Indentation velocity: 3-170 mm/sec 	 <p>MHI Nagasaki Laboratory</p>
<p>Earthquake effects: Water basin vibration tests</p> <ul style="list-style-type: none"> HiTech Research Inc.; Penta-Ocean Construction Co., Ltd. Test specifications: <ul style="list-style-type: none"> Structure types: Gravity-type, gravity-pile combined type Model vibration experiments: Ice-covered sea structures tested using an underwater vibration table, saturated ground conditions. 	 <p>Penta-Ocean Laboratory</p>

ing ice loads that result from flat ice. The data obtained from experiments served as the basis for developing load estimation methods applicable to real-world structures. From 1998 onward, the focus shifted towards experiments and load estimation methods related to ice loads from ridge ice.

Table 7.3 lists the organizations responsible for various aspects of the project and the specifications of the experiments.

7.3 Field Indentation Tests

The JOIA project aimed to achieve two goals—“Ice Load Estimation Program” and “Design Guidelines for Structures

in Ice-Covered Seas”—through a combination of field experiments on natural sea ice, ice model basin experiments with various structural shapes and ice conditions (including flat and ridge ice), and water basin vibration tests.

This section provides a detailed account of the field experiments conducted on natural sea ice at Lake Notoro in Hokkaido. An overview of the Ice Load Estimation Program and the Design Guidelines for Structures in Ice-Covered Seas are presented in sub-sections 7.4 and 7.6.

1) Experimental Process and Site

The objective of the field experiments on natural sea ice, by replicating conditions that closely resemble real-world

conditions, was to validate the results of the ice model basin (indoor) tests. Two key factors contributed to this increased realism: *a)* indentation experiments were performed using actual sea ice, and *b)* experiments were conducted on a scale substantially larger than that of the ice model basin. The results from the field experiments were integrated with the findings from the ice basin experiments to improve the Ice Load Estimation Program.

The experiment site, Futamigaoka Fishing Port on Lake Notoro in Abashiri City, Hokkaido (Fig. 7.3), was chosen based on the following criteria:

- Located in a saltwater lake that is directly connected to the Sea of Okhotsk via a short channel.
- Lake surface reliably freezes during the winter season.
- Quay and surrounding land could be leased for an extended period.
- Site is close to a city that can efficiently provide equipment and personnel for long-term experiments.
- Winter transportation to and from the site is dependable.

Lake Notoro is almost entirely covered with ice during the winter, with the maximum ice thickness typically reaching 30 to 50 cm by February. Being connected to the Sea of Okhotsk, the saltwater in the lake approximates that found in the open sea. Since December and January of the experiment period were devoted to preparations, including creating test ice sheets (refrozen ice sheets), the window for conducting field experiments on natural sea ice—even along the Okhotsk coast, Japan’s coldest coastal area—was limited to the single month of February.



Fig. 7.3 Field experiments (natural sea ice), location: Futamigaoka Fishing Port, Lake Notoro.⁷⁻²⁾

2) Lake Notoro: Characteristics of Refrozen Test Ice

Figure 7.4 depicts the crystal structure of the refrozen ice from Lake Notoro used in the February 2000 experiments. The presence of snowfall led to the formation of distinct layers, from top to bottom: snow, snow ice, granular ice, and columnar ice. For the experiments, the testing was conducted when the granular and columnar ice layers reached the target thickness of approximately 300 mm, measured after remov-

ing the upper layers of snow and snow ice. The saltwater ice from Lake Notoro used in the experiments had the following general characteristics:

- Density: 0.79-0.91 t/m³; Salinity range, 2.0 to 7.7‰ (parts per thousand)
- Compressive Strength: primarily, 1-2 MPa; maximum strength, 4 MPa
- Relationship between bending strength (σ_b) and compressive strength (σ_C): $\sigma_b = 0.23 \times \sigma_C$ (MPa)
- Relationship between shear strength (τ) and compressive strength (σ_C): $\tau = 0.36 \times \sigma_C$ (MPa)

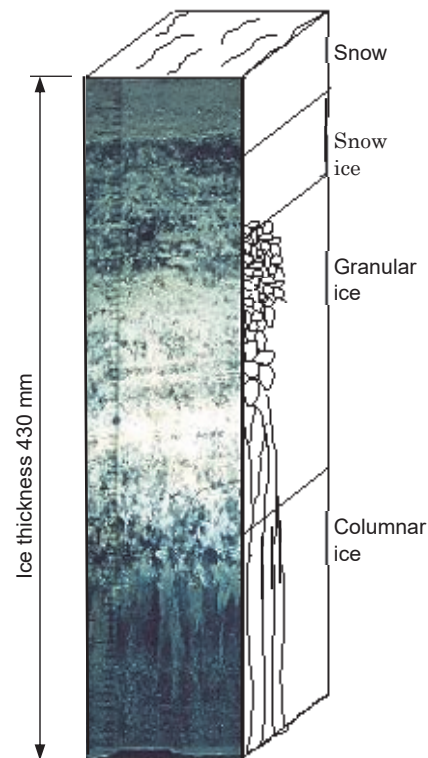


Fig. 7.4 Crystal structure of refrozen (test) ice, Lake Notoro (Feb. 2000).⁷⁻²⁾

3) Experiment Setup and Load Measurement Devices

The indentation experiments were conducted using the quay of the fishing port as a reaction platform, with model structures (indentors) pressed into the test ice sheets. The indentation widths of the model structures, i.e., indentors—1.5, 3.0, 4.5, or 6.0 m (illustrated in Fig. 7.5)—were achieved using a basic indentation device unit (width, 1.5 m) that could be extended wider by joining together various combinations of these basic units and pairs of 0.75-meter wide auxiliary panels.

Each 1.5 m wide basic unit was supported by its own hydraulic servo-jack, capable of applying a maximum force of 100 tons-force (tonf). The indentation velocity (*V*) ranged from 0.03 to 3 cm/sec, with a maximum stroke of 120 cm. The position accuracy during indentation was maintained at ± 1.5 mm through hydraulic servo control, ensuring positional stability despite variations in ice force. Indentation rigidity could be adjusted by inserting disc springs between the jack(s) and

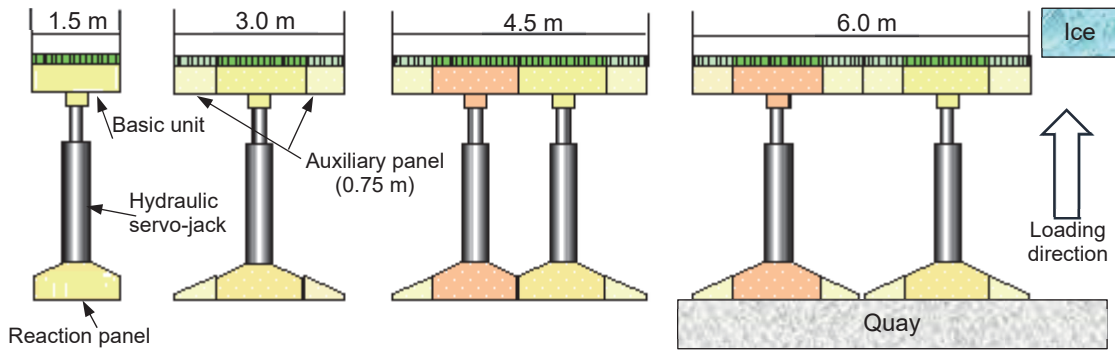


Fig. 7.5 Indentation model structures: width, 1.5 m to 6.0 m (top view).⁷⁻²⁾

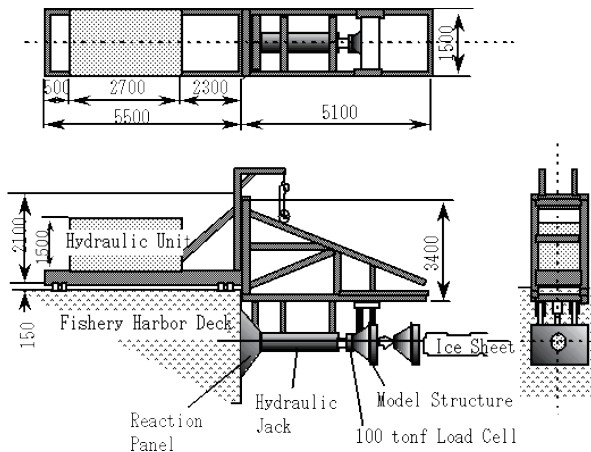


Fig. 7.6 Test structure setup, diagrams: Top view (upper), Side view (lower left), Front view (lower right).⁷⁻²⁾

the indenter. **Figure 7.6** provides an overview of the entire indentation test setup.

The total ice force during indentation was measured using a 100-ton-force load cell positioned between each jack tip and the indenter. The lateral distribution of the local ice load at the contact surface between the ice sheet and each 1.5 m wide basic unit was measured by a set of 15 load cells—one load cell monitoring one pressure plate: each plate, width 100 mm and height 400 mm.

Ice pressure distribution was further monitored using two-dimensional (2D) pressure panel sensors (thickness 0.2 mm, height 238 mm, and width 238 mm) installed on the face of the pressure plates: four panel sensors per basic unit. Each 2D panel sensor consisted of 1,936 pressure-sensing elements arranged in a 44×44 grid. The system's maximum measurement frequency of 127 times per second allowed it to capture relatively fast fracture behaviors, such as ice sheet failure. **Figure 7.7** shows the (15) pressure plates and (four) 2D pressure panel sensors on the front of a (1.5 m wide) basic unit. The pressure plates were also mounted onto the 0.75 auxiliary panels.

This research is believed to be the first employment of 2D pressure panel sensors in ice sheet indentation tests. This innovation enabled 2D pressure measurements at the contact surface between the ice sheet and the indenter as a function

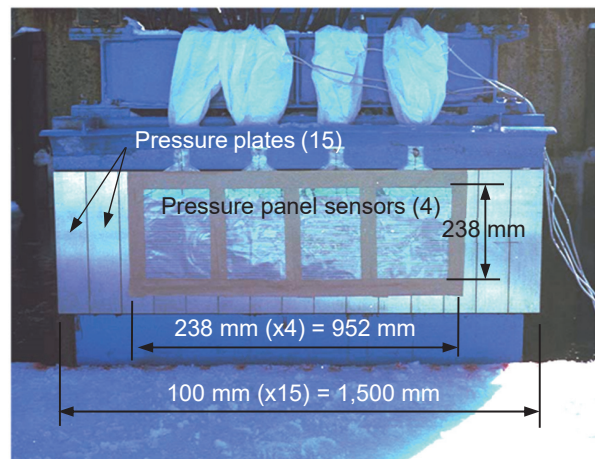


Fig. 7.7 Basic unit structure (1.5 m wide): pressure plates (100 mm wide x15) with 2D pressure panel sensors (238 mm wide x4), photograph.⁷⁻²⁾

of time, enabling visualization of the continuous changes occurring in the ice pressure distribution through a three-dimensional (3D) video format, i.e., fluctuating ice pressure data across the 2D ice sheet-indenter interface as a function of time).

4) Ice Forces: Total and Local

Figure 7.8 depicts the total ice force (indenter 100 tonf Load Cell data) as a function of elapsed time at the contact surface between the ice sheet and the indenter. After initial contact, the ice force increases sharply and, as the contact

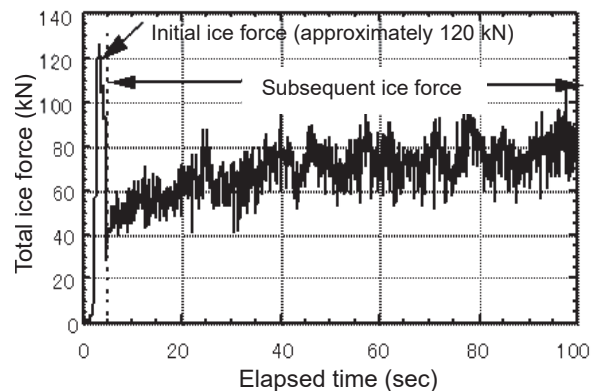


Fig. 7.8 Total ice force vs. elapsed time: Contact surface between ice sheet and indenter.⁷⁻²⁾

area approaches its maximum, an initial peak ice force (~120 kN) occurs. Beyond this point, the ice force remains relatively steady, never exceeding the initial value. This behavior is attributable to the indenter penetrating through an ice sheet that had fractured during the initial failure (maximum ice force) sequence.

Figure 7.9 shows local ice force data over time for four adjacent (100 mm wide and load cell monitored) pressure

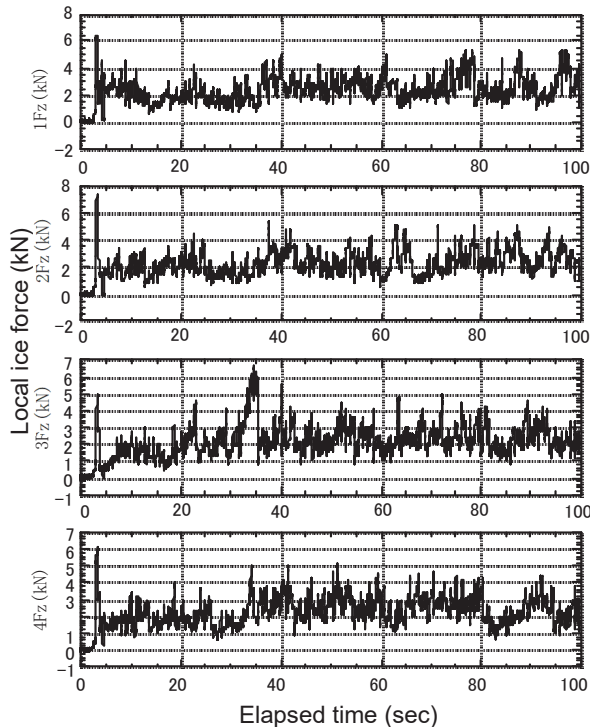


Fig. 7.9 Local ice force vs. time—Ice sheet indentation: (4) Pressure plates 1Fz to 4Fz—Initial ice forces occur simultaneously, but subsequent force peaks occur relatively independently.⁷⁻²⁾

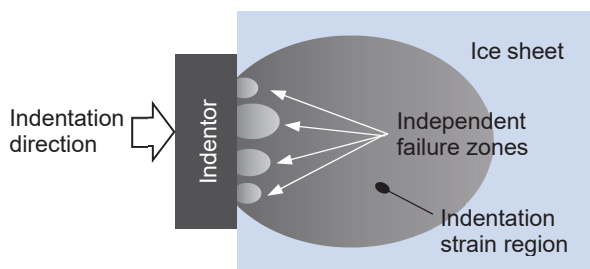


Fig. 7.10 Independent fracture zones: Contact surface between indenter face and ice sheet (top view).⁷⁻²⁾

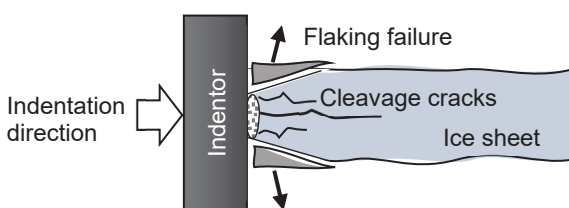


Fig. 7.11 Fracture mode of ice sheet during brittle failure (cross-sectional view).⁷⁻²⁾

plates (1Fz to 4Fz) located on the contact surface between the indenter and the ice sheet. Although these local ice force data appear similar, a close examination shows that the time-dependent variations in the local force data are independent of one another. This indicates that multiple small-scale fracture regions are independently forming at the contact surface (Fig. 7.10). The primary fracture modes observed, see Fig. 7.11, include flaking failure at the top and bottom of the ice sheet originating at the contact surface as well as cleavage cracks propagating horizontally through the ice sheet.

5) Ice Pressure Distribution Using 2D Pressure Sensors

An array of 2D ice pressure sensors mounted on the pressure plates at the front of the indenter measured the time dependent ice pressure distribution across the ice sheet-indenter interface. These real-time observations of the fluctuations in the ice pressure sensor data across the 2D indenter-ice sheet interface were displayed on a computer monitor via a 3D video: The three Ds refer to the x and y axes forming a 2D plane representing the indenter-ice sheet contact face, while the z axis data are the fluctuating ice pressure (MPa) data associated with locations on this 2D plane. Each pressure panel sensor comprised a grid of 44 rows by 44 columns, with each grid point capturing pressure data over an area of 5.4×5.4 mm: four pressure panel sensors on a 1.5 m wide basic indenter unit, see Fig. 7.7.

Figures 7.12 and 7.13 present the experimental results for an indenter with a width of 1.5 m: 0.3 mm/sec indentation speed with 186 mm ice thickness and 3.0 mm/sec indentation speed with 241 mm ice thickness, respectively (note: as described above, the x and y axes form a 2D plane representing the indenter-ice sheet interface, and the z axis data present the ice pressures at individual 2D plane grid points).

At the lower indentation speed (0.3 mm/sec, see Fig. 7.12), the contact area between the ice sheet and the indenter initially increased gradually (Figs. 12 a, b), resulting in a gradual increase in the Ice Force data. The contact area and ice force peaked concurrently—note an almost uniform ice pressure distribution across the contact surface in Fig. 12 c. Subsequently, the pressure distribution shifted downward due to buckling induced by creep failure of the ice sheet (Fig. 12 d).

Thus, under slow indentation rates, where the ice exhibits ductile failure characteristics, the maximum force coincides with a large, uniformly distributed contact area.

In contrast, the faster indentation speed (3.0 mm/sec, Fig. 7.13) resulted in a rapid increase in ice force following contact. Although the contact area was substantial at the peak force, the ice pressure distribution was non-uniform with a sawtooth-like pattern (Figs. 13 e, f). Post peak force, the ice sheet fractured, developing into cleavage cracks propagating horizontally through the ice sheet, Fig. 13 g. During the subsequent progressive failure of the ice sheet, flaking failure occurred, with the ice pressure at the ice sheet-indenter interface reduced to a horizontal linear feature, Fig. 13 h. This

“line-like” ice pressure is consistent with observations by Joensuu and Riska,⁷⁻³ representing a similar ice force interaction mechanism.

The line-like feature typically appears horizontally across the contact surface near the vertical center; however, the ice

pressure distribution remains variable, with peaks randomly shifting horizontally. These findings suggest that at higher indentation speeds, where the ice exhibits brittle failure characteristics, the ice sheet undergoes linear contact and non-simultaneous fracturing.

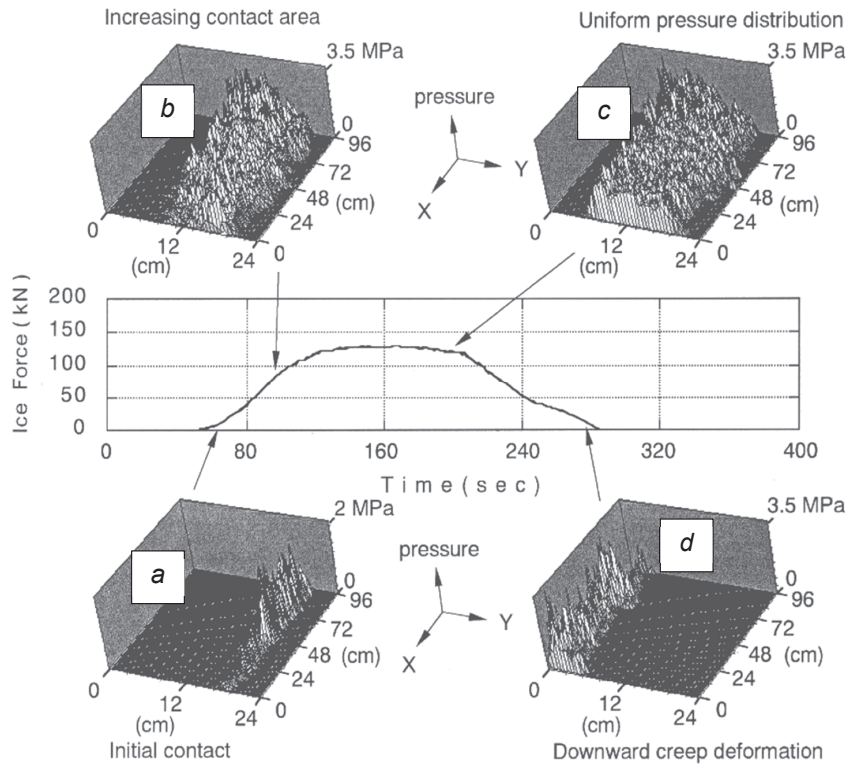


Fig. 7.12 In situ medium-scale vertical indenter test with monitoring of 2D ice sheet Interfacial pressure data (a, b, c, d) and Total ice force as functions of Time: refrozen ice test at 0.3 mm/sec indentation velocity.⁷⁻²

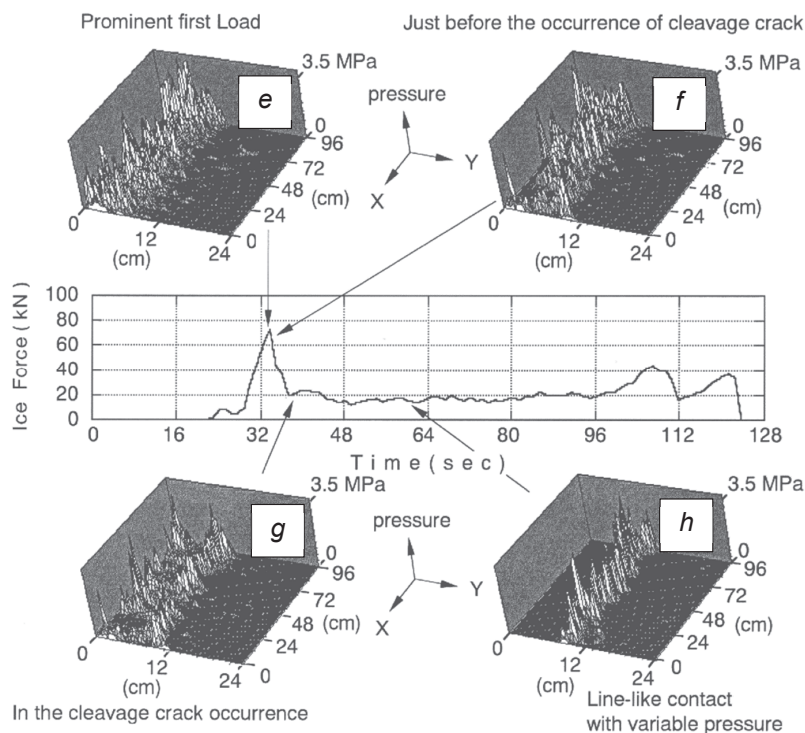


Fig. 7.13 In situ medium-scale vertical indenter test with monitoring of 2D ice sheet Interfacial pressure data (e, f, g, h) and Total ice force as functions of Time: refrozen ice test at 3.0 mm/sec indentation velocity.⁷⁻²

6) Summary: Field Indentation Tests

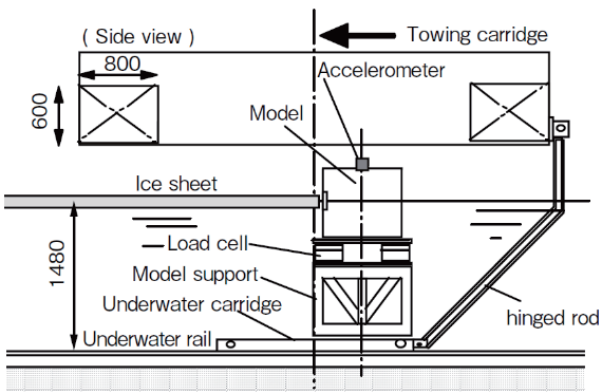
The use of 2D pressure sensor panels in field experiments with natural sea ice made it possible to clarify the pressure distribution at the contact surface between structures and ice sheets as a function of time. During brittle failure of the ice sheet, a horizontal, line-like load distribution was observed across the center of the ice thickness, while ductile failure resulted in a planar load distribution. The ability to observe these phenomena was largely due to the field experiment setting, which allowed the use of thicker ice sheets (up to approximately 400 mm) and an array of relatively large 2D pressure sensors on the 1.5-meter-wide front (face) of the basic indenter unit. For a more detailed discussion on the results of the Field Indentation Tests, I recommend Devinder Sodhi (1998)⁷⁻⁴⁾ and Takahiro Takeuchi (2002).⁷⁻⁵⁾

7.4 Ice Model Basin Experiments: Ice Load Estimation Program

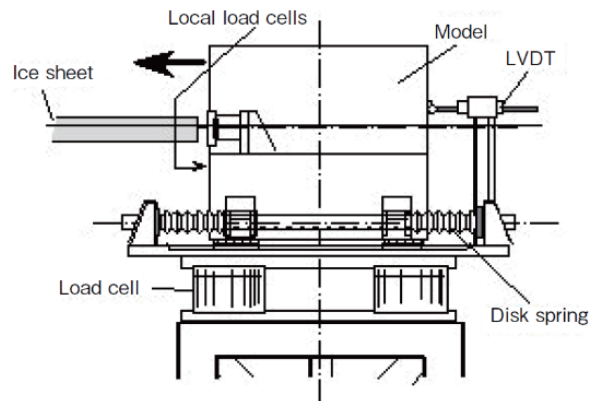
1) Program Development

To aid the designing of structures deployed in ice-covered regions, research experiments were conducted in ice model basins and the Ice Load Estimation Program was developed to more accurately estimate ice loads. The key research activities, starting in 1993, are listed below:

- Investigation: scale effects using square and circular models for indentation tests in an ice model basin, 1993 (Fig. 7.14a).
- Investigation: effect of structural rigidity on ice loads using model indentation tests in an ice model basin, 1994 (Fig. 7.14b).



a) Scale effects testing apparatus: Vertically mounted flat and cylindrical models.



b) Rigidity effect testing apparatus: Structure rigidity, adjustable using disk springs.

Fig. 7.14 Model indentation testing apparatus, diagrams.⁷⁻²⁾

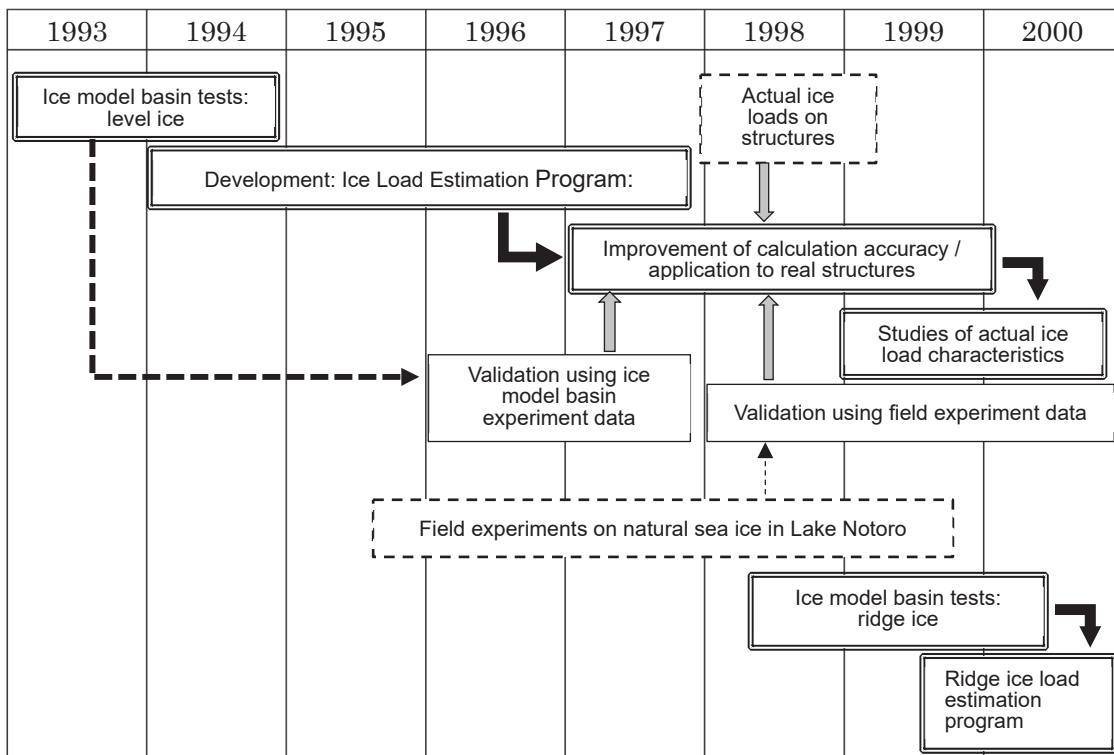


Fig. 7.15 Development flowchart: Ice Load Estimation Program.⁷⁻²⁾

- Development: Ice Load Estimation Program, 1994-1997.
- Validation: Ice Load Estimation Program, 1997-2000.
- Evaluation: reference actual ice loads on structures based on research literature, 1999-2000.
- Investigation: ridge ice loads using an ice tank, 1998-2000.
- Proposal: ridge ice load estimation method, 2000.

Figure 7.14 shows diagrams of the model indentation testing apparatus, and Fig. 7.15 outlines the process of conducting ice tank experiments and developing the Ice Load Estimation Program. This program was initially developed in the early stages of the project and was subsequently validated using data obtained from ice tank experiments and field experiments on in situ natural sea ice, as well as from data obtained on existing structures deployed in ice-covered seas.

2) Ice Load Estimation Program

i) Inputs and Outputs

Figure 7.16 presents a flowchart outlining the input parameters and desired outputs of the Ice Load Estimation Program. The program is divided into three main components:

input data, computation, and output. The input data are the relevant structural characteristics, ice sheet properties, and ground conditions. The program then generates time-series outputs, including structural responses, local and global ice loads, and base loads on the structure. The program was enhanced with an animation feature that visually depicts failure modes, fluctuations in local loads, and structural responses. Additionally, it includes the capability to input seismic waves for assessing the dynamic response of structures under combined ice and seismic loads.

ii) Analysis Scope

The program is designed to analyze vertical wall structures with various waterline shapes, including square, circular, and custom geometries. It also supports analyses of multi-legged structures with up to four legs (does not account for any mutual interaction between legs in ice load calculations). The program integrates failure modes analyzed by NASTRAN (NASA STRuctural ANalysis, a generic structural analysis software program developed by NASA in the late 1960s): The program focuses solely on the waterline shape for ice load calculations, without considering the detailed complex geometry of the total structure. Figure 7.17 illustrates the types of structures that the

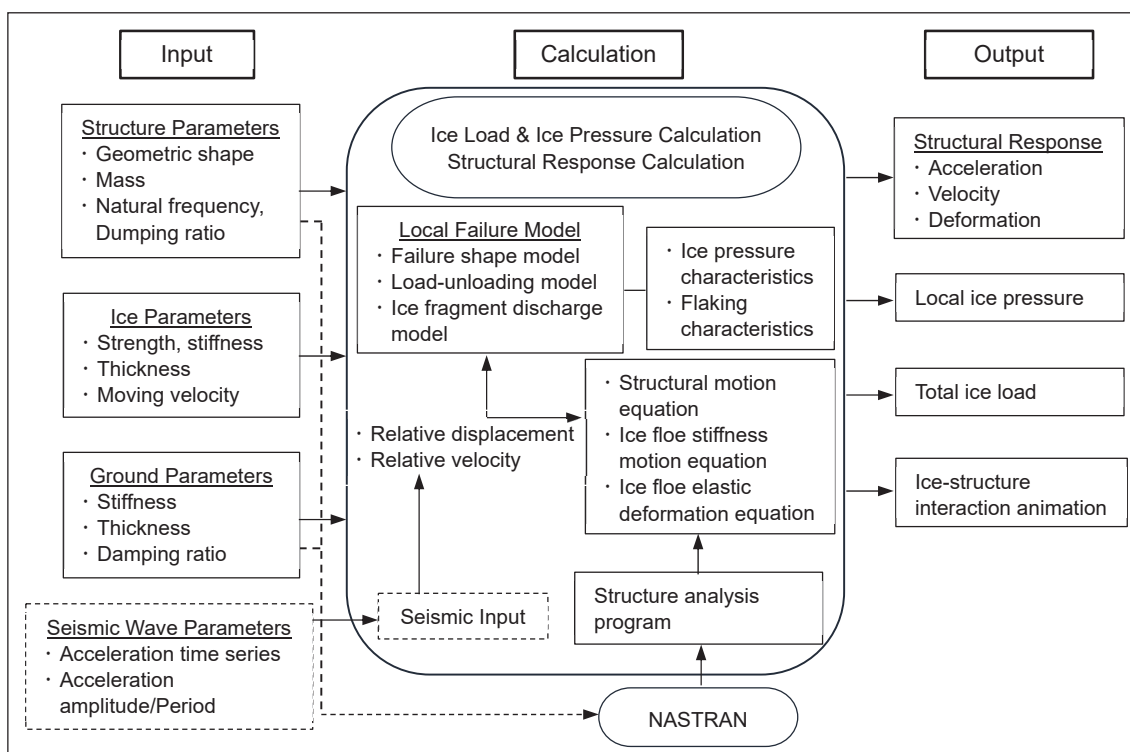


Fig. 7.16 Input-Output flowchart: Ice Load Estimation Program.⁷⁻²⁾

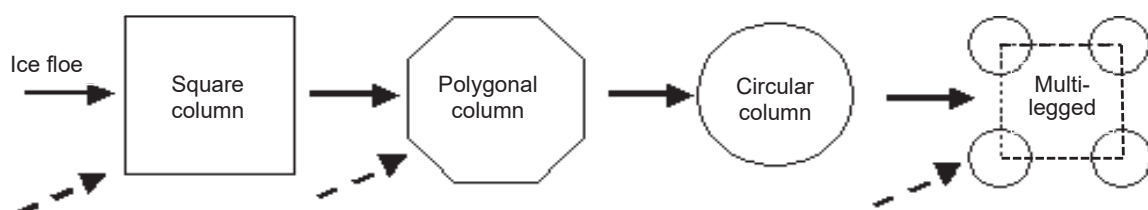


Fig. 7.17 Target structures—waterline shapes: Ice Load Estimation Program.⁷⁻²⁾

Ice Load Estimation Program is designed to analyze.

iii) Analysis Model

The calculation methodology is based on PSSII 2.0 (1995) (Program for Soil-Structure-Ice Interaction), a coupled interaction analysis program for soil, structures, and ice sheets developed by the Technical Research Centre (VTT) of Finland. The program has been refined further with improvements to the local ice sheet failure model (i.e., non-simultaneous multiple small-scale fracture).

7.5 Fundamental Research on Earthquakes in Ice-Covered Regions

1) Seismic Effects in Ice-Covered Regions

Since the Sea of Okhotsk is an earthquake-prone area within an ice-covered region, all marine structures are subject to both ice and seismic loads. Although the annual duration of ice coverage in the Sea of Okhotsk has been decreasing due to global warming, the possibility of simultaneous ice and seismic loads still exists. Sakhalin, located in the southeastern portion of this region, is crossed by numerous active seismic faults running north to south. For oil production facilities built along the eastern coast near these active faults, it is crucial that any seismic design consider the influence of sea ice.

The combination of ice and seismic loads on structures in ice-covered regions has long posed a challenge for designers. Listed below are three design approaches for accommodating both seismic and ice loads:

- a) Design for combined design seismic and ice loads: This approach adds the 100-year return period worst case seismic loads to those of the ice loads.
- b) Design for the larger of either the design seismic or ice loads.
- c) Design for seismic loads combined with typical ice loads: This approach incorporates ice loads based on the average annual maximum ice thickness rather than the 100-year return period worst case ice load.

Design approach **a)** is typically rejected because the simultaneous occurrence of maximum seismic and ice loads is highly improbable. Design approach **b)** has become commonly adopted, as shown in industry standards such as those of the American Petroleum Institute (API) and the Canadian Standards Association (CSA).

The JOIA study adopted design approach **c)** as being the most reasonable for its purposes: the ice load present during an earthquake would be based on the typical annual maximum ice thickness (i.e., 1 m in the Sea of Okhotsk) rather than the 100-year return period worst case ice thickness (i.e., 2 m). The JOIA study proposed the following equation for calculating the combined load F .

$$F = \alpha \varepsilon_i E$$

where E : Design Seismic Load

ε_i : Ice Sheet Influence Coefficient

α : Combined Load Factor

In scenarios where the Design Seismic Load is significantly larger than the Design Ice Load, it is assumed permissible to follow design approach **b)** or, equivalently, approach **c)** with the setting $\varepsilon_i = 1$. However, the rationale behind choosing the larger of the two loads and its impact on safety remains unclear—one of the reasons for the JOIA study.

Given this context, a study of the seismic effects on ice-covered structures in the Sea of Okhotsk was conducted 1996-2000, following the steps summarized below:

- i) Establish design conditions for oil production facilities in ice-covered seas.
- ii) Define the target ice-covered structures for the study.
- iii) Select structural types for ice-covered structures: vertical wall structures, sloping wall structures, gravity-based structures, and hybrid gravity-pile structures.
- iv) Investigate seismic and sea ice conditions in the Sea of Okhotsk.
- v) Assess seismic loads and ice loads.
- vi) Analyze the ground supporting the selected structures and the strength of structural components.
- vii) Develop a method to conduct a coupled vibration analysis on structures that incorporates information about the ground, seawater and sea ice conditions.
- viii) Conduct validation experiments using a large ice-sea vibration tank equipped with a large underwater vibration table.
- ix) Consolidate the research findings into a guideline, i.e., the *Seismic Design Manual*.

2) Parameters: Evaluating Earthquake Effects

Table 7.4 lists the main items evaluated; Fig. 7.18 illustrates the coupled vibration model of ice loads during an

Table 7.4 Key parameters: Evaluating earthquake effects.⁷⁻²⁾

Structure and Foundation	Structural type	Vertical wall, Sloping wall
	Foundation type	Gravity-based, Hybrid gravity-pile
Sea, Ice, Seismic, and Seabed conditions	Water depth	30 m
	Ice thickness	2 m (level ice)
	Horizontal seismic intensity	0.2
	Seabed	Sandy soil
Seismic input parameters	Elastic design level	Level I, 0.2 G
	Elasto-plastic design level	Level II, 0.6 G
	Excitation frequency	0.7 Hz
Analysis method	Modified NKK-VTT model	

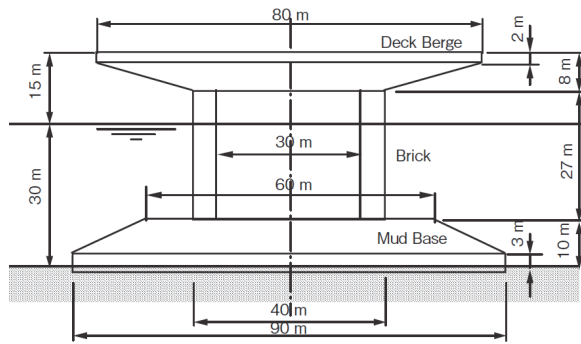
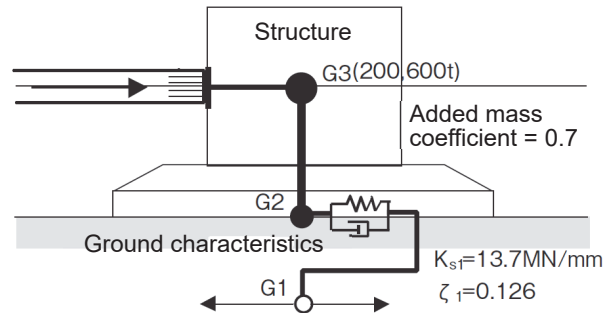


Fig. 7.18 Coupled Vibration Model of earthquake induced ice loads: Gravity-type vertical wall structure with very high rigidity relative to the ground.⁷⁻²⁾



earthquake for a gravity-based vertical wall structure.

3) Seismic Design Manual for Ice-Covered Regions

The seismic impact on structures installed in ice-covered sea areas was evaluated through water basin vibration testing and analysis, with findings compiled into the *Seismic Design Manual for Ice-Covered Regions*. The Sea of Okhotsk, located in a seismic zone, was chosen as the reference area for setting various design conditions. This manual is significant as it represents the first guideline developed specifically for the

design of structures in ice-covered seas affected by seismic activity. **Table 7.5** shows the contents of the *Manual*.

7.6 Design Guidelines for Structures in Ice-Covered Seas

The information in the *Design Guidelines for Structures in Ice-Covered Seas* comprehensively summarizes the research findings of the JOIA Ice Load Research Project. This guideline offers detailed instructions for calculating various

Table 7.5 Contents: Seismic Design Manual for Ice-Covered Regions.⁷⁻²⁾

Seismic Design Manual for Ice-Covered Regions	
<p>Chapter 1: General Provisions</p> <p>1.1 Purpose</p> <p>1.2 Scope of Application</p> <p>1.2.1 Applicable Sea Areas</p> <p>1.2.2 Structural Types</p> <p>1.3 Related Guidelines and Standards</p> <p>Chapter 2: Design Principles</p> <p>2.1 Seismic Design Philosophy</p> <p>2.1.1 Strength-Based Design (Elastic Design)</p> <p>2.1.2 Ductility-Based Design (Elasto-Plastic Design)</p> <p>2.2 Limit State Design Method</p> <p>2.3 Design Workflow</p> <p>Chapter 3: Design Conditions</p> <p>3.1 Functional Requirements</p> <p>3.2 Environmental Conditions</p> <p>3.2.1 Seismic Conditions</p> <p>3.2.2 Sea Ice Conditions</p> <p>3.2.3 Seabed Characteristics</p> <p>Chapter 4: Seismic Loads</p> <p>4.1 Seismic Loads in Icy Seas</p> <p>4.1.1 Seismic Loads in Landfast Sea Ice</p> <p>4.1.2 Seismic Loads in Drift Sea Ice</p> <p>4.1.3 Seismic Loads in Accumulated Ice</p> <p>4.2 Hydrodynamic Pressure Induced by Earthquakes</p> <p>4.2.1 Effects of Sea Ice on Hydrodynamic Pressure</p> <p>4.2.2 Methods for Calculating Hydrodynamic Pressure</p>	<p>Chapter 5: Stability and Structural Integrity</p> <p>5.1 Stability</p> <p>5.1.1 Structural Stability</p> <p>5.1.2 Foundation Stability</p> <p>5.2 Structural Integrity</p> <p>5.2.1 Component Strength</p> <p>5.2.2 Overall Structural Strength</p> <p>5.3 Seismic Resistance of Superstructures and Piping</p> <p>5.4 Performance Criteria for Structures</p> <p>Chapter 6: Seismic Behavior Analysis</p> <p>6.1 Coupled Seismic-Induced Vibration: Sea Ice, Seawater, Structure, and Ground</p> <p>6.1.1 Analysis Model</p> <p>6.1.2 Material Properties and Coefficients</p> <p>6.2 Experimental Studies on Coupled Vibration: Sea Ice, Seawater, Structure, and Ground</p> <p>Chapter 7: Structural Calculations</p> <p>7.1 Safety Verification Formulas</p> <p>7.2 Calculation of Cross-Sectional Force</p> <p>Chapter 8: Safety Evaluation</p> <p>8.1 Failure Modes and Probability of Failure</p> <p>8.2 Reliability Assessment of Ice-Covered Structures</p>

Table 7.6 Contents: Design Guidelines for Structures in Ice-Covered Seas.⁷⁻²⁾

Design Guidelines for Structures in Ice-Covered Seas	
Chapter 1: Introduction	5.1.4 Seismic Loads
1.1 Organization	5.1.5 Total Ice Load
1.2 Basic Concepts	5.1.6 Local Ice Load (P-A Curve)
1.3 Scope of Application	5.2 Load Combinations and Load Factors
Chapter 2: Definitions	Chapter 6: Calculation Examples
2.1 Definitions	6.1 Structures Considered in Calculation Examples
Chapter 3: Environmental Conditions	6.2 Wind Loads
3.1 Meteorology	6.3 Current Loads (Fluid Forces Due to Currents)
3.2 Wind	6.3.1 Gravity-Based Vertical Wall Structures
3.2.1 Basic Concepts	6.3.2 Gravity-Based Sloping Wall Structures
3.2.2 Wind Speed	6.3.3 Hybrid Gravity-Pile Vertical Wall Structures
3.2.3 Data from the Sakhalin Coastal Area	6.4 Wave Loads
3.3 Waves	6.4.1 Design Conditions
3.3.1 Basic Concepts	6.4.2 Wave Analysis
3.3.2 Wave Representation	6.4.3 Calculation of Wave Forces Due to Irregular Waves
3.3.3 Wave Data Collection	6.4.4 Calculation Results
3.3.4 Determining Design Waves	6.5 Ice Loads
3.4 Currents and Tides	6.5.1 Procedure for Calculating Ice Loads
3.4.1 Currents	6.5.2 Selection of Ice Load Calculation Formulas
3.4.2 Tides	6.5.3 Setting Probability Density Functions for Ice Conditions in the Target Sea Area
3.5 Ice Conditions	6.5.4 Probability Distribution of Ice Loads (Cumulative Relative Frequency)
3.5.1 Ice-Covered Areas	6.5.5 Characteristic Values of Ice Loads
3.5.2 Ice Formation Characteristics	6.5.6 Comments on Characteristic Values of Ice Loads
3.5.3 Ice Strength	Appendix
3.6 Earthquakes	Appendix A: Overview of Existing Guidelines
3.6.1 Basic Concepts	Appendix B: Representative Wave Spectra
3.6.2 Seismic Hazard Assessment	Appendix C: Statistical Properties of Ridge Parameters
3.6.3 Evaluation of Seismic Motion	Appendix D: Strength of Level Ice (Reference Strength)
Chapter 4: Environmental Loads	Appendix E: Evaluation of Existing Ice Load Estimation Formulas Based on Molikpaq Ice Load Measurements
4.1 General	Appendix F: Review of Level Ice Load Estimation Formulas for Sloping Structures
4.1.1 Regular Loads	Appendix G: Review of Keel (Unconsolidated Layer) Load Calculation Methods
4.1.2 Operational Loads	Appendix H: Coupled Vibration Response Analysis of Hybrid Gravity-Pile Vertical Wall Structures
4.1.3 Accidental Loads	Appendix I: Study on the Probability of Simultaneous Occurrence of Seismic and Ice Loads
4.1.4 Environmental Loads	Appendix J: Review of Standards Related to Return Periods
4.2 Environmental Loads	Appendix K: Calculation Method for Ridge Ice Encounter Probability
4.2.1 Wind Loads	Appendix L: Derivation of the Proposed P-A Curve
4.2.2 Wave Loads	
4.2.3 Current Loads	
4.2.4 Seismic Loads	
4.2.5 Ice Loads	
4.2.6 Impact of Ice-Structure Interaction on Seismic Loads	
Chapter 5: Characteristic Load Values	
5.1 Characteristic Load Values	
5.1.1 Wind Loads	
5.1.2 Wave Loads	
5.1.3 Current Loads	

loads—such as wind loads, wave loads, current-induced loads, seismic loads, and ice loads—when designing structures in ice-covered regions. **Table 7.6** shows the contents of the *Guidelines*.

7.7 Conclusion

The JOIA Ice Load Research Project, initiated in 1993 and completed in 2000, was a great effort in ice engineering research, involving over 50 research institutions and companies (including observer participants) and more than 100 researchers and engineers. The scope of the project ranged from conducting technical surveys to using field experiments on in situ natural sea ice, ice model basin experiments, and water basin seismic impact tests that led to the development of an ice load estimation program and, ultimately, to the creation of the *Seismic Design Manual for Ice-Covered Regions* and *Design Guidelines for Structures in Ice-Covered Seas*.

From its inception, the JOIA project attracted significant attention both domestically and internationally, with contributions concerning experiments and data analyses from ice researchers worldwide. The project's methodologies, analytical approaches, and commitment to open data dissemination were highly regarded, ultimately enabling Japan's participation in the development of the international standard *ISO 19906 (Petroleum and natural gas industries—Arctic offshore structures)*. The inclusion of the project's findings in this standard represents a major accomplishment.

Despite the successful completion of the JOIA project in 2000, the expected contributions of Japanese companies to the construction of structures and infrastructure development in ice-covered regions have unfortunately failed to meet initial expectations.

From a technical research and development perspective, the primary objective of this project was to establish a rational

method for estimating ice loads on structures in ice-covered seas and to apply this method to the design and construction of such structures. The ice load estimation method that was developed accounts for the dynamic nature of ice loads due to ice sheet fracturing—the method is particularly suited for the behavior analysis of bottom-founded structures under varying loads. **Figure 7.19** (pp.58-59) presents an overview of the JOIA Ice Load Research Project, 1993-2000.

References

- 7-1) Sodhi, D.S., K. Kato, and F.D. Haynes. (1983, Dec.). *Ice Force Measurements on a Bridge Pier in the Ottauquechee River, Vermont*. CRREL Report 83-32.
- 7-2) JOIA. (2000). *FY1993-2000, Marine Petroleum Development Technology Survey: Fundamental Research on Offshore Structures in Extreme Marine Environments — A Study on Ice Loads on Offshore Structures*, Final Report. Japan Ocean Industry Association (JOIA). (in Japanese).
- 7-3) Joensuu, A. and K. Riska. (1989). *Contact Between Ice and a Structure*. Report M-88, Helsinki University of Technology, Laboratory of Naval Architecture and Marine Engineering.
- 7-4) Sodhi, D.S., T. Takeuchi, N. Nakazawa, S. Akagawa, and H. Saeki. (1998, Dec.). Medium-scale indentation tests on sea ice at various speeds. *Cold Regions Science and Technology, Vol. 28, Issue 3*, 161-182.
- 7-5) Takeuchi, T., M. Sakai, S. Akagawa, N. Nakazawa, and H. Saeki. (2001, Dec. 31). On the Factors Influencing the Scaling of Ice Forces. *IUTAM Symposium on Scaling Laws in Ice Mechanics and Ice Dynamic; Proceedings of the IUTAM Symposium held in Fairbanks, Alaska, U.S.A., 13-16 June 2000*, 149-160. Springer Dordrecht. ISBN 978-1-4020-0171-0.
- 7-6) Nakazawa, N. (2022, Mar.). Research and Engineering Development on Sea Ice. *Journal of the Center of the History of Japanese Industrial Technology, Mar. 2022*, 100-186. National Museum of Nature and Science. (in Japanese).

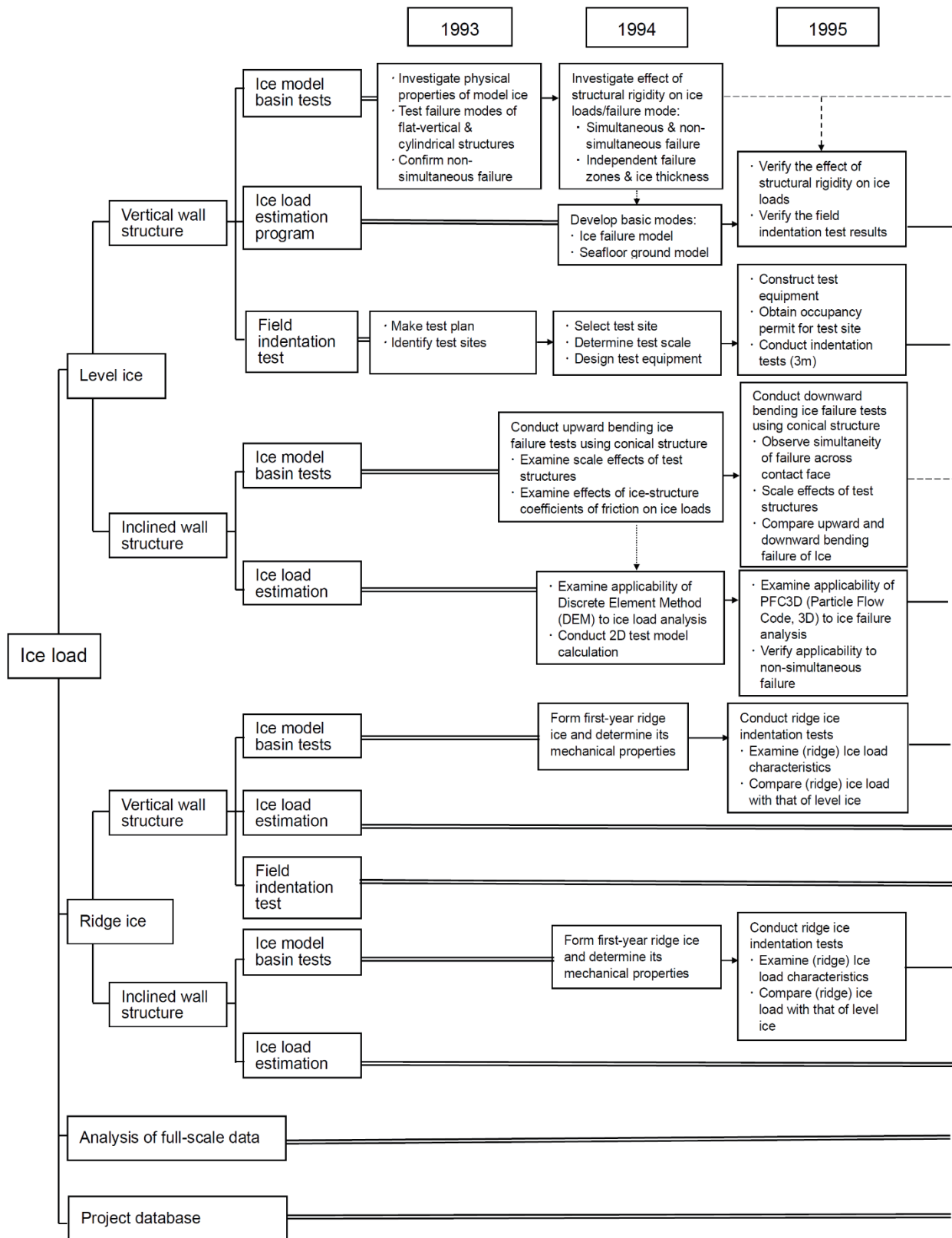


Fig. 7.19 Overview of the JOIA Ice Load Research Project.⁷⁻⁶⁾

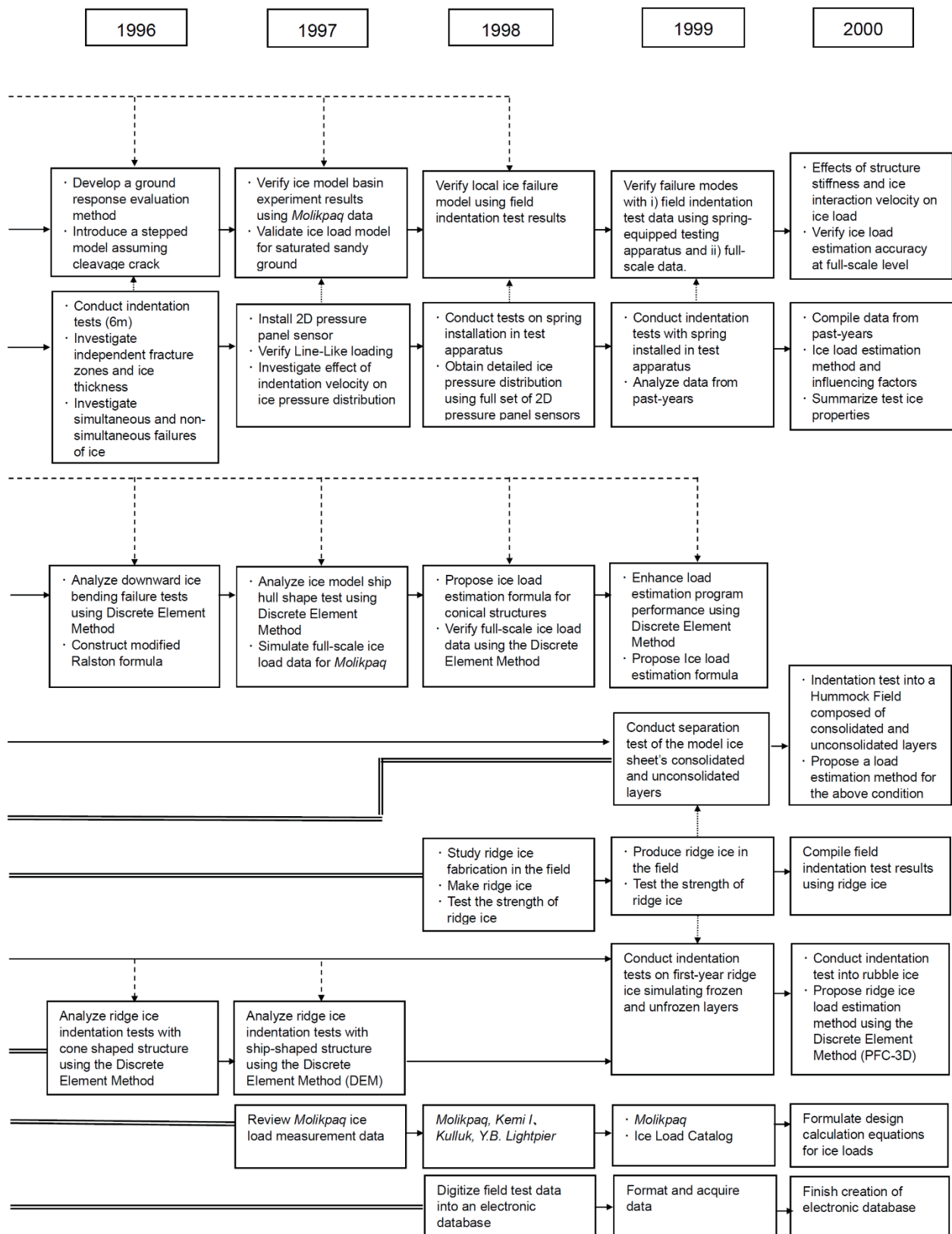


Fig. 7.19 (continued) Overview of the JOIA Ice Load Research Project.⁷⁻⁶⁾

– Addendum 4 –

1) Publication of JOIA Research Results Abroad

The research results of the project have been actively disseminated both domestically and internationally starting in 1994, increasing substantially from 1997 as analyses began to progress, see the table below. Internationally, the results were regularly presented at the following symposia:

- International Society of Offshore and Polar Engineering Conference (ISOPE)
- International Association for Hydro-Environment Engineering and Research (IAHR)
– IAHR International Symposium on Ice
- International Union of Theoretical and Applied Mechanics Conference (IUTAM)

Notably, ISOPE paid particular attention to the JOIA project by establishing the annual JOIA Ice Research Session. This session had become a venue for an ongoing discussion of JOIA project results among international researchers.

Additionally, joint seminars were held with Dartmouth College (Hanover, New Hampshire) and CRREL, and open experiments were conducted with foreign researchers at the natural sea-ice field experiment site on Lake Noto, Abashiri. These efforts contributed to Japan's involvement in the development of ISO 19906.

JOIA Project: Number of Papers Presented at Conferences.

Conference	1994	1995	1996	1997	1998	1999	2000	2001	Total
International	–	–	5	8	19	9	11	11	63
Domestic	1	5	10	6	3	11	4	–	40
Total	1	5	15	14	22	20	15	11	103



JOIA-Dartmouth College Joint Seminar, 1998.



JOIA-CRREL Joint Seminar, 1998.



Experiments open to international researchers, field experiment site, Lake Noto, Abashiri, 1999.



ISOPE JOIA Ice Research Session, 2000.

2) Personnel Involved in the JOIA Ice Load Research Project

The JOIA Ice Load Research Project (1993-2000) involved approximately 50 research institutions and companies, involving over 100 researchers and engineers. In October 2018, a reunion of participants in the JOIA project was attended by Dr. Devinder Sodhi (United States); the project chairperson, Dr. Hiroshi Saeki (then professor at Hokkaido University); and the vice-chairpersons, Dr. Ken-ichi Hirayama (then professor at Iwate University) and Dr. Masayuki Hyodo (then professor at Yamaguchi University); among others (total 23).

As of 2024, many of the project's participants have retired. In Japan, there has been a decline in snow- and ice-related engineering education at universities and research institutions, and industry involvement in ice sea technology also has decreased. Given the reduction in Arctic sea ice due to global warming, with the resulting development of new Arctic shipping routes and continuing exploitation of oil and gas resources, there is a pressing need to rejuvenate Japan's ice engineering research to maintain its competitive edge.



Reunion of participants in the JOIA Ice Load Research Project: October 2018, 23 attendees.
Photograph provided by Dr. Satoshi Akagawa.

8 | Offshore Ice-Resistant Structures

8.1 Types of Offshore Ice-Resistant Structures

In this section, “offshore ice-resistant structures” refers to facilities installed in ice-covered seas, primarily used for oil and natural gas development. **Figure 8.1** presents a general classification of these structures. Offshore facilities in ice-covered regions must not only facilitate resource extraction and transportation but also ensure operational safety. The selection of the appropriate structural type is based on several factors, including water depth, ice thickness, ice movement speed, presence of icebergs, distance from construction location to installation site, and economic considerations. These structures are generally categorized into artificial islands, bottom-mounted structures, and floating structures.

a) Artificial Islands: Typically constructed in shallow coastal waters (up to approximately 15 m in depth),

these structures are formed by piling gravel and sand from the seabed and/or sediment from shore to create an island-like foundation. While offering significant resistance to ice forces, they require large quantities of gravel.

b) Bottom-Mounted (-Founded) Structures: Primarily divided into piled- and gravity-based structures, the choice depends on factors such as water depth, seabed conditions, and the magnitude of ice forces. For gravity-based structures, larger water depths may necessitate a larger foundation to maintain stability.

c) Floating Structures: Often deployed in deeper offshore areas, floating structures are advantageous due to their mobility, allowing them to be relocated once development in a specific area is completed. Ship-shaped designs can enable emergency evacuation from the danger of icebergs.

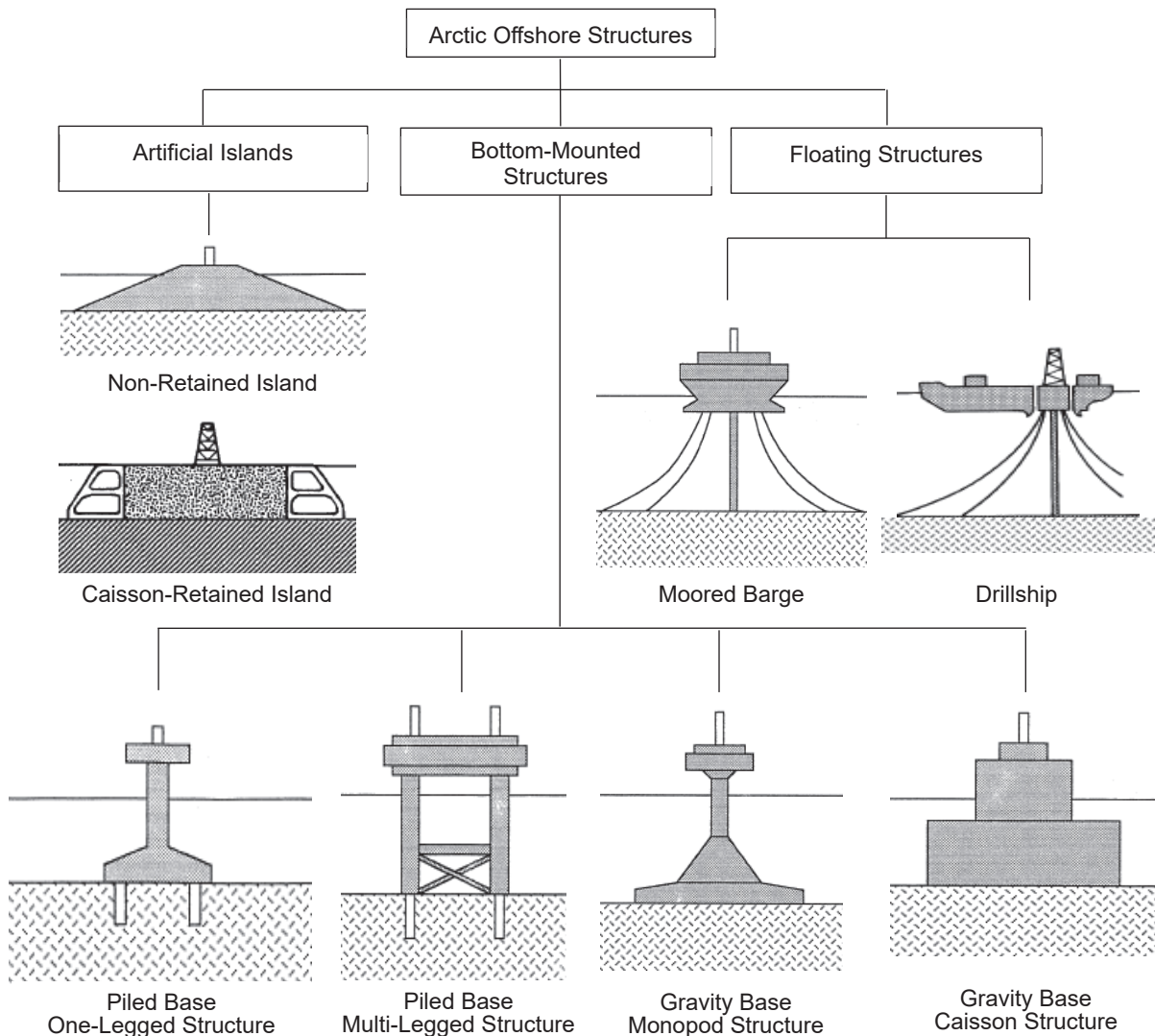


Fig. 8.1 Offshore Ice-Resistant Structures, types: Artificial islands, Bottom-mounted structures, Floating structures.⁵⁻⁴⁾

8.2 Oil and Natural Gas: Beaufort Sea

The discovery of oil and natural gas resources in the North Slope region of the northernmost area of Alaska and Canada and Canada bordering the Beaufort Sea (see Fig. 8.2) during the late 1960s has led to active exploration and development in the Arctic. In the 1970s and 1980s, over 140 exploratory wells were drilled in the Beaufort Sea by the United States and Canada. Figure 8.3 indicates the locations of oil and natural gas exploration in the Canadian sector.

Initially, exploratory drilling was limited to onshore sites. However, activities gradually extended offshore, utilizing existing islands or constructing artificial islands in very shallow waters by transporting sediment from nearby land or using dredged materials for land reclamation and embankment construction. The ice conditions in these areas typically involved landfast ice, i.e., ice that is attached to the shore or seabed



Fig. 8.2 The North Slope, northernmost region of Alaska and Canada bordering the Beaufort Sea: Area within the dashed line shown in Fig. 8.3.⁸⁻¹⁾

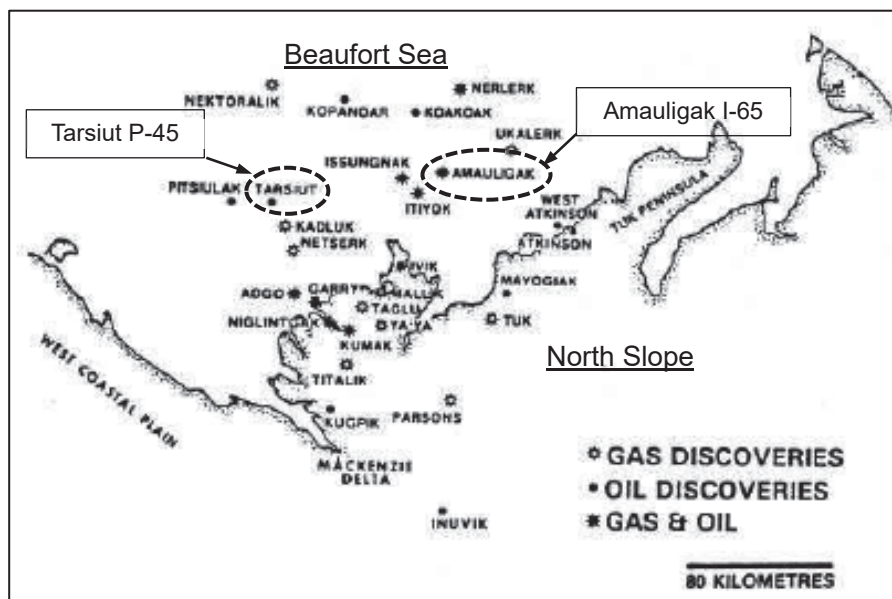


Fig. 8.3 Oil and natural gas exploration sites: North Slope, northernmost area of Canada bordering the Beaufort Sea, 1970s and 1980s (area within the dashed line in Fig. 8.2).⁸⁻¹⁾

and remains stationary, and first-year ice, i.e., ice that forms and melts within a single winter season. Consequently, the ice forces exerted by moving ice sheets were relatively minor.

As exploration moved further offshore, water depths increased, increasing the challenges posed by sea ice, including drifting ice. This led to the consideration of various structural types, as illustrated in Fig. 8.1. The selection of an appropriate structure was evaluated on factors such as the distance from shore to the installation site, water depth at this site, volume of sediment/gravel/sand required, ice thickness, ice movement, presence of icebergs, and duration of the ice season.

8.3 Evolution of Offshore Ice-Resistant Structures

1) Earth-Filled Artificial Islands

In the 1970s, earth-filled artificial islands were constructed in shallow waters by depositing gravel/sand/sediment, either dredged from the seabed near the installation site or transported from land, to create a stable platform for exploration facilities. However, this method was limited to relatively shallow waters, a maximum feasible depth of only a few dozen meters. As the water depth increased, several challenges became apparent. The construction of these islands required large quantities of gravel, which was difficult to source and transport. The construction process was further complicated by the harsh environmental conditions, leading to extended project timelines. Environmental concerns also arose due to the extensive dredging and placement of material into the sea. Moreover, the immobility of these islands posed a significant drawback—each new exploration site required the construction of a new artificial island, resulting in high costs.

Figure 8.4 shows an example of an earth-filled artificial island constructed in the Beaufort Sea, off the coast of Canada.



Fig. 8.4 Earth-filled artificial island, Beaufort Sea, constructed late 1970s, photograph: Structure surrounded by sandbags to withstand external forces from waves and sea ice.⁸⁻¹⁾



Fig. 8.5 Floating drillship, photograph: Support vessels needed to remove sea ice to lessen impact on the drillship.⁸⁻¹⁾

2) Floating Drillship

In the mid-1970s, floating drillships were developed to operate in deeper waters where earth-filled artificial islands were not feasible.

Figure 8.5 shows a drillship deployed by Dome Petroleum in the Beaufort Sea during the summer. The drillship, being anchored in place with mooring lines to prevent changes in position/direction, was vulnerable to collisions from moving ice sheets. To minimize the impact of this ice, support vessels were required to break and remove any surrounding the drillship. Despite these challenges, this design enabled exploration in waters up to approximately 60 m deep.

Figure 8.6 depicts the *Kulluk* (drill barge), a reverse conical floating structure built in 1983. Designed by Gulf Canada Resources and constructed by Mitsui Engineering & Shipbuilding Co., Ltd., the *Kulluk*'s structure was engineered to bend and break ice sheets downward upon impact. This design allowed operations to continue into the early winter season. The structure of the *Kulluk* is described in more detail in Section 8.7.



Fig. 8.6 *Kulluk* (drill barge), reverse conical floating structure, photograph: Built by Mitsui Engineering & Shipbuilding Co., Ltd., 1983.⁸⁻¹⁾

3) Mobile Caisson Islands

The previously mentioned earth-filled artificial islands could operate throughout the year but were limited to shallow waters of only a few dozen meters: they also faced economic and environmental difficulties due to the large quantities of sediment/gravel required. Floating drillships/barges could be used in deeper waters, but they could only operate when sea ice conditions, such as ice thickness and ice forces, were not

severe, making year-round operation difficult.

In the 1980s, the introduction of specialized caisson structure artificial islands enabled operations in deeper waters and permitted year-round activity, even under harsh winter conditions with thick ice. Listed below are five representative types of specialized caisson structures, with specifications listed in Table 8.1:

- a. Tarsiut Caisson
- b. Single Steel Drilling Caisson (SSDC)
- c. Caisson-Retained Island (CRI)
- d. Molikpaq
- e. Super CIDS (Concrete Island Drilling System)

Table 8.1 Mobile Caisson Islands operated in the Beaufort Sea, 1980s onwards.⁸⁻¹⁾

Structure Name	a. Tarsiut	b. SSDC	c. CRI	d. Molikpaq	e. Super CIDS
Annual operating days	365	365	365	365	365
Base area (m ²)	7,947	18,590	10,875	12,383	8,551
Wave height resistance (m)	12	12.2	15	12.2	5.2
Flat Ice thickness resistance (m)	5.6	10	3	10	2
Design Ice Load (MN)	560	900	436	640	640
Design Ice Pressure (MPa)	4.1	8.3	0.7	2.3	2.3
Owner/Operating company	GCR*1	DOME*2	ESSO	GULF Oil	Global Marine
Construction company	CMD*3	Hitachi Zosen	–	IHI, Corp.	NKK

*1Gulf Canada Resources Inc., *2Dome Petroleum Ltd. *3Canadian Marine Drilling Ltd.

8.4 SSDC (Single Steel Drilling Caisson)

1) Conversion: Crude Oil Tanker to Ice-Resistant Oil Drilling Rig

SSDC (Single Steel Drilling Caisson) is an oil drilling rig that was constructed (or more accurately, converted) by Hitachi Zosen Corporation in 1982 and operated in the Beaufort Sea until 2006 (Fig. 8.7). The rig was originally the crude oil tanker *Ujigawa Maru*, completed in 1972 by Kawasaki Heavy Industries at the Sakaide Shipyard (DWT—deadweight tonnage, maximum carrying capacity—of 232,000 t; total length of 320 m). The ship, then named *World Saga*, was acquired by Canadian Marine Drilling and, in 1982, converted from a crude oil tanker to an ice-resistant oil drilling rig at Hitachi Zosen’s Sakai Shipyard (Fig. 8.8). Only the forward portion of the original hull was used, with the reconfigured vessel reinforced to withstand ice by adding 7,000 t of steel and 13,000 t of concrete on the inside of the hull, increasing its thickness by 1 m. The reinforced hull was outfitted with a topside structure weighing about 4,000 t, including an oil derrick, cranes, helipad, and living quarters, transforming it into an ice-resistant drilling rig. In addition, the bow portion of the ship was scrapped.

Upon conversion, the former *World Saga* was renamed the ice-resistant drilling rig SSDC and operated in the Beau-



Fig. 8.7 SSDC, photograph: Actively used for exploration in the Beaufort Sea from the mid-1980s.⁸⁻¹⁾

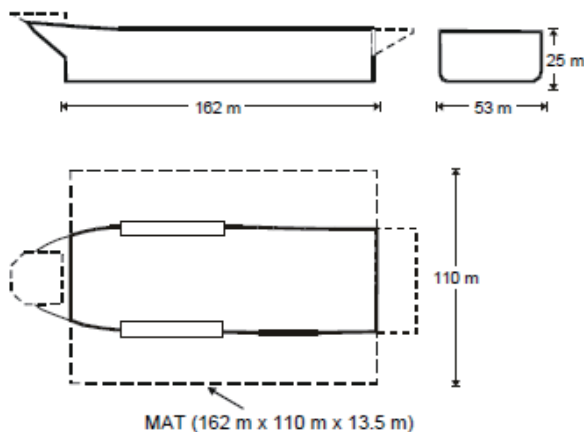


Fig. 8.8 Dimensions: SSDC and MAT.⁸⁻¹⁾

fort Sea from August 1983 until the early 2000s. The SSDC made it possible to conduct year-round operations in ice-covered regions with water depths of around 30 m: classified as a MODU (Mobile Offshore Drilling Unit) by the American Bureau of Shipping. Although the SSDC was designed by a U.S. company, the actual conversion relied on the substantial engineering and technical expertise of Hitachi Zosen Corporation’s “scrap and build” technique in transforming an ordinary tanker into an ice-resistant drilling rig.

2) Submersible barge MAT

Figure 8.9 shows the submersible barge MAT, constructed in 1986 by Hitachi Zosen Corporation for use with the SSDC. This barge featured an innovative design, with steel layers bonded using high-density urethane. Prior to the introduction of MAT, installing the SSDC at the drilling site required extensive seabed preparation, including excavation and the formation of a berm. However, by placing the MAT directly on the seabed, the need for such groundwork was significantly reduced. Additionally, the MAT improved resistance to the ice forces from moving ice sheets, allowing year-round operations. Figure 8.10 illustrates a typical MAT and SSDC installation.



Fig. 8.9 Submersible barge MAT, constructed for SSDC, photograph: Innovative structure—steel layers bonded using high-density urethane.⁸⁻¹⁾



Fig. 8.10 Typical installation, MAT/SSDC in ice-covered seas: Significantly reduced seabed preparation work + Improved resistance to ice forces from drifting ice.⁸⁻¹⁾

8.5 *Molikpaq*: Mobile Arctic Caisson Island

1) World's First Mobile Artificial Island

In the 1970s, structures for resource development in ice-covered seas included earth-filled artificial islands as well as ice islands created by spraying seawater onto ice sheets to form artificial ice foundations. These were primarily used in shallow waters (depths ranging from 0 to a few dozen meters). Later, floating drillships capable of offshore operations were introduced, but they faced challenges related to anchoring in deeper waters and resisting ice forces, which prevented year-round operation. In the 1980s, the SSDC and specialized caisson structures emerged as mobile artificial islands. The caisson method involved filling the interior of the artificial island with sediment, which, through shear mass, helped to withstand ice forces and anchor the island to the seabed.

The *Molikpaq* is the world's first steel-based, bottom-founded ice-resistant structure designed for oil drilling that is also capable of year-round operation even under the harsh ice load conditions of the Beaufort Sea winter. Commissioned by Gulf Canada Resources Inc., the octagonal donut-shaped steel caisson and steel box deck were manufactured at IHI Corporation's Aichi Works, while the topside modules were fabricated in Canada and transported there for installation and integration. The *Molikpaq* was completed in 1984, towed to the Beaufort Sea that same year, and operated at several drilling sites in the region (Fig. 8.11).



Fig. 8.11 *Molikpaq* operating amid moving ice sheets, Beaufort Sea, Canada, photograph.⁸⁻²⁾

2) Relocation and Installation

Molikpaq is composed of three primary sections: steel caisson forming the base of the artificial island, deck, and topside modules (Fig. 8.12). The interior of the donut-shaped caisson, occupied by multiple tanks, functions as ballast with a capacity of approximately 85,000 t. Once the structure is positioned at the drilling site, ballast water is injected into the multiple tanks to anchor the caisson to the pre-leveled seabed.

The hollow core of the steel caisson is then filled with sand, which provides resistance to the horizontal forces exerted by moving ice sheets.

For relocation, a portion of the sand is removed, and the ballast water is drained from the tanks, enabling the structure to float and be towed to a new location. This mobility facilitates efficient oil development operations. Figure 8.13 depicts the installation and relocation process.

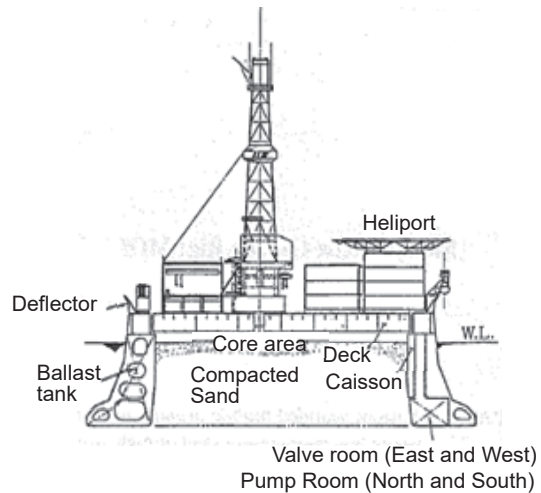


Fig. 8.12 Cross-section of the *Molikpaq*: (bottom to top) Steel Caisson artificial island, Deck section, Topside.⁸⁻³⁾

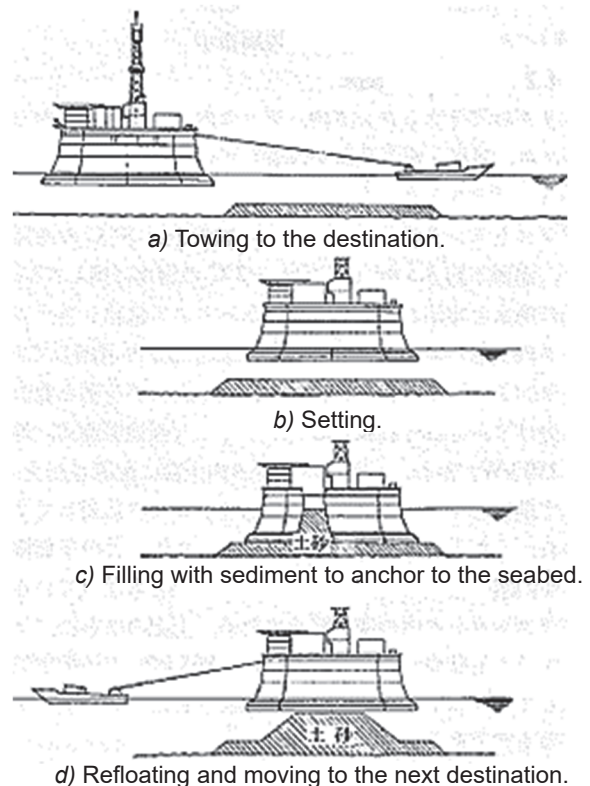


Fig. 8.13 *Molikpaq* usage concept: Location, Installation, Relocation.⁸⁻³⁾

3) Design Features

Molikpaq is not only the world's first mobile artificial island, but is also capable of year-round operation, even under the

challenging winter ice load conditions of the Beaufort Sea. Its specialized caisson structure design features several noteworthy innovations—summarized in **Table 8.2** (details in **Ref. 8-3**):

- i) Mobile bottom-founded artificial island: World’s first example of this type of drilling rig—capable of year-round operation in ice-covered seas with water depths ranging from 15 to 40 m.
- ii) High-strength, low-temperature steel: Caisson design incorporates high-tensile steel specifically designed to withstand ice pressures at temperatures as low as -50°C; certain sections of the base utilize high-tensile steel with a strength of 70 kgf/mm² (686 MPa, Class 70); exterior walls of the caisson sloped to reduce the compressive forces caused by ice growth around the structure.
- iii) Specialized coating: Caisson surfaces near the water-line coated with a special urethane resin to resist/minimize ice adhesion, impact, friction, and low temperatures.
- iv) Anti-freezing measures: To prevent the freezing of seawater and sand inside the ballast tanks and core areas, insulation applied to the top of the ballast tanks and the underside of the deck as well as hot air supplied to these regions. Additionally, extensive heat tracing and insulation applied to exposed pipes.
- v) Independent deck structure: Deck supported by rubber bearings to absorb, through shear deformation, any horizontal displacement of the caisson; deck designed to be entirely independent of the caisson to prevent the transmission of horizontal caisson movement resulting from ice pressure.

Table 8.2 *Molikpaq* specifications.⁸⁻³⁾

Structural Specifications	
Bottom size	111.00 × 111.00 m
Top deck size	86.60 × 86.60 m
Core area size	74.40 × 74.40 m
Height (depth)	29.00 m (to the Top Deck)
Maximum draft when settled	21.34 m
Maximum draft when moving	16.79 m
Gross tonnage	42,317 t
Ballast water capacity	106,250 m ³
Accommodation capacity	100
Maximum drilling depth	6000 m
Operating water depth	15 - 40 m
Classification	ABS A1 Caisson Drilling Unit

4) Construction Method

The construction of *Molikpaq* at IHI’s Aichi Works, see **Fig. 8.14**, involved overcoming numerous challenges, including the structure’s dimensions exceeding the dock width and the need for strict adherence to delivery deadlines. The following description of the construction method, summarized from **Ref. 8-4**, outlines how these challenges were overcome.

The caisson, 111 × 111 m, exceeded the 92-meter width of IHI’s construction dock, so the following construction techniques were employed for the project:

niques were employed for the project:

- i) Pontoon installation: A pontoon (barge) was installed inside the dock, and the caisson was constructed on top of it. The dimensions of the pontoon were determined by the dock’s width and depth, as well as the quay’s water depth required to float and separate the caisson from the pontoon.
- ii) Height adjustment structure: To align the pontoon’s deck level with the ground level of the dockside, the pontoon was placed on an adjustable temporary structure of supports and beams for height adjustment, thus enabling the caisson’s construction on the pontoon despite its dimensions exceeding the site’s dock width.
- iii) Asymmetric positioning: To make effective use of the construction site’s two Goliath cranes, the octagonal caisson was positioned asymmetrically within the dock. This positioning allowed construction activities to be carried out more efficiently, important because of the strict project timeline.
- iv) Launching the caisson: Being the most critical phase of the construction process with no margin for error due to time constraints, a prior structural analysis was conducted on the complex changes in load conditions that would occur to ensure success and safety (caisson, beams, and pontoon treated as an integrated frame structure). At launch, the pontoon, with the caisson still attached, was floated and moved out of the dock.
- v) Deck installation: Deck installed after caisson launching; a 3000-tonf (29.4 MN) class floating crane lifted and placed the large block deck on the 59 rubber bearings installed on the caisson.

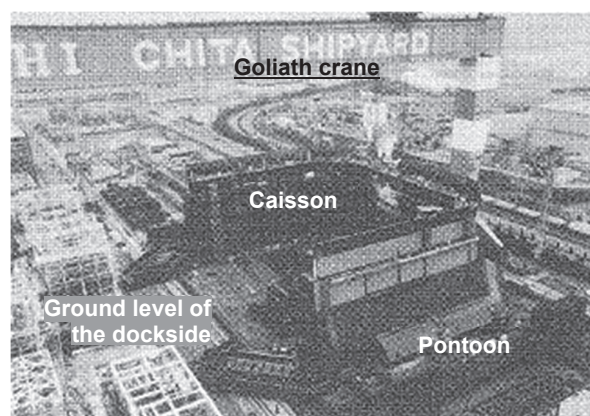


Fig. 8.14 *Molikpaq* under construction, IHI Aichi Works: Caisson, width of 111 m; wider than 92 m wide dock, the left side of the caisson protrudes.⁸⁻³⁾

5) Ice Load Measurements: *Molikpaq*

An international joint project measured ice loads on the *Molikpaq*: Gulf Canada Resources (owner), IHI Corp. (builder), and several oil companies from the United States, Canada, and the United Kingdom. This project collected a substantial amount of ice load data in 1986 at the Amaulikag I-65 site in the Beaufort Sea (see Fig. 8.3). These data provided critical

insights into the accuracy of ice load estimations on offshore ice-resistant structures that significantly influenced the direction of future research on ice load estimation.⁸⁻⁴⁾

The information contained herein provides neither the specifics of the ice load measurements mentioned above, nor the numerous significant results that were obtained from these real-world measurements. For detailed information on the load measurement methods and results, refer to Timco (2002)⁸⁻¹⁾; For a comparison between actual and model test loads, see Kato (1995)⁸⁻⁴⁾.

6) History of *Molikpaq*: Conception to the Arctic Ocean and the Sea of Okhotsk

Molikpaq, commissioned by Gulf Canada Resources Inc.: Swan Wooster Engineering (SWS) (Canada) produced the initial concept and basic design but worked with Ishikawajima-Harima Heavy Industries Co., Ltd. (now IHI Corporation) to produce the detailed design. In collaboration with the client and SWS, IHI developed construction methods, welding techniques for low-temperature steel, specialized coatings, and a thermal insulation construction method.⁸⁻⁴⁾

Molikpaq was completed in April 1984, and on June 11 of the same year, it departed IHI's Aichi Works. Towed by three large tugboats, it arrived in the Beaufort Sea off Canada in early August, where it commenced drilling operations at the Tarsiut P-45 site (refer to Fig. 8.3). The operational history of *Molikpaq* in this region is summarized in **Table 8.3**.

Subsequently, *Molikpaq* was modified at Daewoo Shipbuilding in South Korea to meet the specifications required for the Sakhalin II project in the Sea of Okhotsk. In September 1998, it was relocated to the waters off Sakhalin. As of 2021, *Molikpaq* continues to operate in the Piltun-Astokhkoye-A field, located 16 km offshore. The oil and natural gas produced by *Molikpaq* are transported via pipeline to the Prigorodnoye refinery at the southern tip of Sakhalin, from where they are shipped to Japan and South Korea.

Figure 8.15 shows the route of *Molikpaq* from the Beaufort Sea to Sakhalin; **Fig. 8.16** illustrates its operational site and the pipeline route to Prigorodnoye.



Fig. 8.15 *Molikpaq* route, Beaufort Sea to Sakhalin: modifications made at Daewoo Shipbuilding in South Korea while en route, illustrated by the author.

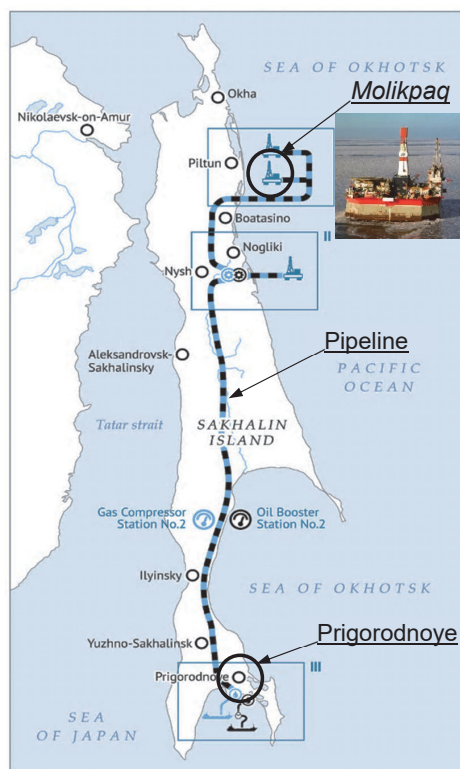


Fig. 8.16 *Molikpaq* location, 2021: oil and natural gas transported via pipeline to Prigorodnoye, refined before shipment to Japan.⁸⁻⁵⁾

Table 8.3 Operational history of *Molikpaq*: Beaufort Sea.⁸⁻⁶⁾

Oil well name	Operator	Operation start date	Operation end date	Water depth (m)
W. TARSUUT P-45	Gulf	1984.9.25	1984.12.24	22
AMAULIGAK I-65	Gulf	1985.9.24	1986.1.21	23
AMAULIGAK I-65A	Gulf	1986.1.28	1986.3.20	23
AMAULIGAK I-65B	Gulf	1986.3.20	1986.9.19	23
AMAULIGAK F-24	Gulf	1987.10.1	1988.8.12	32
AMAULIGAK 2F-24	Gulf	1987.12.22	1988.1.29	32
AMAULIGAK 2F-24A	Gulf	1988.1.30	1988.2.17	32
AMAULIGAK 2F-24B	Gulf	1988.4.15	1988.8.7	32
AMAULIGAK CH NO.1	Gulf	1988.8.12	1988.9.7	32
AMAULIGAK 2F-24BST	Gulf	1988.6.27	1988.8.7	32
ISSERK I-15	Imperial	1989.11.11	1990.1.8	12
Piltun-Astokhkoye	Sakhalin Energy	1990.7.1	In operation	30

8.6 Super CIDS: Mobile Artificial Island

1) World's First Hybrid Structure Artificial Island

Super CIDS (Concrete Island Drilling System), a mobile artificial island specifically conceived for Arctic operations, was designed by Global Marine Development Inc. (GMD, USA) and constructed by Nippon Kokan (now JMU). The design of this offshore oil drilling rig features an innovative hybrid structure combining steel and concrete by incorporating a lightweight, high-strength concrete caisson (Concrete Basic Brick, described below), stacked (vertically) between steel structures on both the top and bottom—a pioneering construction method recognized globally.

The floating Concrete Basic Brick (BB-44) structure, designed to endure substantial ice forces, was constructed in just seven months by a joint venture between Penta-Ocean Construction Co., Ltd. and Shimizu Corporation.

This project also attracted significant attention due to its exceptionally short construction timeline of just nine months: contract awarded to Nippon Kokan, September 1983. Adhering to the schedule, the completed rig was delivered to GMD



Fig. 8.17 Super CIDS mobile artificial island in operation, Beaufort Sea, Alaska, photograph.⁸⁻⁸⁾

on May 30, 1984, and named Glomar Beaufort Sea.⁸⁻⁷⁾ **Figure 8.17** depicts the Super CIDS in operation in the Beaufort Sea.

2) Structural Features

The Super CIDS structure consists of a three-tiered configuration—from the seabed upwards:

- i) Steel Mud Base (SMB): steel structure in contact with the seabed, height of 7.6 m.
- ii) Concrete Basic Brick (BB44): floating concrete sec-

Table 8.4 Structural specifications of Super CIDS.⁸⁻⁷⁾

Classification	ABS, Mobile Offshore Drilling Unit
Principal dimensions	94 m × 89 m × 30 m
Total weight	Approximately 56,000 t
Design conditions	Ambient temperature: -50°C to +26°C
	Seawater temperature: -3°C
	Ice thickness: 1.95 m (winter first-year ice) 7.5 m (summer multi-year ice)
	Water depth: 10.5 m to 16.5 m
	Wave Height: 5.1 m (significant wave height)
Main structures: Construction sites	Deck Storage Barge (DSB): Tsu Works No. 2 Dock.
	Concrete Basic Brick (BB-44): Tsu Works Repair Dock by a joint venture of Penta-Ocean Construction Co., Ltd. and Shimizu Corporation.
	Steel Mud Base (SMB): Tsurumi Works Central Base.

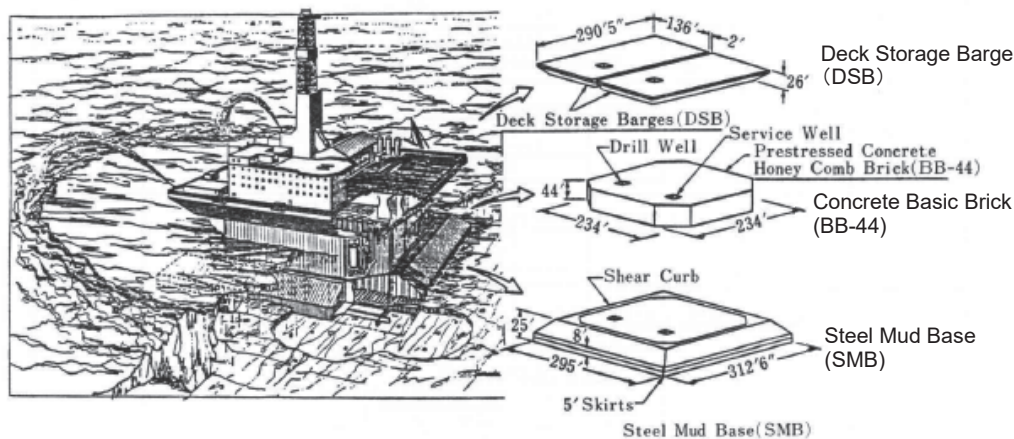


Fig. 8.18 Diagram, three-layer structure of Super CIDS: bottom layer, Steel Mud Base (SMB); middle layer, Concrete Basic Brick (BB-44); top layer, Deck Storage Barge (DSB).⁸⁻⁷⁾

tion, height of 13.4 m.

- iii) Deck Storage Barges (DSB): steel deck barges that house drilling equipment and living quarters, height of 7.9 m.

Each of these three components is a floating structure, allowing mobility. Once on site, the previously floating Steel Mud Base and Concrete Basic Brick sections are submerged by filling them with seawater, but they can be refloated by draining the water. **Table 8.4** provides the structural specifications, and **Fig. 8.18** illustrates the three-layer structure.

3) World's First Freeze-Thaw Resistant High-Strength Lightweight Concrete

One of the most noteworthy aspects of the Super CIDS construction is the use of freeze-thaw resistant high-strength lightweight concrete. The Concrete Basic Brick (BB-44) section, directly encountering the impact of moving ice sheets, is centrally located between the Steel Mud Base (SMB) and the

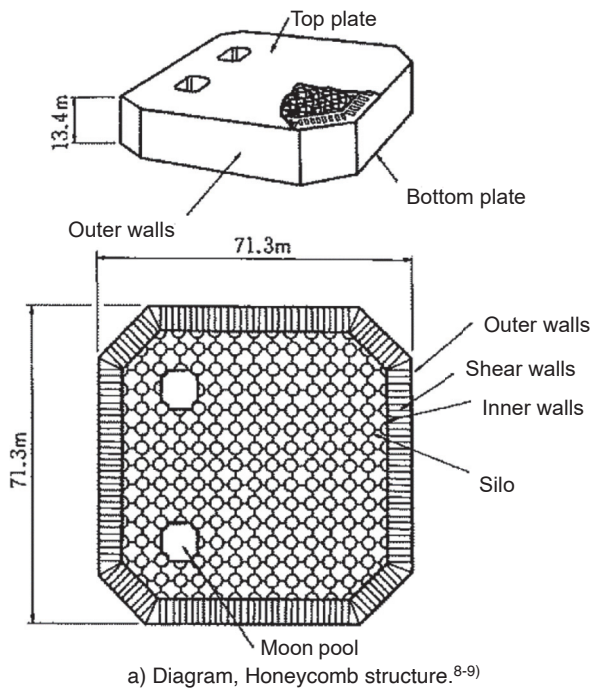


Fig. 8.19 Concrete Basic Brick (BB-44), Super CIDS:
a) Honeycomb structure; b) Construction of Honeycomb structure (aerial view), photograph.

steel Deck Storage Barge (DSB) sections, effectively sandwiching BB-44. As shown in **Fig. 8.19**, the structure of BB-44 is octagonal.

The primary structural components—bottom plate, outer walls, top plate, shear walls, inner walls, silos, and connection walls—together form a honeycomb structure. The shear walls and inner walls are constructed from high-strength conventional concrete, while all other components utilize high-strength lightweight concrete. Each of these materials was required to meet stringent ASTM (American Society for Testing and Materials) freeze-thaw resistance standards: Super CIDS, the first of its kind to use this concrete.

To prevent cracking, a prestress of 35 kgf/cm² (3.5 MPa) was applied horizontally to the top plate, bottom plate, and outer walls. Additionally, the outer, inner, and shear walls were prestressed vertically with deformed PC reinforcing steel bars of ϕ 32 or ϕ 36. The outer and inner walls together with the shear walls form the flanges and webs, respectively, of structures that function as I-beams, supported by the top and bottom plates, designed to resist horizontal ice pressure.⁸⁻⁷⁾

Table 8.5 presents the design compressive strength and unit weight of the concrete used in the floating BB-44 section. Note that the 2021 Japan Society of Civil Engineers' Concrete Standard Specifications' definition of high-strength concrete has a design compressive strength of 60 N/mm²: the concrete used in the BB-44 shown below was considered high strength in the 1980s.

Table 8.5 Concrete specifications:
Concrete Basic Brick (BB-44), Super CIDS.⁸⁻⁹⁾

Parameter	Required Performance
Unit Volume Weight	Lightweight: 1.84 t/m ³ or less Normal weight: 2.48 t/m ³ or less
Design Standard Strength	Lightweight: 45.7 N/mm ² or more Normal weight: 2.48 N/mm ² or more
Total Chloride Content in Concrete	0.06% or less by weight of cement as chlorine
Air Content (at placement)	7±2%
Freeze-Thaw Durability Index	80% or more after 300 freeze-thaw cycles: based on ASTM C666 Method A

4) Ice-Resistant Structure

The reasons for selecting concrete structures for the Super CIDS, beyond economic considerations, are as follows:⁸⁻⁹⁾

- i) Excellent strength characteristics at low temperatures, with minimal issues related to low-temperature brittleness.
- ii) Sufficient resistance to freeze-thaw cycles.
- iii) Structural integrity capable of withstanding localized concentrated loads from ice.
- iv) Durability against waves and spray.
- v) Sufficient weight to provide the necessary horizontal resistance to ice and wave forces.
- vi) Ease of maintenance in the severe natural environment of the Arctic Ocean.

5) Construction and Project Management System

The contract for Super CIDS was awarded on September 7, 1983, with completion set for May 30, 1984—a remarkably short construction period of just nine months. Considering that only seven months was allotted to construct the floating concrete section BB-44 with special high-strength lightweight concrete, stringent project management practices, including meticulous schedule and quality control, were vital (see Fig. 8.20).

The complexity and strictness of the inspection and control system were driven by several factors listed below:⁸⁻⁹⁾

- i) Certification requirements: As a floating and mobile artificial island, the structure had to pass inspections and receive certifications as a vessel from both the United States Coast Guard (USCG) and the American Bureau of Shipping (ABS).
- ii) Multiple stakeholder involvement: The project involved multiple stakeholders with their own dedicated inspectors conducting rigorous inspections from various perspectives.
- iii) Design challenges: The initial design provided by the owner consisted of only ten basic drawings, from which all the detailed design drawings had to be developed.

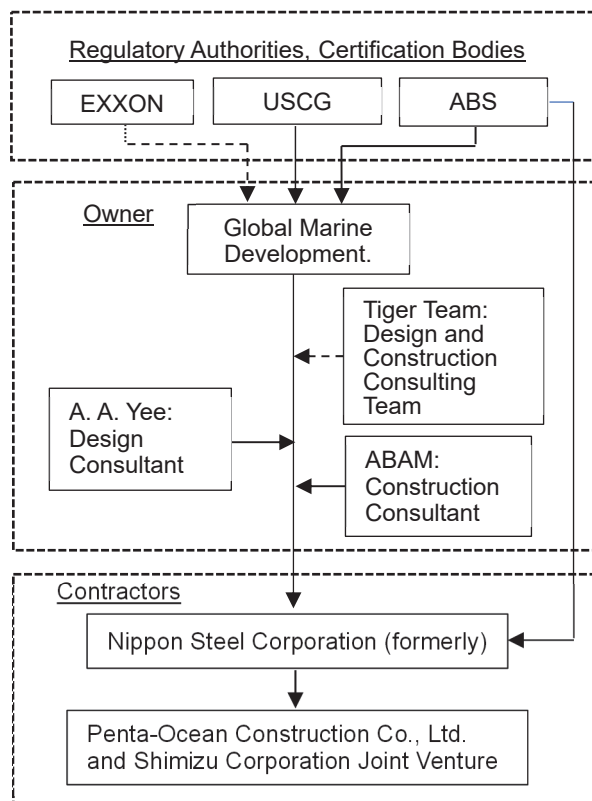


Fig. 8.20 Project Management and Quality Control System: Concrete Basic Brick (BB-44).⁸⁻⁹⁾

6) Conclusion

This section draws heavily on the work of Hiroshi Watanabe (1984)⁸⁻⁷⁾ and Yoshiro Ono et al. (1985)⁸⁻⁹⁾. Watanabe concludes his paper with the following remarks that capture

the profound sense of accomplishment and the pioneering spirit of the engineers who completed this world-first project in such a short period:

After completion, the artificial island, towed by two 20,000-horsepower tugboats, set sail in early June 1984. About two months later, it arrived in the Beaufort Sea off the coast of Alaska. The drilling operations, which began in November of the same year, proceeded smoothly, with two wells already drilled. The rig has been operating safely without any trouble to date.

This offshore structure construction project presented several significant challenges:

- i) An exceptionally short project timeline.
- ii) The project required precise fabrication using high-strength lightweight concrete with excellent freeze-thaw resistance.
- iii) The construction involved a complex offshore stacking of large structural components.
- iv) The project uniquely brought together the expertise of shipbuilders and construction companies to develop a new product.

For us, this was an incredibly meaningful experience and a first in many respects. Thanks to the dedicated efforts and cooperation of all involved, the project was successfully completed.

Receiving the Japan Petroleum Institute Award for Technological Progress has been an encouragement to all involved, and we are determined to continue embracing new technological challenges.⁸⁻⁷⁾ (trans. by author)

It is worth noting that the Super CIDS received the 1984 Japan Petroleum Institute Award for Technological Progress and the Japan Society of Civil Engineers Technology Award.

8.7 Kulluk: Floating Drilling Unit

1) World's First Mobile Floating Drilling Unit

The *Kulluk*, classified as a Conical Drilling Unit (CDU), was the world's first mobile floating oil drilling rig designed for the Arctic Ocean: built in 1983 by Mitsui Engineering & Shipbuilding Co., Ltd. and delivered in April 1983 to Gulf Canada Resources, Inc.⁸⁻¹¹⁾ It was developed to operate in the challenging polar environment, where the supply of drilling materials was difficult—The *Kulluk* aimed to extend the continuous operation period from the approximately 120 days typical of conventional drillships to over 200 days.

Unlike previous structures such as the SSDC, *Molikpaq*, and Super CIDS, which were bottom-founded, the *Kulluk* presented an almost circular floating structural shape, secured in position by wire mooring ropes.

Figures 8.21 and 8.22 show the *Kulluk* in operation encircled by sea ice in the Beaufort Sea, Canada, and diagrams of its general structural with notable inverted conical profile, respectively; Table 8.6 presents structural specifications.



Fig. 8.21 *Kulluk* operating amidst sea ice, Beaufort Sea, Canada, photograph.⁸⁻¹⁾

Table 8.6 *Kulluk* structural specifications.⁸⁻¹¹⁾

Category	Specifications
Classification	ABS, +A1, Barge, Drilling Unit
Structural Shape	Inverted cone floating structure
Main Dimensions	Length: 83.78 m, Width: 84.48 m
Radius	40.50 m (Main deck level)
Depth	18.50 m
Draft	12.50 m (max. during transit)
Gross Tonnage	29,147 t
Personnel Capacity (max.)	108
Drilling Depth (max.)	6,100 m
Ice Thickness	1.2 m
Temperature	Air: -50°C, Seawater: -2°C
Hull Structure Compliance	a) Arctic Pollution Prevention Class 1V b) ABS Ice Strengthened Class 1AA

2) Structural Features

The *Kulluk*, an oil drilling barge, had several distinctive features tailored for operations in ice-covered seas. In particular, its structure was based on a 24-sided regular polygon (in plan view) with an inverted-cone cross-sectional shape (see Fig. 8.22)—unprecedented at the time. Below are the key structural features:⁸⁻¹¹⁾

- i) Hull shape: *Kulluk*'s inverted-cone shape, see Fig. 8.22, designed to reduce ice loads by bending and breaking incoming ice sheets downward.
- ii) Hull structure: Each deck from the keel to the main deck divided into 15-degree segments, with each segment reinforced with robust radial web plates extending from the (inner) moon pool to the outer hull to provide strength against ice pressures.
- iii) Mooring system: *Kulluk* moored radially using 12 winches with 3.5-inch (89 mm) diameter wire ropes.
- iv) Riser protection from floating ice debris: Protection for the riser pipes provided by ice deflectors installed around the hull and an ice shield of the hull.
- v) Cold-resistant steel plates: Structural components made of high-tensile steel with sufficient toughness to withstand ice forces at temperatures as low as -50°C (air) and -2°C (seawater)—welding joint toughness designed to be equivalent to that of the steel plates.
- vi) Corrosion protection for hull plates: Hull coated with 1 to 2.5 mm of 100% solid polyurethane, offering excellent resistance to impact, abrasion, extreme cold, and seawater to provide long-term durability.

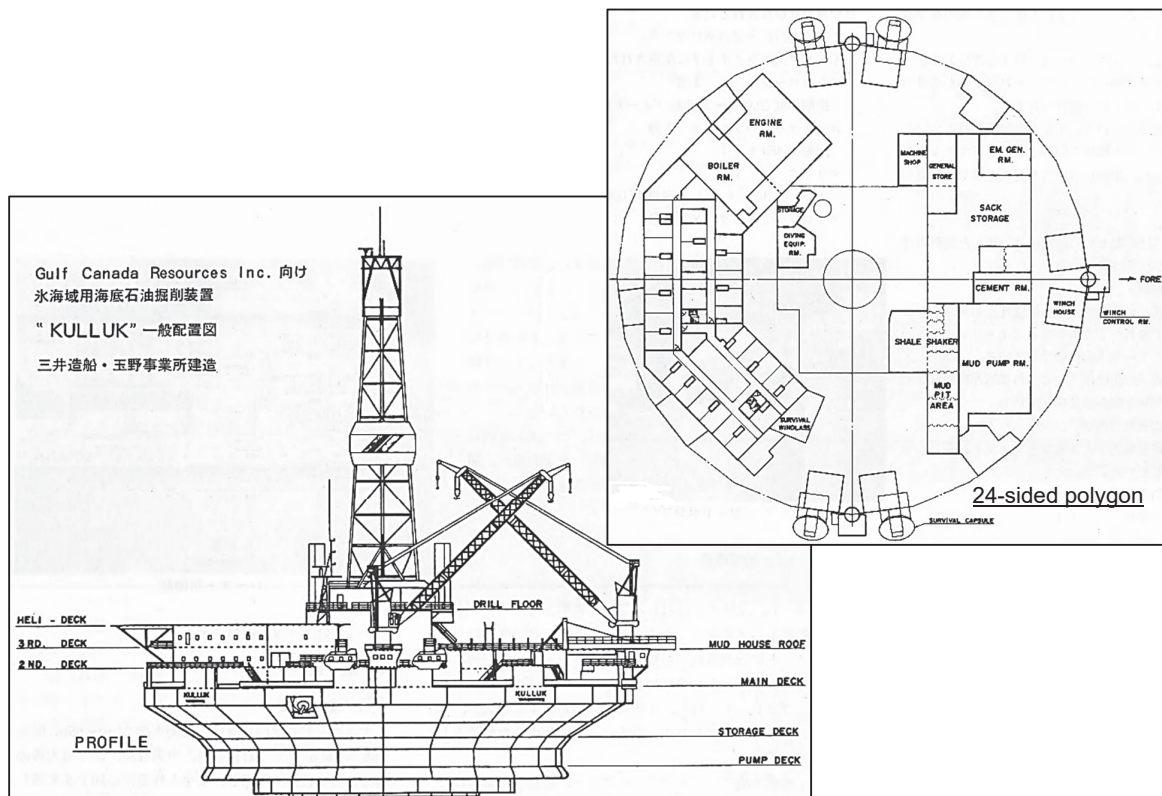


Fig. 8.22 *Kulluk*, structure diagrams: Side view (left), inverted cone in cross-section; Plan view (top right), nearly circular 24-sided polygon.⁸⁻¹¹⁾

- vii) Corrosion protection for exposed and internal areas: Goal of achieving a maintenance-free finish by employing a heavy-duty anti-corrosion system that featured a base coat of alkali silicate solution and zinc dust inorganic paint, followed by epoxy paint.
- viii) Living quarters: Designed for up to 108 personnel—55 double-occupancy rooms, offices, dining hall, movie room, recreation facilities, medical room, and shop to ensure a comfortable living environment for workers in polar conditions.

3) Operational History: Aftermath of the *Kulluk*

The *Kulluk* left Mitsui Engineering & Shipbuilding’s Tama-no Works in April 1983, loaded drilling equipment in the Aleutian Islands, and began drilling operations in the Beaufort Sea, Canada, in August of the same year. Its operational history in the Beaufort Sea is listed in **Table 8.7**: 10 wells drilled between August 1983 and September 1989.

The *Kulluk* was operated by Gulf Canada Resources from 1983 to 1993, after which it remained inactive for nearly a decade. In 2005, it was sold to Shell Oil, refurbished, and operated off Alaska’s North Slope. However, in December 2012, while being towed to its winter home port of Seattle, the *Kulluk* ran aground after the towline from the tugboat snapped. Although it was transported to Singapore for repairs, Shell ultimately decided to decommission the *Kulluk*, and it was dismantled in China in March 2014.

8.8 Ice Boom in Lake Saroma: Drift Ice Inflow Control Facility

1) Lake Saroma: Japan’s Largest Brackish Lake

Lake Saroma, the largest brackish lake in Japan, is located along the northeastern coastline of Hokkaido. Facing and connected to the Sea of Okhotsk, the lake spans the cities of Kitami, Saroma Town, and Yubetsu Town: surface area of 150.96 km², surface elevation of 0.0 m MSL (Mean Sea Level), maximum depth of 19.6 m, average depth of 8.7 m, and circumference of 92 km. In terms of surface area, it is the third largest lake in Japan, following Lake Biwa and Lake Kasumigaura.

As shown in **Fig. 8.23**, Lake Saroma is separated from the Sea of Okhotsk by a narrow sandbar that extends 25 km. However, it connects to the open sea through two inlets: The First inlet, approximately 250 m wide, is the one located closer to the middle of the sandbar; the Second inlet is about 50 m wide. The lake is classified as a marine area under Japan’s fisheries law and known for its thriving aquaculture, particularly scallop and oyster farming. Additionally, the lake supports the production of various marine species such as salmon, as well as the native Hokkai shrimp, making it a vital site for sustainable fishery operations.

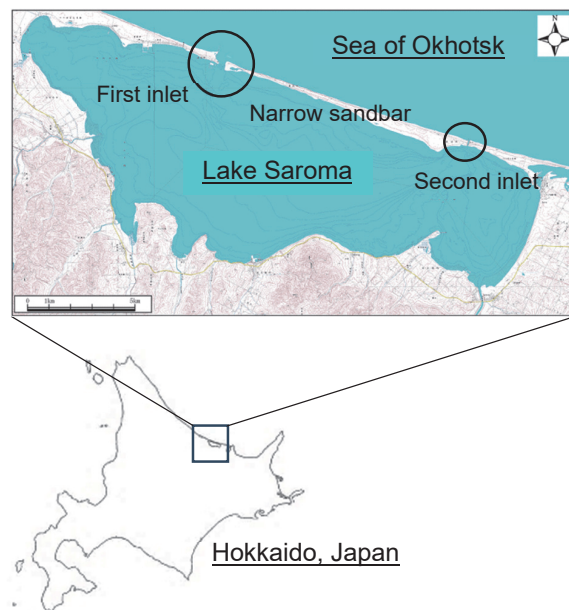


Fig. 8.23 Lake Saroma, location of First and Second inlets connecting to the Sea of Okhotsk: Both inlets located centrally in the sandbar—First Inlet, about 250 m wide; Second Inlet, about 50 m wide.

2) Inflow of Drift ice: Damage to Aquaculture

Drift ice typically arrives in Japan along the coast of the Sea of Okhotsk between late January and early February. Historically, the lake usually freezes over during the winter, so the fully frozen lake would prevent entry of any drift ice.

Table 8.7 *Kulluk*: Operational history in the Beaufort Sea.⁸⁻⁶⁾

Well Name	Operator	Drilling start date	Drilling end date	Water depth (m)
PITSIULAK A-05	Gulf	1983.8.22	1984.7.26	27
AMAULIGAK I-44	Gulf	1983.10.7	1983.11.15	20
AMAULIGAK J-44	Gulf	1983.11.16	1984.9.23	31
NERLERK J-67	Dome	1984.9.26	1985.10.24	45
AKPAK P-35	Gulf	1984.10.17	1985.11.8	41
AKPAK 2P-35	Gulf	1985.7.8	1985.8.14	41
AAGNERK E-56	Gulf	1985.10.28	1986.6.26	20
AMAULIGAK O-86	Gulf	1988.6.30	1988.8.26	20
IMMIUGAK N-05	Gulf	1989.6.1	1989.6.10	32
IMMIUGAK A-06	Gulf	1989.6.16	1989.9.22	53

However, if the drift ice arrives before the lake is fully frozen, as shown in **Fig. 8.24**, it can flow into the lake through its two inlets and cause significant damage to aquaculture facilities.

The complete freezing of Lake Saroma has been occurring later in the season since the 1970s. In the 1960s, lake freeze over (surface completely frozen) typically occurred from mid to late December, but by the 1990s, this event had shifted to late January/early February. In 1974, the lake did not fully freeze over, leading to an inflow of drift ice that caused ¥2.3 billion in damage to aquaculture facilities. Similar incidents of damage occurred frequently since then (see **Fig. 8.25**). In addition to facilities damage, any drift ice that remained in the lake could obstruct the departure of fishing vessels from port after the drift ice that had landed on the coast detaches and moves offshore in the spring (from March to April), necessitating icebreaking operations. These challenges often resulted in significant revenue losses.

As a result, counter measures were considered to prevent the inflow of drift ice into Lake Saroma, leading to the installation of an ice boom, a protective structure designed to control the entry of ice sheets into the lake. After the main facilities of the ice boom were completed in 1998, there have been no reported incidents of damage to aquaculture facilities caused by drift ice or of delays to resuming fishing operations in the Sea of Okhotsk immediately after the coastal ice drifts offshore.



Fig. 8.24 Aerial photograph: First lake inlet, drift ice entering Lake Saroma before installation of ice boom.⁸⁻¹²⁾

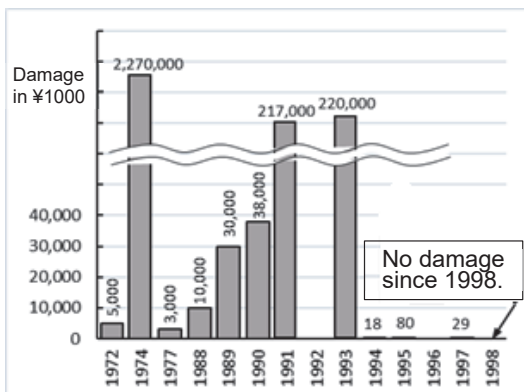


Fig. 8.25 Lake Saroma: Damage to aquaculture facilities from influx of drift ice—no damage reported since 1998.^{8-12, 13)}

3) Structure: Ice Boom

The ice boom at Lake Saroma was conceived as part of a project by the Hokkaido Regional Development Bureau: designed by the bureau's Abashiri Development and Construction Department and constructed by Nishimuragumi Co., Ltd. (Yubetsu, Hokkaido). Construction began in 1994, the ice boom became operational in 1998, and related facilities were completed in 2001.

The ice boom was installed on the lake side of the First inlet to Lake Saroma. Centered approximately 400 m inland from the lake's inlet, the fixed support structure of the ice boom consists of (14) pillars at intervals of 110 m, forming a semicircle: each pillar comprising four steel pipe piles driven into the lakebed and connected by an upper concrete section. These pillars are connected by 130 m long main wire cables with attached 1.2-meter diameter cylindrical floats. The ice boom is composed of net wires suspending horizontal chains underwater from the main wire cables and floats, which together with additional horizontal net wires form a net-like barrier capable of withstanding a load of approximately 500 tons per section transmitted to the pillars as tension through the main wires.

Below is a summary of the design conditions of the Lake Saroma ice boom; **Fig. 8.26** illustrates structural details of the ice boom.

- Flow velocity: General section (located at ends) 1.0m/sec; Special section (central portion) 1.4 m/sec
- Wind speed (10 m above water surface): 20 m/sec
- Wave height (Significant wave height): 4.1 m
- Wave period: 12.5 s
- Ice condition: unconsolidated ice floes
- Representative ice floe diameter: 5 m

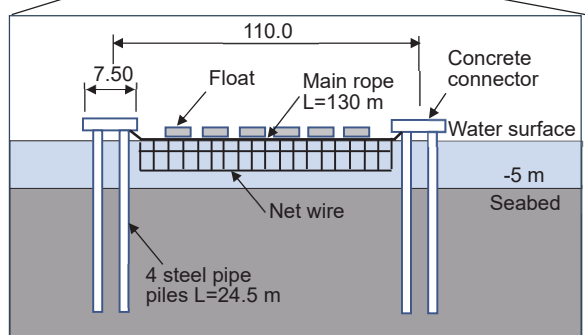
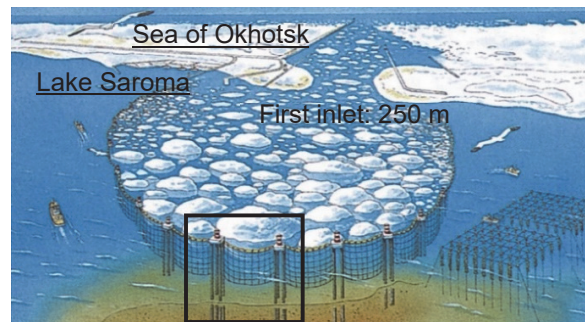


Fig. 8.26 Ice Boom structure: upper diagram, overall conceptual view; lower diagram, details of ice boom between support pillars.⁸⁻¹³⁾

- Ice thickness: over 2 m
- Total length of accumulated ice against the ice boom: 1250 m

4) Ice Boom, Drift Ice Control Structure: Highly Evaluated Internationally

The ice boom at Lake Saroma was the world's first ice control structure specifically designed to manage drift ice (sea ice). Prior to this, ice booms were primarily used in rivers in the United States and Canada to capture relatively small ice fragments during the early stages of ice formation: effective in flows with velocities below 0.7 m/sec, based on installed experience.

On the other hand, controlling the thicker and larger drift ice fragments that occur under normal conditions, where flow velocities can exceed 1 m/sec and wave forces can exist, required the development of new design methodologies beyond existing knowledge and practices. Additionally, it was necessary to consider the impact of sediment drift, seawater exchange, and the presence of scenic areas such as national parks.

The Lake Saroma Fishing Port Drift Ice Inflow Countermeasure Committee, established in 1991, led the discussion and development of this project. The structural design, choice of materials, and design of the floats all resulted from a series of technological advancements achieved through research conducted by a team led by Dr. Hiroshi Saeki, then a professor at Hokkaido University's Faculty of Engineering. The design methodology, presented in a keynote lecture at the 1992 IAHR Ice Symposium, received high praise from leading ice engineering nations.⁸⁻¹³⁾

The photo in Fig. 8.27 shows the installed ice boom effectively preventing the inflow of drift ice into Lake Saroma.

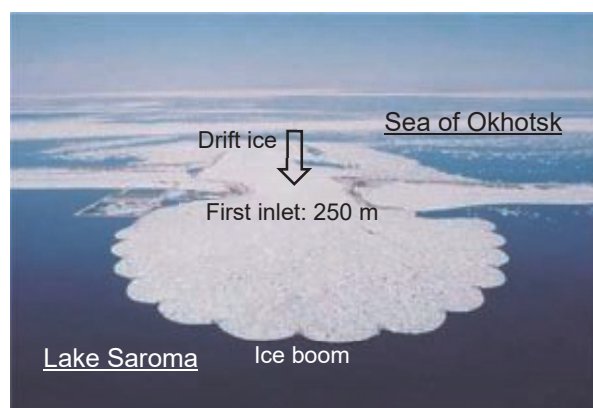


Fig. 8.27 Aerial photograph: Ice inflow prevented by ice boom, First inlet, Lake Saroma.⁸⁻¹²⁾

8.9 Conclusion

The 1980s saw Japanese shipbuilding companies playing a significant role in constructing oil drilling platforms for icy seas. Additionally, in 1998, the world's first drift ice control boom was constructed in Lake Saroma. In summary, the time-

line below places these developments in a context of global events:

- 1956: Japan becomes leading shipbuilding nation.
- October 1973: First oil shock.
- January 1979: Second oil shock.
- March 1982: World's first tanker-to-SSDC conversion completed.
- April 1983: World's first mobile floating drilling unit, *Kulluk*, completed.
- April 1984: World's first mobile artificial island, *Molikpaq*, completed.
- May 1984: World's first hybrid system artificial island, Super CIDS, completed.
- September 1985: Onset of rapid yen appreciation following the Plaza Accord.
- 1998: World's first large-scale ice boom designed to control drifting sea ice began operation.

Japan's shipbuilding industry experienced rapid growth from the 1960s to the mid-1970s. However, the two oil shocks led to a decline in demand, turning the industry into a structurally depressed sector. This was further compounded by the sharp appreciation of the yen following the 1985 Plaza Accord, forcing the industry to undergo structural adjustments, such as downsizing and streamlining. By 1988, South Korea had nearly equaled Japan's shipbuilding output.

In response to the drop in shipbuilding after the oil shocks, Japan sought new business opportunities in marine structures, particularly in building oil drilling facilities in icy regions, which had gained attention as a new frontier for resource development. However, Japan faced challenges in securing contracts for ice-resistant structures due to a lack of experience in marine structures, the stringent requirements set by major oil companies (specifications, deadlines, etc.), and a reduced price competitiveness resulting from a strengthening yen.

Despite the Japanese shipbuilding industry's global reputation for high quality, advanced research and development capabilities, and strict adherence to deadlines, its entry into the market for ice-resistant structures coincided with a period of significant political and economic upheaval worldwide, a matter of unfortunate timing beyond its control.

References

- 8-1) Timco, G. W. and Johnston, M. E. (2002, Nov.). *Caisson Structures in the Beaufort Sea 1982-1990: Characteristics, Instrumentation and Ice Loads*. Technical Report, CHC-TR-003. Canadian Hydraulics Centre, National Research Council of Canada.
- 8-2) IHI Co., Ltd.: Offshore Group, Ship & Offshore Engineering Department. (2000, Dec. 27). *MORIKPAQ (1984), PRINCIPAL CHARACTERISTICS*.
https://www.ihico.jp/offshore/morikpaq_e.htm
- 8-3) IHI. (1984, Nov.). Mobile Arctic Caisson Rig: MOLIKPAQ for Gulf Canada Resources Inc. (Canada). *IHI Engineering Review*, Vol. 24, No. 6, 445-450. (in Japanese).
- 8-4) Kato, K. and Y. Kumakura. (1995). Prediction of Ice Forces on

- Arctic Structure MOLIKPAQ. *Journal of the Society of Naval Architects of Japan*, Vol. 177, 141-146. (in Japanese).
- 8-5) Gazprom. (viewed December 2022).
https://www.gazprom.com/f/posts/39/853008/map_sakhalin_2_e2016-10-17.png.
- 8-6) Callow, L. (2013, Mar.). UPDATED, *Oil and Gas Exploration & Development Activity Forecast, Canadian Beaufort Sea 2013-2028*. Beaufort Regional Environmental Assessment, Aboriginal Affairs and Northern Development Canada.
- 8-7) Watanabe, H. (1986). Construction of the Mobile Drilling Platform (Super CIDS) for Arctic Use. *Sekiyu Gakkaishi*, Vol. 29, No. 3, 201-211. (in Japanese).
- 8-8) Shimizu Corp. (n.d.). *Mobile Artificial Island for Oil Drilling SuperCIDS* [trans. from Japanese].
https://www.shimz.co.jp/works/jp_har_198403_supersizzu.html.
- 8-9) Ono, Y., T. Suzuki, M. Niwa, and M. Iguro. (1985). Construction of Mobile Arctic Drilling Island. *Journal of Japan Society of Civil Engineers*, No. 354/V-2, 43-52. (in Japanese).
- 8-10) Indo, M. (2021, Mar. 20). *Future Vision - Shimizu Dream* [in Japanese]. Presentation materials of Rikuryo Alumni Association.
- 8-11) MES. (1983). Overview of KULLUK, the World's First Offshore Oil Drilling Unit for Arctic Use. *Journal of the Japan Society of Naval Architects and Ocean Engineers*, Vol. 36, No. 7, 69-75. (in Japanese).
- 8-12) Hokkaido Regional Development Bureau. (n.d.). *Key Technologies in Fishing Ports, Measures to Prevent the Inflow of Drift Ice Using Ice Booms* [trans. from Japanese].
https://www.hkd.mlit.go.jp/ky/ki/kouhou/70th/full/data/03/03/03-03_02.pdf.
- 8-13) Hirayama, K. (1995). Ice Boom in Lake Saroma—World's First Ice Control Structure to Prevent Drift Ice. *Journal of Japan Society of Civil Engineers*, Vol.80 No.9, 6-9. (in Japanese).

- Addendum 5 -

Ice Boom: Lake Saroma



“Protecting Aquaculture Facilities From Drift Ice: Ice Boom Rope [Re-]Installation Begins [for Winter], Saroma”
(November 28, 2013, Hokkaido Shimbun Press)



A net designed to hold back drift ice. During non-winter seasons, it is brought ashore and kept in storage, awaiting its next deployment during the following drift ice season.

Zero Drift Ice Damage and Enhanced Fisheries Productivity

Since the completion of the first ice boom in the first inlet area of Lake Saroma in 1998, no damage to aquaculture facilities from drift ice has been reported. Although it is impossible to recover previous losses, e.g., exceeding 2 billion yen in 1974, the installation of the ice boom has embodied the local determination to prevent future damage. Prior to the introduction of the ice boom, fishery workers had to manually breakup the drift ice within Saroma Lake, diverting significant labor from their core operations. Now, this effort can be redirected toward aquaculture activities. In this way, the ice boom has contributed not only to reducing economic risks but also to improving operational productivity.

“We can now focus on our main work!”

“When drift ice enters the lake, the ropes suspending scallop spat are often severed, making it impossible to retrieve them. To prevent this, we used to go out during the drift ice season on boats equipped with excavators to break the ice. It was extremely labor-intensive — even with 30 people, the task took a full day. Thanks to the ice boom, we no longer need to perform this work, and we no longer worry about damage to our aquaculture facilities. We are truly grateful.”

(Voice of a local fisherman)

Nishimura Gumi Corp. (n.d.). *Ice Boom* [trans. from Japanese]. https://www.nishimura.co.jp/construction_example/project1/

9 | Icebreakers of Japan

9.1 New Arctic Research Vessel

1) Japan's First Arctic Research Vessel: *Mirai II*

In December 2020, the Japanese government approved the construction of a new “Arctic Research Vessel” (named *Mirai II* in 2023) to be designed with icebreaking capabilities. And on August 27, 2021, the Japan Agency for Marine-Earth Science and Technology (JAMSTEC) awarded the construction contract to JMU. The construction is expected to take five years, with the vessel scheduled to enter service in 2026.

While Japan has a history of Antarctic research vessels, starting with the *Soya*, this will be the first Japanese vessel specifically designed for research in the Arctic with ice-breaking capabilities. Although JAMSTEC’s oceanographic research vessel *Mirai* conducted observations in the Arctic Ocean during the summer of 2021, its lack of such icebreaking capabilities prevented entry into ice-covered waters.

The *Mirai II* (see Fig. 9.1) will be capable of continuously



Fig. 9.1 Artist rendering: *Mirai II*, arctic research vessel.⁹⁻¹⁾

breaking through flat ice up to 1.2 m thick, enabling a wide range of new research activities in the Arctic such as sea ice monitoring, biological and resource surveys, and meteorological observations. Table 9.1 compares key specifications of the *Mirai II* with those of the currently active Antarctic research vessel, the second-generation *Shirase*, a vessel of similar size, but *Shirase* with somewhat superior icebreaking capabilities.

2) Key Requirements and Socioeconomic Impact of the Arctic Research Vessel

Prior to designing Japan’s first dedicated Arctic research vessel, a panel of experts organized by the Ministry of Education, Culture, Sports, Science, and Technology (MEXT) examined various aspects and published their results in December 2020.⁹⁻³⁾ The report specifies the following performance requirements for the Arctic research vessel:

- i) The vessel should maintain the observation capabilities of the existing *Mirai* while incorporating new equipment such as scientific fish finders.
- ii) The vessel design should balance necessary icebreaking and ice resistance capabilities with an ability to conduct observations in both ice-covered and open water conditions.
- iii) The vessel should be equipped with an advanced navigation support system to ensure safe and efficient operations under icy conditions.
- iv) A dual-fuel engine (capable of running on both marine fuel oil and liquefied natural gas) should be used to reduce environmental impact and improve fuel efficiency.
- v) The vessel should have a reliable dynamic positioning system and an efficient propulsion system.

Table 9.1 Details: *Mirai II* and *Shirase* (second-generation).

Detail	<i>Mirai II</i> ⁹⁻¹⁾	<i>Shirase</i> ⁹⁻²⁾
Operator	JAMSTEC	Maritime Self-Defense Force
Builder	JMU	JMU
Commissioning	2026(planned)	May 2009
Construction Cost	est. 33.5 billion yen	37.6 billion yen
Gross Tonnage	13,000 t	12,650 t
Overall Length	128 m	138.0 m
Beam (Width)	23 m	28.0 m
Depth: deck to keel	12.5 m	15.9 m
Draft	8 m	9.2 m
Icebreaking Capability ¹⁾	Flat first-year ice, 1.2 m thick	Flat first-year ice, 1.5 m thick
Ice Class Rating	PC 4 ²⁾	PC 2 ³⁾
Personnel Capacity	97 ⁴⁾	259 ⁵⁾

1): Icebreaking capability at 3.0 knots (approx. 5.6 km/h).

2): PC 4: Year-round navigation in thick first-year ice with some multiyear ice.

3): PC 2: Year-round navigation in moderate multiyear ice.

4): 34 crew, 63 researchers/engineers.

5): 179 crew, 80 researchers/passengers.

- vi) Facilities for operating remotely operated vehicles (ROVs) and autonomous underwater vehicles (AUVs) should be included.
- vii) The vessel should have the capability to operate helicopters for safety, ice observation, and other purposes.
- viii) The vessel should provide sufficient laboratory space and communication networks to support research and analysis.
- ix) The vessel should provide a living environment that incorporates gender and other international standards to create a suitable international platform.
- x) The vessel should be capable of supporting disaster-relief efforts in stricken areas such as during heavy rains.

The inclusion of features such as the dual-fuel engine (iv), consideration of international standards in the living environment (ix), and capability to support disaster-stricken areas (x) reflects the vessel’s commitment to current societal needs. The report also anticipates several socioeconomic benefits from the construction of the Arctic research vessel, as detailed in the following:

Given the limited number of vessels currently operating in the Arctic, there is a lack of information necessary for the development of ships and navigation equipment suited for ice-covered waters. The operation of the Arctic research vessel, equipped with a hull response measurement system, will enable the collection of data on meteorological and oceanographic conditions, hull loads, and equipment performance in the Arctic and other maritime regions. This data will enhance Japan’s shipbuilding capabilities, particularly in designing and constructing vessels with superior fuel efficiency and safety in both ice-covered and open waters, potentially leading to increased orders for Arctic-route vessels and marine equipment.

Additionally, the incorporated hull response measurement system will enable monitoring cumulative stress on the hull to optimize maintenance costs and reduce the risk of maritime accidents—capabilities expected to enhance Japan’s influence in setting appropriate ship regulations and improving maritime safety standards. (trans. from Japanese)

3) Costs: Arctic Research Vessel

The estimated costs reported for the construction, operation, and maintenance required to meet the key requirements of the Arctic research vessel are outlined in **Table 9.2**.⁹⁻³⁾ The

report also compares these costs to those of similar icebreaking research vessels from Germany and the United Kingdom, concluding that the costs for Japan’s first Arctic research vessel are reasonable, as seen below.

- Germany: Construction cost, 27 billion yen; annual operating cost, 2.86 billion yen.
- United Kingdom: Construction cost, 30.3 billion yen; annual operating cost, 2.6 billion yen.

9.2 Antarctic Research Vessels

1) Japan’s Antarctic Research Vessels

The history of Japan’s Antarctic research vessels began with the *Soya* (in service from 1956 to 1962), followed by the *Fuji* (in service from 1965 to 1983), the first-generation *Shirase* (in service from 1982 to 2005), and the second-generation *Shirase* (2009 commissioned, still in service as of 2024). According to K. Nezu (2010), the following are the unique characteristics required of Japan’s Antarctic research vessels.⁹⁻²⁾

The primary role of an Antarctic research vessel is to reliably transport the research team and necessary supplies for their activities to Antarctica. The location of Japan’s Showa Station at Lützow-Holm Bay presents severe sea ice conditions, characterized by fixed ice that can be difficult to navigate through even during the Antarctic summer. In many other countries’ bases, the sea ice disappears during the summer, making the transportation of supplies relatively easy. However, Japan’s Antarctic research vessels require a high level of icebreaking capability to penetrate this fixed ice, through which even an icebreaker with a continuous icebreaking capability of about 1 m might struggle.

In addition to icebreaking capabilities, these vessels must also transport a large amount of supplies—over 1,000 tons necessary for a year’s operation—on a single voyage from Japan via Australia. Countries located in the Southern Hemisphere can distribute the transportation of supplies across multiple trips with icebreakers, and other countries such as the U.S. can utilize aircraft for effective transportation to their bases. However, securing a runway near Showa Station is not feasible due to geographical conditions and the characteristics of the surrounding ice. Therefore, Japan’s Antarctic research vessels must have the ability to break through the fixed ice of Lützow-Holm

Table 9.2 Costs: Arctic Research Vessel *Mirai II*.⁹⁻³⁾

Cost Item	Amount	Remarks
Total Construction Cost	est. ¥33.5 billion	Includes construction of the basic ship and installation of observation equipment, etc.
Cost of Observation Equipment	est. ¥1 billion	ROV, AUV, etc.
30-Year Operational Cost	est. ¥78 billion	Annual operational cost: est. ¥2.6 billion
Major Overhaul Cost	est. ¥3 billion	–
30-Year Total Cost	est. ¥115.5 billion	Total cost on annual basis: est. ¥3.85 billion

Bay, while carrying over 1,000 tons of supplies and at least two helicopters. Moreover, these vessels must also possess research capabilities, making them uniquely capable in ways that are unmatched by any other icebreaker in the world. (trans. by author)

2) Soya

The *Soya* was originally built in 1938 as an ice-strengthened cargo ship at the Kawanami Kogyo Co., Ltd. Koyagi Island Shipyard in Nagasaki Prefecture. It served in the Pacific War (WW2) and, postwar, as a repatriation ship and a lighthouse supply vessel (Fig. 9.2). *Soya* was Japan’s first Antarctic research vessel, participating in six Antarctic expeditions from November 1956 to April 1962. After its service as an Antarctic research vessel, it continued to serve as a patrol vessel for the Japan Coast Guard until decommissioning in 1978. Since 1979, the *Soya* has been preserved and displayed, moored in front of the Museum of Maritime Science in Tokyo.



Fig. 9.2 Lighthouse supply ship *Soya* at start of conversion into an Antarctic research vessel, photograph.⁹⁻⁴⁾

3) Antarctic Research Ships: *Fuji* and First *Shirase*

Japan’s Antarctic research began with the repurposing of the lighthouse supply vessel *Soya*. However, its first dedicated Antarctic research vessel, *Fuji*, was built in 1965. The *Fuji* served for 18 years until being succeeded by the first *Shirase* in 1982. The most significant difference between these two vessels was the enhancement of continuous icebreaking capability from 1.0 m to 1.5 m—an improvement necessitated by *Fuji* only being able to reach Showa Station six times out of 18 attempts as well as situations where it became immobilized by thick ice.

During the design phase of the first *Shirase*, Japan did not yet have an ice model basin. Therefore, the initial hull design relied on theoretical methods previously systematized primarily by Russian researchers for evaluating icebreaking resistance. Subsequent testing at HSVA (Hamburg Ship Model Basin) in Germany was conducted to refine the hull shape. With its enhanced icebreaking capabilities, the first *Shirase* was able to reliably reach Showa Station.

Table 9.3 provides the main specifications of Japan’s Antarctic research vessels from *Soya* onwards.

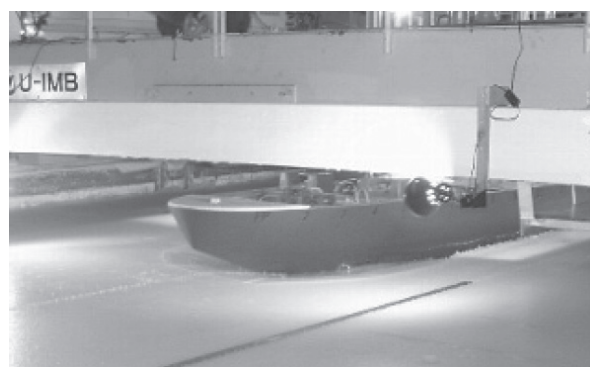


Fig. 9.3 Model testing, photograph: Second *Shirase*, ice tank at JMU.⁹⁻²⁾

Table 9.3 Key specifications of antarctic research vessels: *Soya* onwards.^{9-2, 5)}

Vessel Name	<i>Soya</i>	<i>Fuji</i>	(First) <i>Shirase</i>	(Second) <i>Shirase</i>
Commissioned	1956	1965	1982	2009
Antarctic Operation	7 years	18 years	25 years	Currently active
Antarctic Expeditions	1st to 6th Expeditions	7th to 24th Expeditions	25th to 49th Expeditions	51st and onwards
Length	84 m	100 m	134 m	138 m
Beam	12.8 m	22 m	28 m	28 m
Depth: Deck to Keel	7.0 m	11.8 m	14.5 m	15.9 m
Draft	5.8 m	8.3 m	9.2 m	9.2 m
Standard Displacement	2,736 t	5,250 t	11,650 t	12,650 t
Displacement—Fully Loaded	4,235 t	9,120 t	18,990 t	20,370 t
Cargo Capacity	400 t	400 t	1,000 t	1,100 t
Maximum Speed	14 kn	17 kn	19 kn	19 kn
Maximum Output (Horsepower)	2,400	11,900	30,000	30,000
Continuous Icebreaking Capability (at 3 kn)	1 m	1 m	1.5 m	1.5 m
Crew	94	182	174	179

Note: The 50th Antarctic Research Expedition conducted summer operations using the Australian icebreaker *Aurora Australis* for alternate transportation.

4) Second *Shirase*: Design Considerations

i) Ice Model Basin Experiments

The first *Shirase* supported 25 Antarctic expeditions from 1982 until its retirement in 2008; the second *Shirase* was completed in 2009. Based on the mission success rate of the first *Shirase*, the continuous icebreaking capability of 1.5 m was considered sufficient with no need for further enhancement. However, in areas with multi-year ice thicker than 2 m or exhibiting chaotic ice, icebreaking vessels must perform ramming icebreaking, i.e., the ship accelerating and ramming the ice, using the additional kinetic energy from the run-up to break through. The impact of ramming events on travel time and fuel consumption is significant. Therefore, to further stabilize mission schedules, the hull shape of the second *Shirase* was optimized to improve ramming performance with a hull design developed through model experiments conducted in the ice model basin at Universal Shipbuilding Corporation (now JMU), the vessel builder (Fig. 9.3).

ii) Bow Shape

The ship's bow angle (inclination to the horizontal) near the waterline and the frame lines of the bow are particularly important on icebreakers, being designed to be more efficient by being shallower. Since icebreaking is more efficiently achieved, i.e., requiring less force, by bending rather than by crushing the ice, shallower angles result in an icebreaking ship pushing ice sheets downward to break through them as it moves forward. However, if the bow angle is too shallow, the ship may ride up excessively onto the ice sheets, or the increased contact area between the hull and the ice can lead to higher frictional resistance.

Figure 9.4 illustrates the bow shapes of the *Fuji*, the first *Shirase*, and the second *Shirase*. When the *Fuji* was designed, the bow angle was set at 30 degrees in the belief that a bow angle in the range of 25 to 30 degrees was optimal. During the planning of the first *Shirase*, ice model basin tests resulted in a hull design with an enhanced icebreaking capability at a reduced bow angle of 21 degrees. The 19 degree bow angle of the second *Shirase* is not significantly different from that of its predecessor, but the hull shape at the waterline was altered to more easily penetrate ice sheets to increase the distance

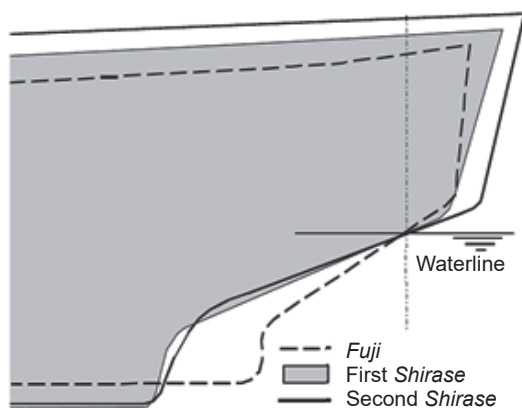


Fig. 9.4 Bow shapes—Angle: *Fuji*, 30 degrees; first *Shirase*, 21 degrees; second *Shirase*, 19 degrees.⁹⁻²⁾

advanced during ramming.⁹⁻²⁾

iii) Icebreaking Assist Water Spraying System

A water spraying system was installed in the second *Shirase* to improve icebreaking performance. The heavy snowfall commonly occurring in areas around Showa Station can reduce the distance advanced during ramming to less than half that experienced when the sea ice is bare; the water spraying system reduces the frictional resistance between the snow/sea ice and the hull by spraying water from nozzles located at the bow above the waterline onto the ice sheet. As this system is particularly effective when dry snow is heavily accumulated on the ice, the icebreaking performance has been improved during Antarctic voyages to Showa Station. Figure 9.5 shows the operation of the water spraying system in an ice-free sea area.⁹⁻²⁾



Fig. 9.5 Second *Shirase* icebreaking enhancement—Sprinkler system, photograph: System sprays water from bow nozzles to reduce friction between snow/sea ice and the ship.⁹⁻²⁾

iv) Double-Hull Structure

The second *Shirase* adopted a double-hull structure, where the space between the fuel tanks and the hull's outer plating can prevent fuel from leaking if only the outer hull is damaged, see Fig. 9.6. In contrast, the single-hull design of the

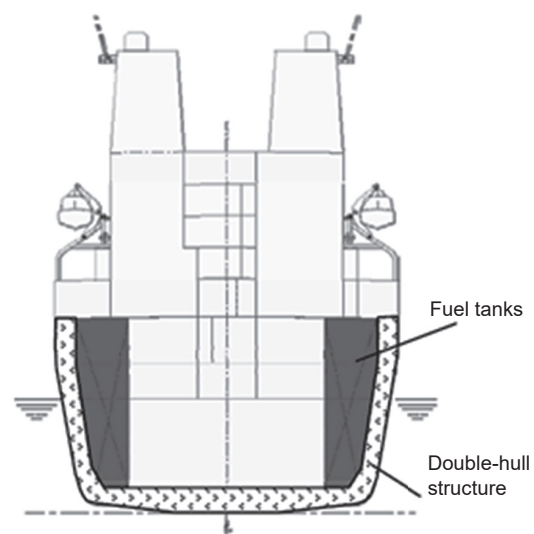


Fig. 9.6 Second *Shirase* double-hull structure: Design prevents fuel leakage from damaged outer hull.⁹⁻²⁾

first *Shirase* posed a risk of fuel leakage from a collision or grounding: The amount of fuel being carried is substantial as it is for its own use as well as to supply various fuels to Showa Station.

Since much of the description of Antarctic research vessels in this section is based on K. Nezu (2010) (Ref. 9-2), this reference is recommended for further details.

9.3 Arctic Sea Routes

1) Northeast Passage and Northwest Passage

The relatively recent rapid reduction of sea ice in the Arctic Ocean has brought increased attention to the use of Arctic Sea routes for the transportation of goods and Arctic cruises. Since the 2000s, shipping through the Arctic Sea routes, increasing gradually at first, has been rising each year. While the navigable period for the Arctic Sea routes (Fig. 9.7) fluctuates depending on various meteorological conditions, as of 2021, navigation is generally possible from around August to October.

The two primary trans-Arctic routes are the Russian route along the coast of Russia (Northeast Passage), and the Canadian route through the territorial waters of Canada (Northwest Passage). As of 2021, the Russian route is the one being used

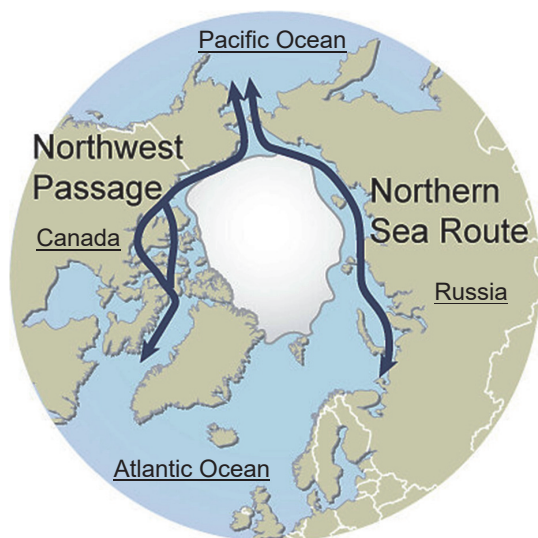


Fig. 9.7 Arctic Sea Routes, 2020: Northern Sea Route (Russian portion of Northeast Passage) and Northwest Passage.⁹⁻⁶⁾

for transporting goods to Japan. For example, when shipping between Rotterdam and Yokohama, the southern route through the Suez Canal is 18,400 km, while that via the Russian Arctic route is only 11,100 km, about 40% shorter. This shorter route offers advantages such as reduced transit time and fuel savings as well as avoiding piracy. However, as of 2022, questions remain about its economic feasibility due to costs associated with Russian icebreaker escort services and the need for ice-class vessels, as well as the growing concern over the environmental impact of increased ship traffic through the Arctic.

2) Increasing Traffic: Northeast Passage

Table 9.4 presents an overview of the vessels navigating the Russian route from June to December between 2017 and 2020, showing the number of voyages increasing yearly from 49 in 2017 to 133 in 2020. Notably, transit voyages (no stops at Arctic ports) between Europe and Asia doubled to 65 from 2019 to 2020. In particular, the significant increase in the number of cargo ships and tankers was driven largely by the growth in LNG tanker traffic to the Yamal Peninsula LNG terminal (Yamal LNG Project, liquified natural gas, Russia), which began operations in December 2017.

As Arctic sea ice continues to decline and resource development in the Arctic region intensifies, the number of vessels navigating the Arctic Sea routes is expected to continue rising. However, the routes are subject to significant influence from the political interests of concerned nations such as the United States, Canada and Russia, bordering the Arctic Sea, as well as China, which has invested in the Yamal LNG project and views the Arctic Sea as the “Polar Silk Road,” a part of its broader geopolitical strategy.

3) Icebreaking LNG Vessels: Yamal LNG Project

The increasing use of the Arctic Sea routes has likewise increased the demand for vessels with icebreaking capabilities or ice-resistant features. In the Yamal LNG Project, the LNG is transported to Europe and East Asia using icebreaking-capable ships. Mitsui O.S.K. Lines, Ltd. (MOL) plays a significant role in this transportation, and by 2024, the company is expected to own and manage 14 icebreaking LNG ships, with all of these vessels being built at shipyards in South Korea and China. As of now, Japanese shipbuilders have yet to establish a track record in constructing commercial vessels for the Arctic Sea.

Table 9.4 Arctic Sea voyage summary: Northern Sea Route (Russian portion of Northeast Passage).⁹⁻⁷⁾

Year		2017	2018	2019	2020
Total Voyages		49	60	87	133
Navigation Type	Arctic Route Port Calls* ¹	20	31	55	68
	Transit Voyages* ²	29	29	32	65
Vessel Type	Cargo Ships, Tankers	32	48	76	109
	Cruise Ships	3	1	4	1
	Others (Tugs, etc.)	6	10	7	23

*¹ Arctic Route Port Calls: Vessels stopping at ports along the Arctic Sea route.

*² Transit Voyages: Vessels using the Arctic Sea route as a passage without stopping at any ports along the route.

Figure 9.8 shows the first icebreaking LNG ship for the Yamal LNG Project, built in South Korea by Daewoo Shipbuilding & Marine Engineering Co., Ltd.



Fig. 9.8 World's first icebreaking LNG carrier, *Vladimir Rusanov*, photograph: Daewoo Shipbuilding, South Korea, Dec. 2017; maximum icebreaking capability, 2.1 m (in reverse).⁹⁻⁸⁾

9.4 Conclusion

Japan's history with icebreaking ships dates back to the pre-WW2 period when icebreakers were deployed in Karafuto (now Sakhalin). However, the *Soya*, repurposed from a lighthouse supply vessel into an Antarctic research vessel in 1956, is Japan's first well-known icebreaker. *Soya* was followed by the *Fuji* in 1965, the first-generation *Shirase* in 1982, and the second-generation *Shirase* in 2009. In 2021, Japan made the decision to construct its first research vessel equipped with icebreaking capabilities specifically designed for Arctic research. Despite Japan's shipbuilders having steadily accumulated icebreaker technology through the construction of Antarctic research vessels, they currently have not built any icebreaking vessels for international markets.

Japan's shipbuilding industry, although once dominating the global market with a 50% share, as of 2020, ranked third in terms of total volume (measured in Gross tonnage (GT)) of ships built and delivered, behind China and South Korea. The Japanese industry lacks the financial strength seen in the other countries, where large shipbuilding companies have been

formed through mergers supported by government guidance and assistance—a contributing factor to Japan's reluctance to pursue orders for building icebreaking vessels intended for the Arctic route.

References

- 9-1) JAMSTEC (Japan Agency for Marine-Earth Science and Technology). (2021, Aug. 27). *Contract Signed for Construction of Arctic Research Vessel* [in Japanese]. http://www.jamstec.go.jp/j/about/press_release/20210827_2/.
- 9-2) Nezu, K. (2010). The New Antarctic Research Vessel *Shirase*. *Journal of the JIME (Japan Institute of Marine Engineering)*, Vol. 45, No.2, 32-37. (in Japanese).
- 9-3) Expert Panel on Utilization Strategies and Cost-Effectiveness of the Arctic Research Vessel. (2020, Dec.). *Review of Utilization Strategies and Cost-Effectiveness of the Arctic Research Vessel*, Report. Ministry of Education, Culture, Sports, Science and Technology (MEXT). (in Japanese).
- 9-4) Museum of Maritime Science. (n.d.). *History in [sic] "SOYA."* <https://funenokagakukan.or.jp/soya/history/road>. (in Japanese).
- 9-5) MEXT. (2019, May 24). [Materials distributed], 24th External Evaluation Committee Meeting of the Headquarters for Antarctic Research Promotion. Ministry of Education, Culture, Sports, Science and Technology (MEXT).
- 9-6) GRID-Arendal. (2024). *Arctic sea routes - Northern sea route and Northwest passage*. <https://www.grida.no/resources/7859>.
- 9-7) MLIT. (2021, Mar. 23). *Results of Joint Research on Understanding Navigation Conditions in the Arctic Ocean Using Satellite AIS* [Press Release, trans. from Japanese]. National Institute for Land and Infrastructure Management, Ministry of Land, Infrastructure, Transport and Tourism (MLIT).
- 9-8) Mitsui O.S.K. Lines. (2018, Mar. 29). *Ice-Breaking LNG Carrier "VLADIMIR RUSANOV" for Yamal LNG Project Started the First Loading Operation in the Yamal LNG Plant at Sabetta Port—Operational Commencement with MOL's 1st Vessel for World's First Ice-Breaking LNG Carrier Project*, Press Release [in Japanese]. <https://www.mol.co.jp/pr/2018/18022.html>.

10 | Epilogue

Japan's systematic research on snow and ice began in the 1930s with studies on snow damage by the Snow Regions Agricultural Research Center in Shonai City, Yamagata Prefecture, and Dr. Ukichiro Nakaya's pioneering work on snow crystals at Hokkaido University (Chapter 4).

Although initially focused on snow, the start of Antarctic expeditions in 1956 and the discovery of oil and natural gas resources in the Arctic Ocean during the 1960s resulted in a rapid expansion of research on ice engineering. The conversion of the *Soya* into an icebreaker and the construction of Antarctic research vessels, starting with the *Fuji*, significantly advanced Japan's icebreaker technology (Chapter 9). In addition, Arctic resource development served as a catalyst for universities and industry to initiate engineering studies on the interaction between sea ice and structures as well as the design and construction of ice-resistant structures.

Starting in the 1970s, institutions like Hokkaido University, Iwate University, and the University of Tokyo have advanced engineering research on ice, with company researchers and engineers conducting studies at leading international research institutes, such as the U.S. Army CRREL, the National Research Council Canada (NRC), and the HSVA in Germany (Chapter 5). These research efforts led to the construction of world-first structural types of arctic offshore drilling platforms by Japanese shipbuilders in the 1980s, e.g., *SSDC*, *Kulluk*, *Molikpaq*, and *Super CIDS* (Chapter 8). Around the same time, the Ship Research Institute (now the National Maritime Research Institute), Nippon Kokan, and Mitsubishi Heavy Industries began operating ice model basins for research on ice-resistant structures, enabling the 1980s to be a formative period for Japan's ice engineering and shipbuilding capabilities (Chapter 6).

In 1993, the JOIA Ice Load Research Project was initiated with the collaboration of academia, industry, and the government to further develop Japan's ice engineering technology (Chapter 7). This project yielded numerous significant results, including the world's largest in situ sea ice indentation experiments, pioneering experiments and analyses using ice model basins, and the establishment of special sessions at international conferences as well as joint research with overseas scientists. These efforts also led to Japan's involvement in the development of ISO19906, the international standard for the design of Arctic offshore structures.

Despite these research and development achievements and construction successes, Japanese companies did not gain a competitive edge in the global market for Arctic offshore structures. The unique market dynamics of this sector, i.e., greatly influenced by fluctuating oil prices, unpredictable market size, and stringent construction specifications and deadlines, as well as competition from emerging competitors like South Korea and China, posed significant challenges. This

result paralleled a transitioning of the overall structure of Japan's industrial base from large traditional, resource-intensive industries to more modern, efficient, and technology-driven industries. As a result, even with Japan's superior construction technology, quality, and reliability in meeting deadlines, the ice engineering business proved to be a difficult venture.

On September 16, 2021, Arctic sea ice reached its annual minimum extent—4.72 million km². Arctic sea ice typically reaches its minimum extent each September and its maximum in March. The September 2021 average extent was 4.92 million km², the 12th smallest in 47 years of satellite records—the 15 smallest of these sea ice extents since records began in 1974 occurred during the 15 years from 2007 to 2021. In addition to this remarkable indicator of the changing Arctic environment, the thickness of the ice is decreasing, resulting in a significant reduction in sea ice volume.

Global warming is an undeniable reality: With the Arctic region experiencing the most pronounced temperature increases, its sea ice is rapidly diminishing. As summer sea ice continues to decline, the use of Arctic shipping routes is expected to increase. The exploitation of fossil resources—one of the primary reasons for studying sea ice—is recognized to be a major factor in accelerated global warming, ultimately resulting in the loss of sea ice: a deeply troubling outcome for the field of ice engineering.

The diminishing sea ice in the Arctic presents a new frontier where Japan's advanced technology can make a significant contribution. *Mirai II*, Japan's new research vessel scheduled to enter service in 2026 with a capability to operate in the icy Arctic seas, holds great promise for researchers, engineers, and companies (Chapter 9). As Japan already has innovative companies using satellites and providing Arctic sea ice information to ships domestically and internationally, we look forward to the launch of *Mirai II* opening up more opportunities for company researchers and engineers to participate in Arctic research and promote the emergence of new polar technologies.

The primary focus of this book is the engineering research and technological developments that have occurred in the field of ice engineering since the 1970s: a period concurrent with the author's over 40 years of involvement in this area that began in the late 1970s during a university sea ice graduation research project. I hope that this perspective will lead to a better understanding and greater appreciation not only for the advancements seen in this field but also for the efforts put forth by the researchers themselves as well as the associated institutions, private and governmental.

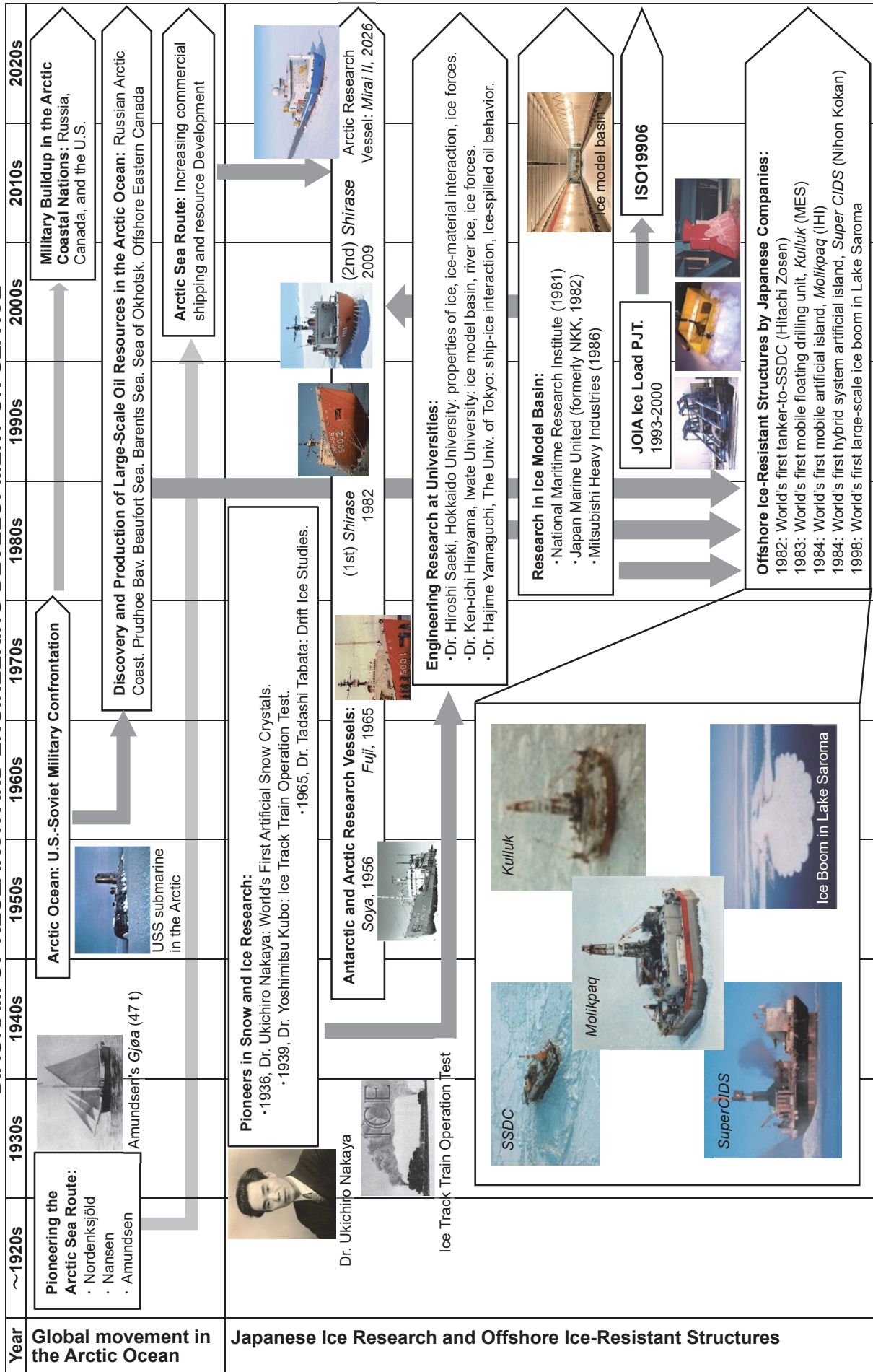
■ Acknowledgements

The author would like to express his gratitude to the following individuals and organizations for their valuable advice and the provision of materials that greatly contributed to the writing of this book:

Dr. Satoshi Akagawa
Dr. Makoto Ota
Dr. Shinji Kioka
Dr. Akira Kurokawa
Dr. Masanori Kobayashi
Dr. Norikazu Maeno
Dr. Yutaka Yamauchi
Dr. Robert Frederking (Canada)
Prof. Takahiro Takeuchi
Ms. Sachi Itagaki
Ms. Fujiko Nakaya
IHI Corporation
Japan Agency for Marine-Earth Science and Technology (JAMSTEC)
Shimizu Corporation
Japan Marine United Corporation (JMU)
Ukichiro Nakaya Museum of Snow and Ice
Mitsubishi Heavy Industries, Ltd.
Japan Foundation for Maritime Science, Museum of Maritime Science
Kyoto University of Foreign Studies
International Research Center for Japanese Studies
Nishimura-Gumi Co., Ltd.
Hokkaido University, Institute of Low Temperature Science

The author would like to express his special gratitude to Mr. Eiji L. Suenaga for his significant contribution to this English version of the original Japanese. Without his expertise in sea ice engineering and experience in writing technical papers in English, this version would not have been possible: University of California, Los Angeles, (UCLA) College of Engineering—B.S. (1966) and M.S. (1969) and School for International Training (Brattleboro, Vermont)—M.A. (1989) in teaching. After working in the aerospace industry and the military-industrial complex in southern California, he relocated to Japan, where he was a research fellow at Hokkaido University in the field of sea ice engineering under Professor H. Saeki. Subsequently, he taught at several universities located in Japan, including the Kanazawa Institute of Technology, Kanazawa, and the City University of New York-Lehman College, Hiroshima campus.

DIAGRAM OF RESEARCH AND ENGINEERING DEVELOPMENT ON SEA ICE



SURVEY OF INDUSTRIAL TECHNOLOGY HISTORY ARCHIVE

No.	Name	Year	Creator / Manufacturer	Location (as of 2022)	Reason for Selection
Research Apparatus / Research Report					
1	Artificial snow crystal production apparatus	1936	Ukichiro Nakaya, Hokkaido Imperial University	Institute of Low Temperature Science, Hokkaido University	World's first artificial snow crystal production apparatus
2	Research report on river ice, in particular railroad tracks across ice-covered rivers	1941	Yoshimitsu Kubo, South Manchuria Railway Company	Engineering Library, Nagoya University	Foundational research of ice engineering—conducting ice track train operation test
Drift Ice Observation Apparatus					
3	C-band wide-area drift ice observation radar	1965	Hokkaido University	Mombetsu, Hokkaido	World's first radar system (C-band) for observing drift ice
4	X-band doppler radar	2005	Hokkaido University	Mombetsu, Hokkaido	World's first use of this type of radar for observing sea ice and snow clouds
Ice Model Basin					
5	Ice Model Basin	1981	National Maritime Research Institute (NSRI)	Mitaka City, Tokyo	Japan's first, the world's eighth, large ice model basin facility
6	Ice Model Basin	1982	Japan Marine United Corporation (JMU)	Tsu City, Mie	Japan's second ice model basin (first private company operator)
Offshore Ice-Resistant Structures					
7	SSDC (Single Steel Drilling Caisson)	1983	Hitachi Zosen Corporation	Herschel Island, Canada	World's first tanker-to-ODR (oil drilling rig) conversion
8	<i>Molitpaq</i> (Mobile Arctic Caisson Island)	1984	IHI Corporation	Offshore Sakhalin, Sea of Okhotsk	World's first mobile artificial island
9	Super CIDS (Concrete Island Drilling System)	1984	Nippon Kokan (now JMU)	Offshore Sakhalin, Sea of Okhotsk	World's first hybrid structure (combining steel and concrete) artificial island
10	Ice Boom (Drift Ice Inflow Control Facility)	1998	Hokkaido Regional Development Bureau	Lake Saroma, Hokkaido	World's first large-scale ice boom designed to control drifting sea ice
Antarctic/Arctic Research Vessels					
11	<i>Soya</i> : 1st to 6th Antarctic Expeditions	1956	Ministry of Education, Culture, Sports, Science and Technology (MEXT)	Aomi Kita-futo Park, Shinagawa, Tokyo	Japan's first Antarctic research vessel (originally built as a cargo ship)
12	<i>Fuji</i> : 7th to 24th Antarctic Expeditions	1965	MEXT	Nagoya Maritime Museum, Nagoya, Aichi	Japan's first dedicated Antarctic research vessel
13	(First) <i>Shirase</i> : 25th to 49th Antarctic Expeditions	1982	MEXT	Funabashi, Chiba	Supported 25 Antarctic expeditions from 1982 to 2008
14	(Second) <i>Shirase</i> : 51st and onwards Antarctic Expeditions	2009	MEXT	Yokosuka, Kanagawa	Development model tests conducted in the ice model basin at JMU—in service as of 2024
15	<i>Mirai II</i> : scheduled to enter service to Arctic in 2026	2026	MEXT	Mutsu, Aomori (home port)	Japan's first Arctic research vessel